

# **The Synthesis and Characterization of Novel Rhodium Alkenyl Complexes and Rhodacycloalkanes**

Emma Hager



University of Cape Town

2007

The copyright of this thesis vests in the author. No quotation from it or information derived from it is to be published without full acknowledgement of the source. The thesis is to be used for private study or non-commercial research purposes only.

Published by the University of Cape Town (UCT) in terms of the non-exclusive license granted to UCT by the author.

## ABSTRACT

The rhodium dimers  $[\text{Cp}^*\text{RhCl}_2]_2$  and  $[\text{Cp}^*\text{RhBr}_2]_2$  were reacted with alkenyl Grignard reagents  $\text{MgBr}(\text{CH}_2)_n\text{CH}=\text{CH}_2$  ( $n = 1 - 4, 6, 8, 9$ ) in an attempt to form bis-alkenyl complexes that would be potential precursors to rhodium-containing metallacycloalkanes. The shorter-chain Grignard reagents ( $n = 1 - 3$ ) produced novel rhodium allylic complexes of composition  $\text{Cp}^*\text{RhBr}(\eta^3\text{-allyl-R})$  where  $\text{R} = \text{H}, \text{CH}_3, \text{CH}_2\text{CH}_3$ . These were isolated as stable crystals and were fully characterized by analytical and spectroscopic methods. An X-ray crystal structure obtained for one of the complexes ( $\text{R} = \text{CH}_2\text{CH}_3$ ) confirmed the allylic structure of the complex.

The use of longer-chain reagents ( $n = 3, 4, 6, 8, 9$ ) resulted in the formation of the novel bis-alkenyl complexes  $\text{Cp}^*\text{Rh}(\{\text{CH}_2\}_n\text{CH}=\text{CH}_2)_2(\text{H}_2\text{O})$ . The bis-alkenyl complexes were obtained as yellow oils that were found to be stable in air and non-chlorinated solvents, but unstable in chlorinated solvents. They were characterized by NMR, MS and elemental analysis.

Ring-closing metathesis (RCM) reactions were carried out on two of the bis-alkenyl complexes ( $n = 4, 6$ ) in the presence of Grubbs' first-generation catalyst. NMR evidence indicated that the corresponding 11- and 15-membered ring rhodacycloalkenes had been formed.

The rhodium phosphine precursors  $\text{Cp}^*\text{RhCl}_2(\text{PR}_3)$  ( $\text{PR}_3 = \text{PPh}_3, \text{PMePh}_2, \text{PMe}_2\text{Ph}$ ) were prepared and reacted with the di-Grignard reagents  $\text{MgBr}-(\text{CH}_2)_n\text{-MgBr}$  ( $n = 7, 8, 9$ ) to form a series of medium-sized rhodacycloalkanes that were larger than any synthesized previously. The rhodacycles were found to be quite unstable at room temperature. Thermal decomposition studies were conducted on some of the complexes and the major organic products were analyzed by GC-MS. In most cases the major products were 1- and 2-alkenes and n-alkanes. It was found that the nature of the tertiary phosphine ligand affected the types of decomposition products formed.

## Abbreviations

bipy	bipyridyl
<i>ca</i>	approximately
COD	cycloocta-1,5-diene
Cp*	pentamethylcyclopentadienyl
DCM	dichloromethane
dppe	1,2-bis(diphenylphosphino)ethane
dippe	1,2-bis(diisopropylphosphino)ethane
Eq.	equation
FAB	fast atom bombardment
GC	gas chromatography
GC-MS	gas chromatography - mass spectrometry
IR	infrared
L	ligand
L <sub>n</sub>	ligand system
mp.	melting point
NMR	nuclear magnetic resonance
PPh <sub>3</sub>	triphenylphosphine
RCM	ring-closing metathesis
S	solvent
sty	styrene

## Acknowledgements

I wish to extend my thanks to the following people:

To my supervisors, Prof John Moss and Dr Greg Smith, for your invaluable support and guidance throughout my MSc. project. Thank you both for your optimism and sense of humour.

To Dr Akella Sivaramakrishna, who always found time to help and encourage both myself and other students in our laboratory. Thank you for your kindness and your patience.

To all those involved in the various aspects of analysis of my complexes, and who contributed so greatly to my project: Feng, Noel, Pete, Hong, Piero and Tommy of Wits University.

To all members of the UCT Organometallic Research Group: during the past few years I have learned so much, but, as importantly, I have met some wonderful people and made good friends. Thank you for so many smiles and so much laughter in the lab.

To other friends and members of family who have encouraged and supported me, especially over the last few years.

To my immediate family, Catherine and Matthew, and especially to my parents, Brenda and Christopher, for your love and support throughout my life. Thank you.

# TABLE OF CONTENTS

ABSTRACT	i
CONFERENCE CONTRIBUTIONS	ii
ABBREVIATIONS	iii
ACKNOWLEDGEMENTS	iv
TABLE OF CONTENTS	v

## Chapter 1

### **General Introduction: The preparation of dialkyl complexes and metallacycloalkanes of group 8 – 10 transition metals and their applications in catalysis**

1.1	Introduction	1
1.2	Synthesis of metal dialkyl complexes	2
1.2.1	The reaction of metal halide complexes with carbon nucleophiles	3
1.2.2	The reaction of anionic or nucleophilic metal complexes with carbon electrophiles	3
1.2.3	Generation of dialkyls from trialkyl complexes	4
1.3	Known, isolated dialkyl complexes of group 8 – 10 metals	4
1.4	Reactivities of metal dialkyl species	7

1.4.1	Radical reactions	7
1.4.2	$\beta$ -hydride elimination	8
1.4.3	$\alpha$ -hydride abstraction	9
1.4.4	Reductive elimination	10
1.4.5	Alkyl migration	14
1.4.6	Alkene insertion	16
1.5	Catalytic applications of metal dialkyl species	17
1.5.1	Carbon-carbon cross-coupling reactions	17
1.5.2	Cyclization and cyclooligomerization reactions	22
1.5.3	Other examples of applications of metal dialkyl complexes	23
1.6	Summary of Chapter 1	24
1.7	Aims and objectives of this project	25
1.7.1	The focus of this project	25
1.7.2	Approaches to the synthesis of rhodacycloalkanes	26
1.8	References	27

## Chapter 2

### **Results and discussion: reactions of rhodium precursors with alkenyl Grignard reagents**

2.1	Introduction	36
2.2	Rhodium starting materials	37
2.2.1	Synthesis of rhodium chloride complexes	37
2.2.2	Characterization of rhodium chloride complexes	39
2.2.3	Synthesis and characterization of rhodium iodide complexes	40

2.2.4	Synthesis and characterization of rhodium bromide complex	40
2.3	Reactions of alkenyl Grignard reagents with rhodium precursors	41
2.4	Reactions of rhodium complexes with short-chain versus long-chain alkenyl Grignard reagents	43
2.5	Allyl complexes	44
2.5.1	Synthesis of allyl complexes	44
2.5.2	NMR spectra of allyl complexes	47
2.5.3	The effect of different solvents on the complex	48
2.5.4	Mass spectrometry of allyl complexes	50
2.5.5	X-ray crystal structure of Cp*RhBr( $\eta^3$ -1-ethylallyl)	50
2.5.6	Mechanism of formation of the allyl complex	51
2.6	Bis-alkenyl complexes	54
2.6.1	Synthesis of bis-alkenyl complexes	54
2.6.2	Microanalysis results for bis-alkenyl complexes	56
2.6.3	NMR spectra of the bis-alkenyl complexes	58
2.6.4	The absence of allylic product with long-chain alkenyl Grignard reagents	60
2.6.5	Reaction mechanism for formation of the complex	62
2.7	Ring-closing reactions	63
2.8	Summary of Chapter 2	65
2.9	References	67

## Chapter 3

### Results and discussion: reactions of rhodium precursors with di-Grignard reagents

3.1	Introduction	69
3.2	Reactions of rhodium complexes with di-Grignard reagents	70
3.2.1	Di-Grignard reagents	70
3.2.2	The di-Grignard reaction: chloride versus iodide starting materials	71
3.2.3	NMR characterization of rhodacycloalkanes	72
3.2.4	Other characterization methods	73
3.3	Decomposition studies	74
3.4	Summary of Chapter 3	77
3.5	References	78

## Chapter 4

### Experimental Details

4.1	General	80
4.2	Synthesis of Grignard reagents	80
4.3	Synthesis of di-Grignard reagents	81
4.4	Synthesis of rhodium starting materials	81
4.4.1	[Cp*RhCl <sub>2</sub> ] <sub>2</sub>	81

4.4.2	Cp*RhCl <sub>2</sub> (PPh <sub>3</sub> )	82
4.4.3	Cp*RhCl <sub>2</sub> (PMePh <sub>2</sub> )	83
4.4.4	Cp*RhCl <sub>2</sub> (PMe <sub>2</sub> Ph)	83
4.4.5	[Cp*RhI <sub>2</sub> ] <sub>2</sub>	83
4.4.6	Cp*RhI <sub>2</sub> (PPh <sub>3</sub> )	84
4.4.7	[Cp*RhBr <sub>2</sub> ] <sub>2</sub>	84
4.5	Rhodium alkenyl complexes	84
4.5.1	Reaction of [Cp*RhBr <sub>2</sub> ] <sub>2</sub> with MgBr-CH <sub>2</sub> CH=CH <sub>2</sub>	84
4.5.2	Reaction of [Cp*RhBr <sub>2</sub> ] <sub>2</sub> with MgBr-(CH <sub>2</sub> ) <sub>2</sub> CH=CH <sub>2</sub>	85
4.5.3	Reaction of [Cp*RhBr <sub>2</sub> ] <sub>2</sub> with MgBr-(CH <sub>2</sub> ) <sub>3</sub> CH=CH <sub>2</sub>	86
4.5.4	Reaction of [Cp*RhCl <sub>2</sub> ] <sub>2</sub> with MgBr-(CH <sub>2</sub> ) <sub>3</sub> CH=CH <sub>2</sub>	86
4.5.5	Reaction of [Cp*RhCl <sub>2</sub> ] <sub>2</sub> with MgBr-(CH <sub>2</sub> ) <sub>4</sub> CH=CH <sub>2</sub>	87
4.5.6	Reaction of [Cp*RhCl <sub>2</sub> ] <sub>2</sub> with MgBr-(CH <sub>2</sub> ) <sub>6</sub> CH=CH <sub>2</sub>	87
4.5.7	Reaction of [Cp*RhCl <sub>2</sub> ] <sub>2</sub> with MgBr-(CH <sub>2</sub> ) <sub>8</sub> CH=CH <sub>2</sub>	88
4.5.8	Reaction of [Cp*RhCl <sub>2</sub> ] <sub>2</sub> with MgBr-(CH <sub>2</sub> ) <sub>9</sub> CH=CH <sub>2</sub>	88
4.6	Reactions of rhodium complexes with di-Grignard reagents	89
4.6.1	Reaction of Cp*RhCl <sub>2</sub> (PPh <sub>3</sub> ) with MgBr-(CH <sub>2</sub> ) <sub>7</sub> -MgBr	89
4.6.2	Reaction of Cp*RhCl <sub>2</sub> (PMePh <sub>2</sub> ) with MgBr-(CH <sub>2</sub> ) <sub>7</sub> -MgBr	89
4.6.3	Reaction of Cp*RhCl <sub>2</sub> (PMe <sub>2</sub> Ph) with MgBr-(CH <sub>2</sub> ) <sub>7</sub> -MgBr	90
4.6.4	Reaction of Cp*RhCl <sub>2</sub> (PPh <sub>3</sub> ) with MgBr-(CH <sub>2</sub> ) <sub>8</sub> -MgBr	90
4.6.5	Reaction of Cp*RhCl <sub>2</sub> (PPh <sub>3</sub> ) with MgBr-(CH <sub>2</sub> ) <sub>9</sub> -MgBr	91
4.7	Determination of X-ray crystal structure of <b>30</b>	91
4.8	Thermal decomposition studies	92
4.9	References	93

## **Chapter 5**

### **Conclusions and future work**

94

## Chapter 1

# General Introduction: The preparation of dialkyl complexes and metallacycloalkanes of group 8 – 10 transition metals and their applications in catalysis

### 1.1 Introduction

Transition metal complexes containing one or more metal-carbon single bonds (Figure 1.1) are ubiquitous in the field of organometallic chemistry,<sup>1</sup> where the  $\sigma$ -bonded organic group may constitute an alkyl, aryl, acyl or vinyl moiety.

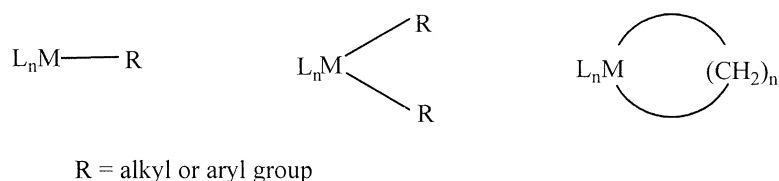


**Figure 1.1** Representations of a metal alkyl, metal dialkyl and metallacycloalkane

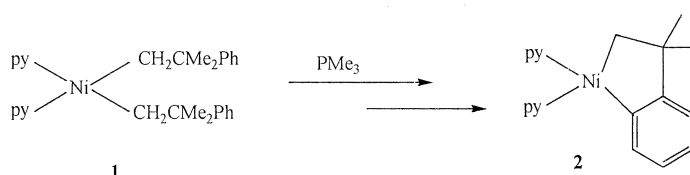
Monoalkyl or -aryl species are particularly abundant and their structures and applications have been widely reported. Reactivity patterns (such as  $\beta$ -H elimination, hydride abstraction) have also been extensively studied<sup>1</sup> and their mechanisms discussed.

Dialkyl metal complexes contain two M-C  $\sigma$ -bonds. These less well-known complexes naturally exhibit similar reactivity to their monoalkyl counterparts. However, the presence of the second alkyl or aryl group allows for the occurrence of reactions not possible in monoalkyls.<sup>2</sup> The most striking example of this is the potential for intramolecular coupling of the two carbon groups in dialkyl species.<sup>1,2</sup>

Metallacycloalkanes also contain two M-C single bonds. In this case, the attachments to the metal centre occur via two different carbons on the *same* alkyl chain, so forming a cyclic complex. The principles of reactivity are again comparable to other types of metal alkyls except that the carbon ring, more inflexible than a free alkyl

chain, can impose restraints on the reactivity of metallacycles. Their chemistry and decomposition behaviour are therefore somewhat different from those of the structurally similar dialkyls.<sup>3</sup>

Metallacycloalkanes are generally observed to be more stable than the metal dialkyls. For example, Scheme 1.1 depicts the action of trimethylphosphine on nickel dialkyl complex **1** to form nickelacycloalkane **2**. The metallacycle was shown to be much more stable than the complex from which it was derived.<sup>4</sup>



**Scheme 1.1**

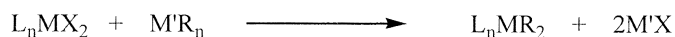
Because of their unique reactivity, metal complexes with more than one M-C bond play essential roles, both as catalyst precursors and as intermediates, in numerous catalytic reactions.<sup>5</sup> Although complexes with three or four bonded alkyl groups are known,<sup>6</sup> the present review will focus specifically on the synthesis and applications of metal species with two metal-carbon bonds. A literature survey reveals that much of the work done in this area focuses on the early transition metal complexes and their use in oligomerization and polymerization catalysis.<sup>7-10</sup> This present review discusses complexes of the later transition metals; specifically, those belonging to groups 8, 9 and 10. In particular, the metal dialkyls, their reactivities and applications will be highlighted, as a review of metallacycloalkanes has been published recently.<sup>5</sup>

## **1.2 Synthesis of metal dialkyl complexes**

There are several methods for the preparation of metal alkyl complexes. Some of these have been applied to the formation of their dialkyl counterparts.

### 1.2.1 The reaction of metal halide complexes with carbon nucleophiles

This is by far the most common synthetic method for both dialkyl metal complexes and metallacycloalkanes.<sup>11</sup> Neutral or cationic dihalides react with organometallic alkylating reagents to afford the dialkylated product (Equation 1.1).



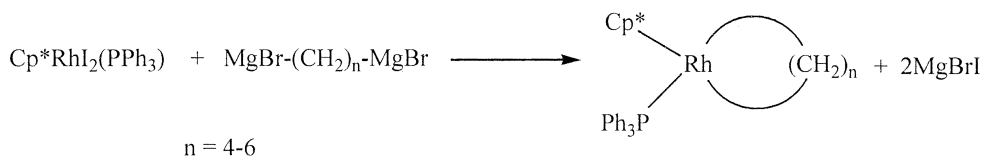
M' = MgBr, Li, Al, Zn

X = Cl, Br, I

R = alkyl, aryl, vinyl

Eq. 1.1

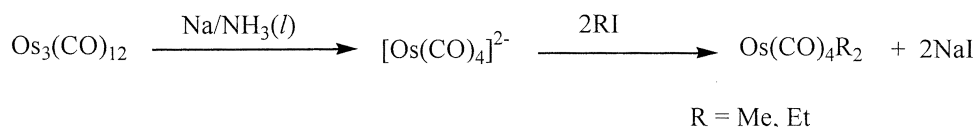
Metallacycloalkanes can be similarly prepared using a single equivalent of  $\alpha,\omega$ -dilithium or di-Grignard reagent. Substitution of the halide atoms by both ends of the alkyl chain occurs. Diversi *et al.* have prepared small-ring rhodacycloalkanes by this method<sup>12, 13</sup> (Equation 1.2).



Eq. 1.2

### 1.2.2 The reaction of anionic or nucleophilic metal complexes with carbon electrophiles.

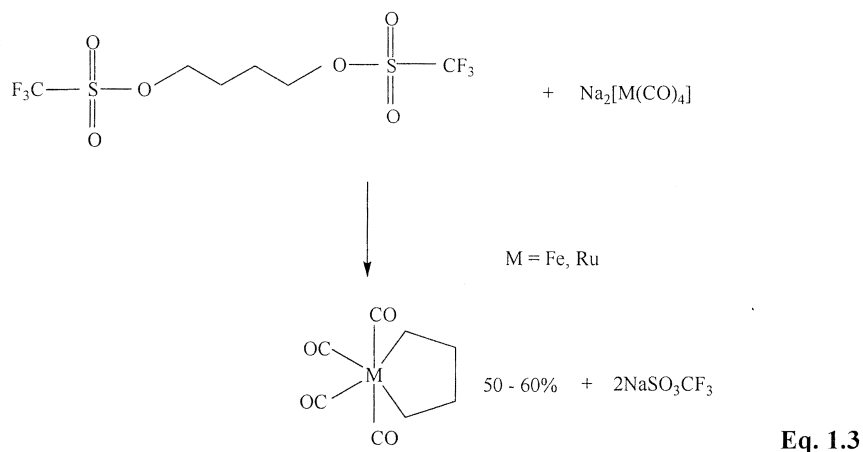
Anions generated from carbonyl metal complexes will react with alkyl halides to yield alkylated products.<sup>11, 14, 15</sup> For example,  $\text{Os}_3(\text{CO})_{12}$  can be alkylated to form mononuclear dialkyl complexes (Scheme 1.2).



Scheme 1.2

Another example is seen in many cobalt complexes: cobalt(III) dialkyls are often synthesized from more nucleophilic cobalt(I) intermediates.<sup>16</sup>

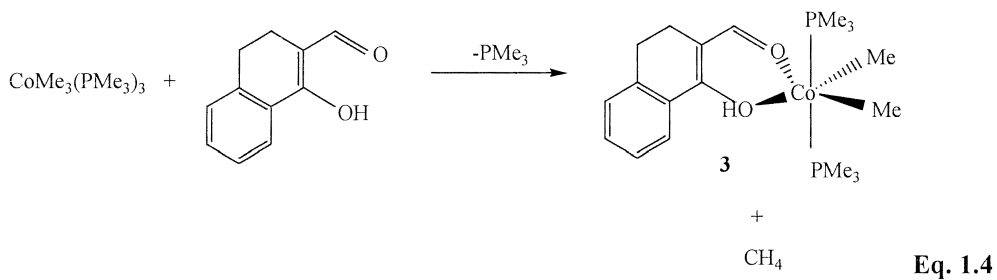
Metallacycles, too, can be synthesized using this method. Iron and ruthenium metallacyclopentanes have been made by the addition of butyl ditriflate to the metal tetracarbonyl dianion <sup>17</sup> (Equation 1.3).



### 1.2.3 Generation of dialkyls from trialkyl complexes

Trialkyl complexes can react to produce an alkane and a dialkyl complex.<sup>18</sup>

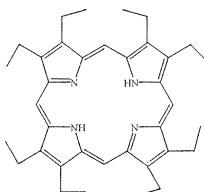
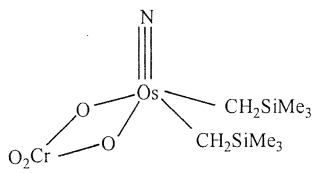
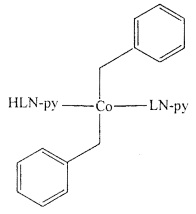
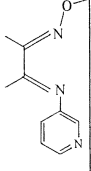
Equation 1.4 shows how a cobalt trimethyl complex is converted to dimethyl complex **3** with the release of methane.

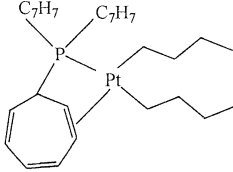
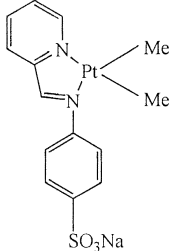


## 1.3 Known, isolated dialkyl complexes of group 8 -10 metals

There are many different types of known dialkyl or diaryl metal complexes. However it is often observed that the type of complex synthesized is common to a certain metal. Table 1.1 summarizes common dialkyl complex forms for the group 8 to 10 metals.

**Table 1.1 Examples of the more common types of dialkyl complexes of group 8 – 10 metals.**

Metal	Common form of dialkyl complex	Examples	Reference
Fe	Fe(bipy) <sub>2</sub> R <sub>2</sub> is common	Fe(bipy) <sub>2</sub> Et <sub>2</sub> , Fe(bipy) <sub>2</sub> ( <i>i</i> -Pr) <sub>2</sub> Fe(dippe)(CH <sub>2</sub> CMe <sub>2</sub> Ph) <sub>2</sub>	19, 20 21
Ru	Some ruthenium porphyrin complexes are known <sup>22–26</sup> as well as more conventional types of complex	[Ru(N)(OH) <sub>2</sub> Me <sub>2</sub> ][PPh <sub>4</sub> ] Ru(OEP)Ph <sub>2</sub> OEP = octaethylporphyrin: 	27 25
Os	Sometimes seen as carbonyl complexes with CO and other ligands. Some examples of Os complexes containing a chromium moiety; these heterobimetallic complexes are good oxidation catalysts <sup>28–30</sup> . Also some osmium porphyrins.	Os(CO) <sub>4</sub> Me <sub>2</sub> , Os(CO) <sub>4</sub> Et <sub>2</sub> 	14, 15 28
Co	Often in the form of macrocyclic complexes that mimic the coenzyme cobalamin (vitamin B12) <sup>16</sup> . Mono- and dialkyl cobalt complexes are used as models for studying the biological properties of this essential enzyme.	Co(acac)(bipy)( <i>n</i> -C <sub>3</sub> H <sub>7</sub> ) <sub>2</sub>  where LN-py = 	31 16

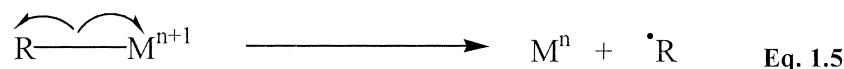
Metal	Common form of dialkyl complex	Examples	Reference
Rh	Usually 18e <sup>-</sup> complexes, often with Cp or Cp* ligands	Cp*RhMePh(CO) Rh(CH <sub>3</sub> )(CH <sub>2</sub> OCH <sub>3</sub> )(PMe <sub>3</sub> ) <sub>3</sub> Br	32 33
Ir	Usually 18e <sup>-</sup> complexes, often with Cp or Cp* ligands	Cp*IrMe(C <sub>6</sub> H <sub>4</sub> X)(DMSO) where X = H, Cl, Br, CF <sub>3</sub> etc.	34
Ni	NiR <sub>2</sub> L <sub>2</sub> complexes are known, where L is nitrogen or phosphorus donor ligand <sup>35</sup> .	Ni(dppe)Et <sub>2</sub> Ni(dippe)(CH <sub>2</sub> SiMe <sub>3</sub> ) <sub>2</sub>	36 37
Pd	PdR <sub>2</sub> L <sub>2</sub>	Pd(dppe)(CH <sub>2</sub> CMe <sub>2</sub> Ph) <sub>2</sub> Pd(PPh <sub>2</sub> Me) <sub>2</sub> Me <sub>2</sub>	38 39
Pt	PtR <sub>2</sub> L <sub>2</sub> and Pt(cod)R <sub>2</sub> (often used as precursor to derivatives with N- or P-donor ligand) <sup>38</sup> .	 <p>Platinum dibutyl complex with a bidentate phosphane ligand</p>	40
		 <p>A water-soluble complex with sulfonate-substituted iminopyridine ligand</p>	41

## 1.4 Reactivities of metal dialkyl species

Like monoalkyl complexes, dialkyl species can react or decompose in numerous ways. Many of these reactions form crucial steps in catalytic cycles. It is therefore vital to have a good understanding of their mechanisms and the factors that promote or impede their occurrence. Some of the more pertinent reactivity pathways are discussed below.

### *1.4.1 Radical reactions*

Metal-carbon bonds can experience homolytic fission to produce radical species (Equation 1.5). This reaction can often be photolytically induced. Some metal centres, namely Fe(III),<sup>20</sup> Ru(III)<sup>42</sup> and Co(III),<sup>43</sup> are more likely than others to undergo radical splitting.

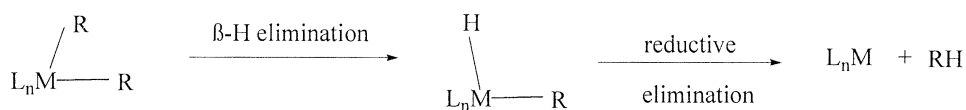


A dialkyl metal complex is able to produce *two* alkyl radical intermediates; these, then, may couple to form a new organic product.<sup>20</sup>

Radical reactions are especially important in cobalt chemistry.<sup>43, 44</sup> Vitamin B<sub>12</sub>, a cobalt-containing corrinoid complex, is an essential coenzyme in human metabolism. Its catalysis of some important reaction pathways in the body is known to be initiated by homolysis of the metal-carbon bond.<sup>43, 44</sup> Although the complex itself is a monoalkyl species, numerous cobalt corrinoid or macrocyclic complexes, both mono- and dialkyl, have been synthesized and used as model compounds for the investigation of the chemistry of this fascinating biological molecule.<sup>43</sup>

### 1.4.2 $\beta$ -hydride elimination

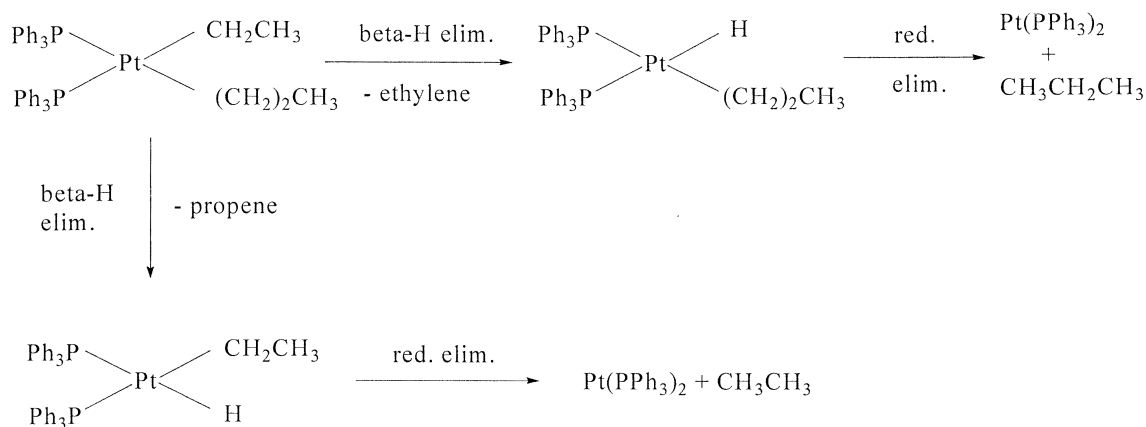
A literature survey reveals that a large proportion of stable, isolable transition metal dialkyl complexes are those in which there are no H-atoms bonded to the carbon at the position *beta* to the metal centre. Dimethyl species are particularly abundant, but complexes containing benzyl (CH<sub>2</sub>Ph) or *t*-butyl (CMe<sub>3</sub>) moieties, for example, are also found. This can be explained by the general belief that  $\beta$ -H-containing metal alkyls undergo facile  **$\beta$ -hydride elimination**, possibly the most frequently observed thermal decomposition pathway for this class of compounds.<sup>45</sup> Scheme 1.3 shows the process for metal dialkyls.



**Scheme 1.3**

In certain cases the decomposition is complete after the  $\beta$ -H step. The stable  $\eta^2$ -coordinated Pt(0) precursor Pt(Et<sub>3</sub>P)<sub>2</sub>( $\eta^2$ -C<sub>2</sub>H<sub>4</sub>), for example, is easily prepared via the  $\beta$ -H elimination of Et<sub>2</sub>Pt(PEt<sub>3</sub>)<sub>2</sub>.<sup>46</sup> Usually however, the newly-formed olefin ligand dissociates so that the final products of the decomposition pathway are metal hydride and alkene. In the case of metal dialkyls, the elimination product, after alkene dissociation, is an alkyl-hydrido complex. This can further decompose by *reductive elimination*, a coupling of the R and H groups, to yield an alkane.

Obviously, the greater the number of accessible  $\beta$ -hydrogens in the complex, the greater the likelihood of  $\beta$ -H elimination occurring. Yamamoto *et al.* illustrated this after carrying out a study on mixed-alkyl platinum(II) complexes<sup>47</sup> (Scheme 1.4).



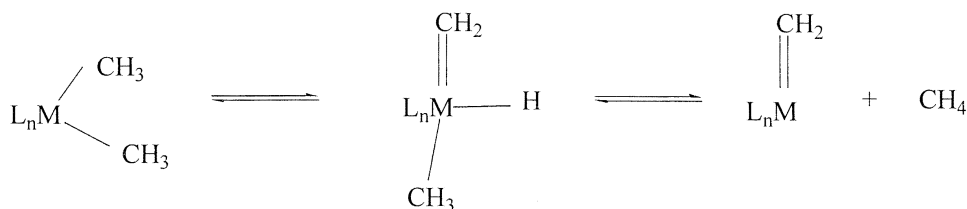
**Scheme 1.4**

The ratios of ethane:ethene and propene:propane generated were found to be 0.64 and 0.60 respectively. This showed that the ethyl group was participating in  $\beta$ -elimination approximately 1.5 times faster than was the propyl group. The results make sense in light of the fact that the ratio of  $\beta$ -hydrogens in an ethyl group versus a propyl group is 3:2.

The higher stability of metallacycloalkanes compared to metal dialkyl complexes can in part be explained by the suppression of  $\beta$ -H elimination in metallacycles.<sup>45, 48</sup> The cyclic chain is often not flexible enough to rotate into the conformation necessary for elimination to occur. Rigid 5- and 6-membered metallacycles appear to be particularly resistant to this type of decomposition.

#### 1.4.3 $\alpha$ -hydride abstraction

Transition metal alkyls or dialkyls with no  $\beta$ -hydrogens, such as dimethyl complexes, may undergo thermal decomposition via other, less common routes. One of these is  $\alpha$ -hydride abstraction, the mechanism of which is outlined in Scheme 1.5.



**Scheme 1.5**

The process is more often observed with early transition metal complexes<sup>49, 50</sup> like tantalum, but there are a few examples for the elements in groups 8-10. Complex **4** (Figure 1.2) is the first example of a square planar iridium methylidene complex,<sup>49</sup> formed by light-induced  $\alpha$ -elimination of the (methyl)(neopentyl) starting complex.

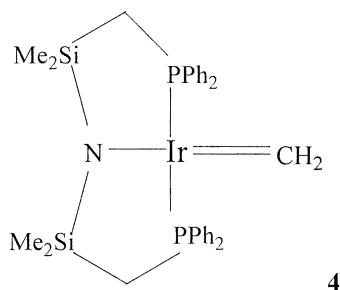
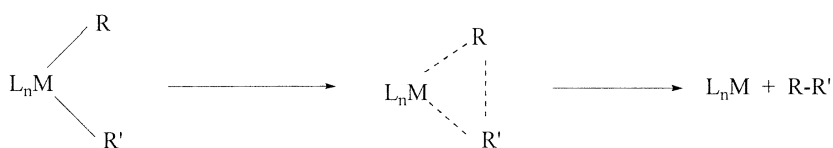


**Figure 1.2** An iridium alkylidene complex

#### 1.4.4 Reductive elimination

Alkyl-halo, alkyl-hydrido, or dihydrido metal complexes can react via reductive elimination to yield the products of coupling of the groups concerned: alkyl halide, alkane or dihydrogen respectively. The ability of dialkyls to react in this way leads to the formation of new carbon-carbon bonds (Scheme 1.6), an aspect of considerable interest and importance in several catalytic reactions, some of which are of industrial importance.<sup>39, 48, 51 - 53</sup>



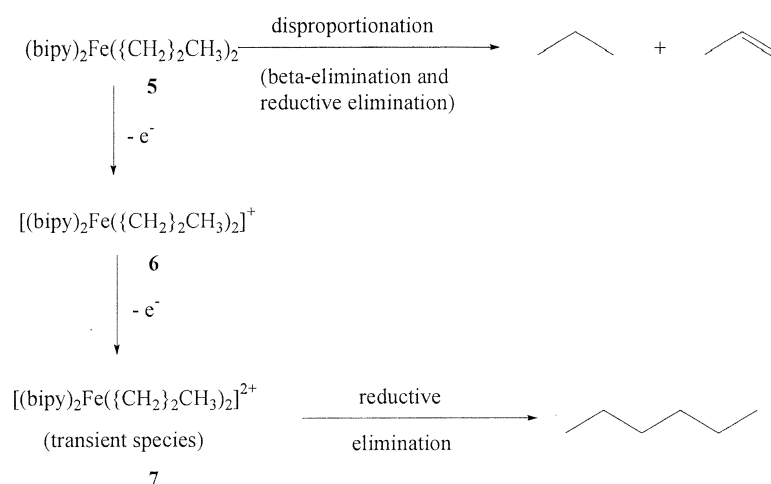
**Scheme 1.6**

As Scheme 1.6 indicates, it is necessary for the two coupling groups to be situated *cis* to each other for coupling to occur.<sup>39, 45, 48, 50, 54</sup> A study by Yamamoto and co-workers showed how palladium dialkyls with different stereochemical configurations would decompose through different pathways.<sup>54</sup> Palladium complex *cis*-PdEt<sub>2</sub>(PR<sub>3</sub>)<sub>2</sub> is able to undergo a facile reductive elimination step to give the ethyl-ethyl coupling product butane. However, the *trans* isomer is unable to do this, and prefers the  $\beta$ -H elimination decomposition route.

Gillie and Stille<sup>39</sup> demonstrated that *trans*-PdMe<sub>2</sub>(PMePh<sub>2</sub>)<sub>2</sub> did not undergo reductive elimination under normal conditions. However, when placed in polar, coordinating solvents (THF, DMF), it was able to isomerize to the *cis* form, and the coupling product ethane could be detected.

The inevitable decrease of a metal centre's oxidation number following reductive elimination makes the process more favourable for metals in higher oxidation states.<sup>39, 45, 52</sup> Thus the use of oxidants can promote the coupling reaction.<sup>45, 55</sup> For instance, the rhodium complex Cp\*RhMe<sub>2</sub>(Me<sub>2</sub>SO) decomposes in acid to give mostly methane with a small amount of ethane (1-5%). The introduction of one-electron oxidizers, such as AgBF<sub>4</sub> or iodine, into the system greatly enhances the percentage of the coupling product ethane.<sup>56</sup>

Kochi *et al* showed a similar trend with a series of neutral [Fe(bipy)<sub>2</sub>R<sub>2</sub>] complexes (R = Et, n-Pr, n-Bu; n = 0, 1, 2) and the electrochemically oxidized products [Fe(bipy)<sub>2</sub>R<sub>2</sub>]<sup>n+</sup> (n = 1, 2).<sup>20</sup> The neutral dialkyliron(II) complexes **5** decomposed slowly via a disproportionation mechanism, whereas the transient dicationic Fe(IV) analogues **7** rapidly broke down to release reductive elimination products (Scheme 1.7).



**Scheme 1.7**

One other observation is that reductive elimination involving alkyl-acyl<sup>45, 53, 57</sup> or alkyl-vinyl<sup>53</sup> coupling occurs much more readily than when alkyl-alkyl coupling is

involved. It was seen that dialkyl-monoacyl  $\text{PtMe}_2(\text{COMe})\text{XL}_2$  complexes that decomposed via this pathway afforded the acyl-alkyl product propanone rather than the dialkyl product ethane.<sup>58</sup> Yamamoto *et al.* demonstrated that cobalt complex **8** (Figure 1.3) is stable and not susceptible to reductive elimination; however, its acyl relative **9** reacts smoothly to yield the diethylketone product.<sup>59</sup>

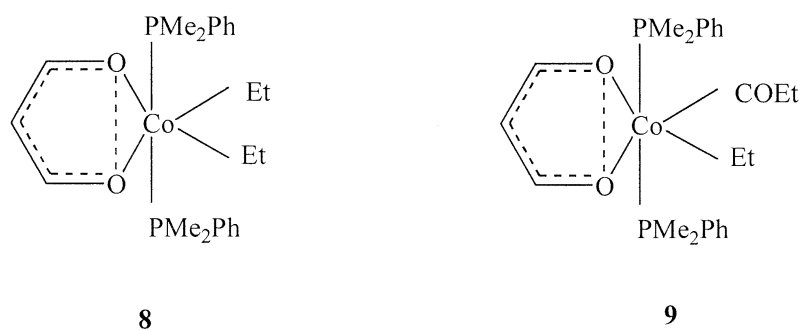
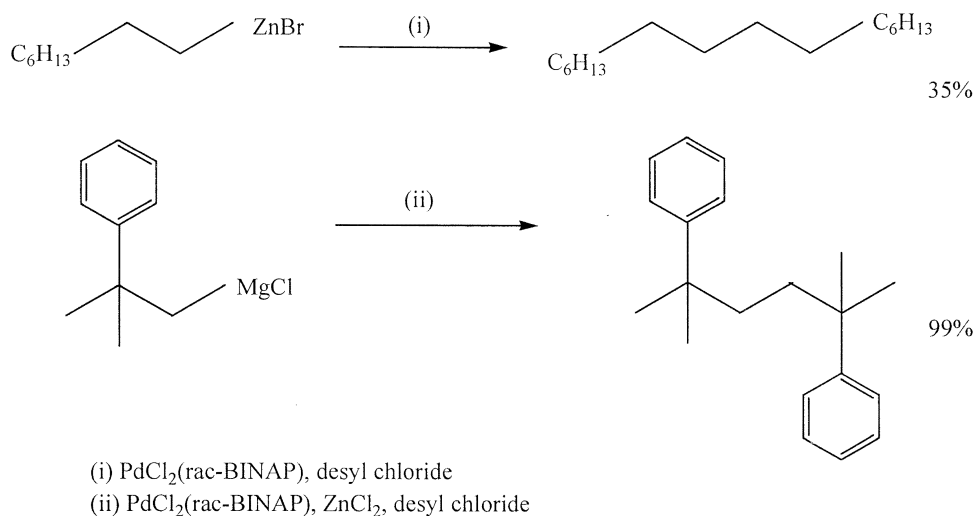


**Figure 1.3** A cobalt dialkyl complex and a cobalt alkyl acyl complex

Although reductive elimination is such a useful process from synthetic and industrial points of view, it is not always favoured by metal dialkyls as a decomposition pathway, and must compete with other, more facile pathways.<sup>52, 53, 60, 61</sup> Lei and Xhang<sup>60</sup> have examined several palladium-catalyzed  $\text{C}_{\text{sp}^3}\text{-C}_{\text{sp}^3}$  coupling reactions in which a key feature is the formation of a Pd-dialkyl intermediate that can undergo reductive elimination to generate the product. While the coupling of carbon chains bearing no  $\beta$ -hydrogens proved to be an efficient and high-yield process, those involving alkyl chains with  $\beta$ -hydrogens proceeded with more difficulty (Scheme 1.8). The results implied that a  $\beta$ -H elimination process was in competition with the desired reductive elimination step.



**Scheme 1.8**

In the case of palladium *cis*-dialkyl complexes, reductive elimination *does* seem to be a favoured decomposition pathway.<sup>38, 39, 62</sup> *cis*- $\text{Pd}(\text{CH}_2\text{SiMe}_3)_2(\text{PMe}_2)_2$ , for example, decomposes to give  $\text{Me}_3\text{SiCH}_2\text{CH}_2\text{SiMe}_3$ .<sup>38</sup> The thermally unstable  $\text{Pd}(\text{Me})(\text{Sty})(\text{PPh}_2\text{Me})_2$  undergoes reductive elimination at low temperatures to give propenylbenzene.<sup>62</sup> Gentle heating of diaryl complex **10** (Figure 1.4) causes its decomposition via reductive elimination to produce 4-methoxy-2',6'-difluorobiphenyl.<sup>63</sup>

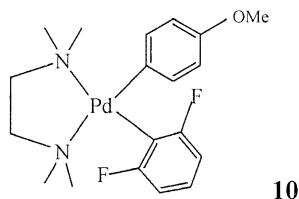


**Figure 1.4** This palladium diaryl complex decomposes via reductive elimination upon gentle heating.

Nickel, too, can sometimes undergo reductive elimination quite readily<sup>64, 65</sup>. The complex  $\text{Ni}(\text{bipy})(\text{CN})(\text{C}_6\text{H}_4\text{CN}-m)$  undergoes rapid elimination of  $\text{CNC}_6\text{H}_4\text{CN}$  in the presence of acetonitrile.<sup>65</sup> Complexes **11** - **14** (Figure 1.5) decompose to give the organic coupling products butane or heptane.<sup>64</sup>

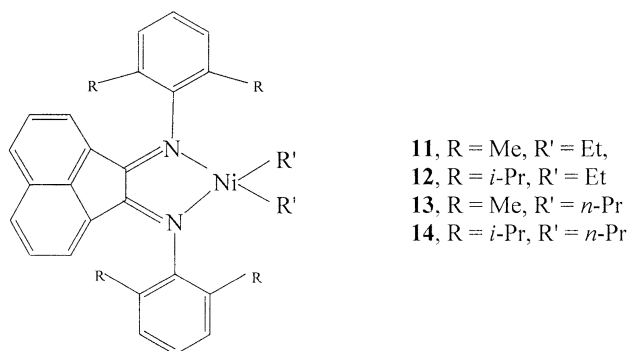
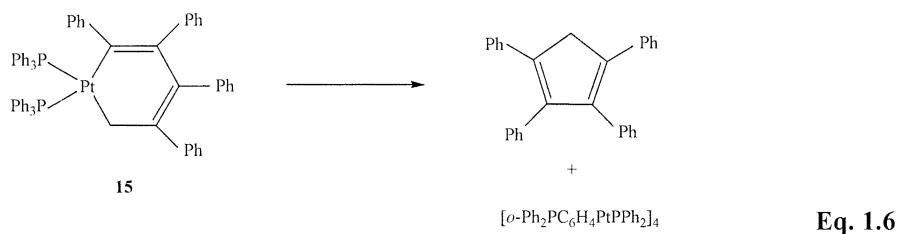


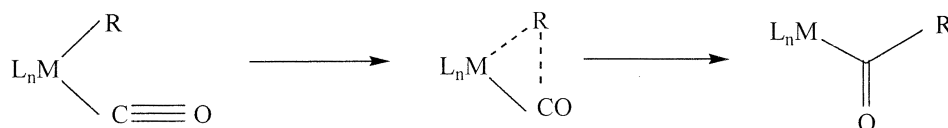
**Figure 1.5** A series of Ni( $\alpha$ -diimine) complexes that undergo facile reductive elimination

Reductive elimination in small-ring metallacycles is not common, because the process would lead to thermodynamically strained organic products like cyclobutane.<sup>3</sup> However, complexes with more than 5 ring members can decompose to give cyclic products. Equation 1.6 shows the formation of tetraphenylcyclopentadiene from the reductive elimination of platinumacycle **15**.<sup>66</sup>



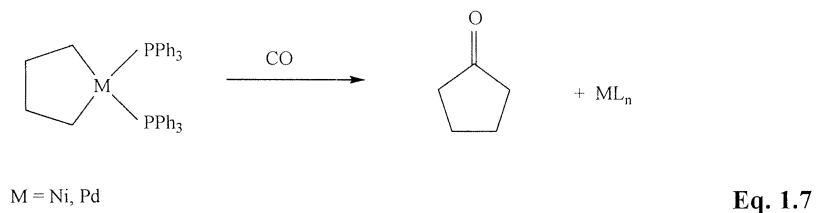
#### 1.4.5 Alkyl migration

Alkyl migration (often referred to as carbonyl insertion) describes the shifting of an alkyl ligand from a metal centre to a CO ligand bonded *cis* to the alkyl on the metal centre (Scheme 1.9).<sup>45</sup>



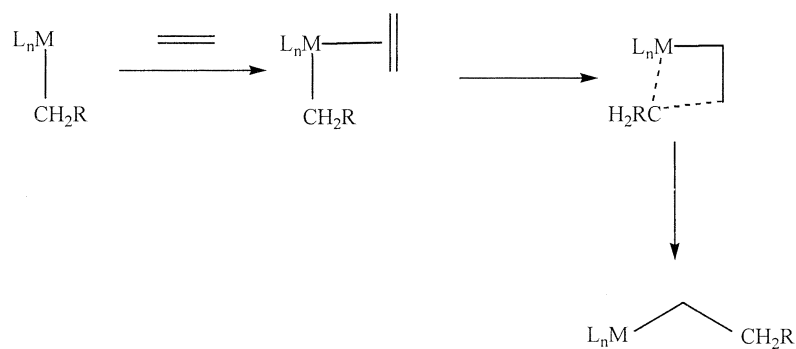
**Scheme 1.9**





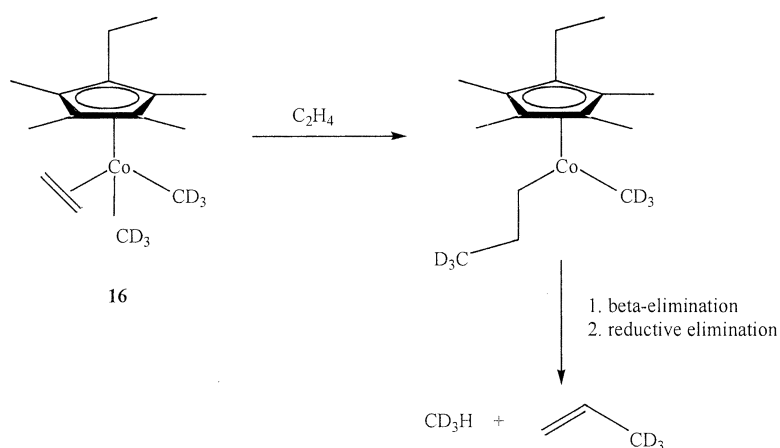
### 1.4.6 Alkene insertion

Olefins can be inserted into metal-carbon  $\sigma$ -bonds to form extended-chain alkyls through the general mechanism outlined in Scheme 1.11.<sup>72</sup>



**Scheme 1.11**

Pardy gained some insight into this process when carrying out a study on a deuterated dimethyl cobalt complex **16**<sup>73</sup> (Scheme 1.12).



**Scheme 1.12**

Extension of the carbon chain by consecutive insertion of multiple alkene molecules into a metal-carbon  $\sigma$ -bond is what makes this process a crucial step in alkene oligomerization and polymerization reactions.

## **1.5 Catalytic applications of metal dialkyl species**

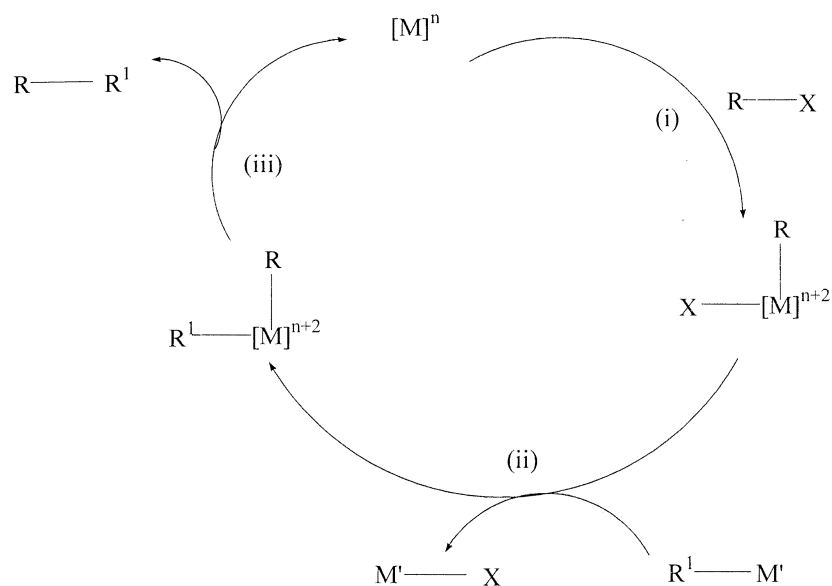
It is by virtue of their unique and rapid reactivity that transition metal dialkyls form such an important class of metal complexes in the field of catalysis. For this reason, their most important catalytic applications are those in which the metal dialkyl or metallacycloalkane is formed as a transient, non-isolable intermediate that breaks down to form the organic product. Section 1.3 was concerned primarily with well-characterized isolated species as models for studying reactivity patterns, but this will not necessarily be the case with much of section 1.4.

The previous segment of this review also dealt with metal alkyls in a very literal sense: methyl, ethyl, propyl and butyl complexes were often discussed. It should be noted that the “alkyl” moiety may in fact comprise acyl, vinyl, allyl or aryl groups, and these are expected to exhibit patterns of reactivity that are similar to those shown by the dialkyls.

### *1.5.1 Carbon-carbon cross-coupling reactions*

Development of methodologies for the creation of new carbon-carbon bonds is a constant challenge in combinatorial chemistry, and is especially relevant in the synthesis of natural products.<sup>74 - 77</sup> Cross-coupling reactions catalyzed by transition metals constitute what is probably the most useful method of achieving these bond formations.<sup>78, 79</sup> The field is dominated by palladium chemistry,<sup>80</sup> but other late transition metals like Ni, Rh, Pt and Ru have also been known to catalyze the reactions.

A simplified mechanism of cross-coupling is depicted in Scheme 1.13. This is the mechanism that occurs in systems of palladium and many of the other metal-catalyzed reactions.



X = halide, triflate  
 R = alkyl, aryl, vinyl etc.  
 M' = MgBr, Li, Zn, Sn etc.

**Scheme 1.13**

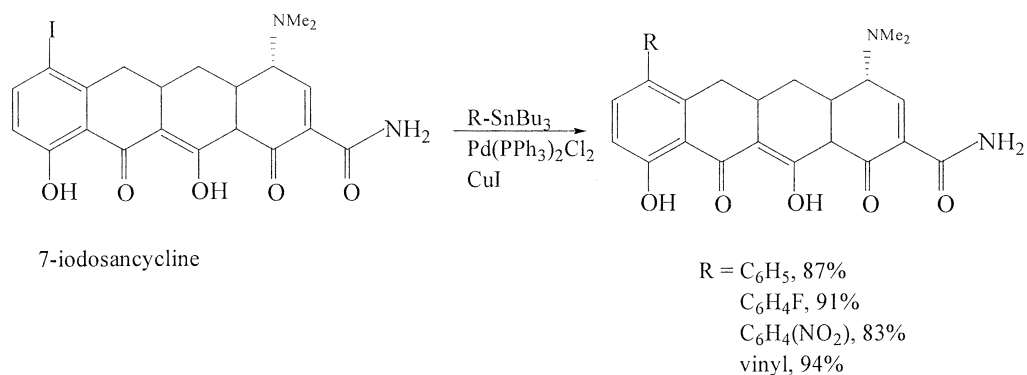
The crucial step in the cycle is the formation of the dialkyl, which undergoes reductive elimination to release the coupled product. It is important to realise that in most cases the dialkyl complexes, though formed, are not isolated due their high reactivities. Therefore, the examples discussed here do not deal directly with the dialkyl complexes, but rather with the catalyst systems that produce them.

In general, the oxidatively added group R would be an aryl, vinyl or allyl group rather than an alkyl. This precludes  $\beta$ -hydride elimination that would occur rapidly with an alkyl group,<sup>81, 82</sup> ending the cross-coupling catalysis. There were few efficient  $C_{sp^3}$  alkyl-alkyl coupling systems known until quite recently,<sup>83</sup> but selected examples of those that do exist will be discussed.

### Palladium systems

Among the more well-known palladium-catalyzed cross-coupling reactions are the Stille,<sup>80, 84, 85</sup> Suzuki<sup>77, 80, 86</sup> and Sonogashira couplings.<sup>80, 87</sup>

These reactions have traditionally involved the addition of *aryl* halides to various organometallic reagents. Stille coupling has been used, for example, in the convenient synthesis of derivatives of the antibiotic tetracycline (Scheme 1.14), in hopes that the new derivatives would show good antibiotic activity against multi-drug-resistant bacteria.<sup>85</sup>

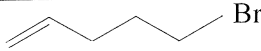
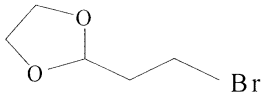
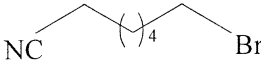


**Scheme 1.14**

Naturally, it would be useful to be able to apply these methods using alkyl halides *with*  $\beta$ -hydrogens. Pioneering research done by Fu and others has proved worthwhile in achieving this end. Use of appropriate ligands is essential. Certain ligands (usually the bulky, strongly-donating molecules) can prevent either the formation of a coordinatively unsaturated metal-alkyl intermediate, or the co-planar geometry required before  $\beta$ -H elimination can take place.<sup>83</sup>

Fu and Menzel discovered that a Pd/P(*t*-Bu)<sub>2</sub>Me catalyst system, unlike most other palladium systems, was able to effect the cross-coupling of C<sub>sp</sub><sup>3</sup> alkyl halides with various alkenyltin reagents.<sup>84</sup> Table 1.2 gives examples of some of the yields that were obtained for various reagents.

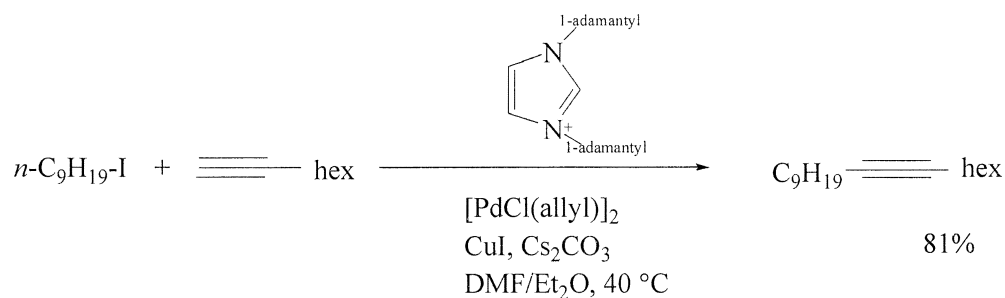
**Table 1.2 Cross-coupling product yields for reaction catalyzed by  $[(\pi\text{-allyl})\text{PdCl}_2]$  in the presence of  $\text{P}(t\text{-Bu})\text{Me}_2$  ligand**

Alkyl halide (R-Br)	Tin reagent	Yield (%)
	$\text{Bu}_3\text{Sn}-\text{CH}=\text{CH}-\text{C}_7\text{H}_{15}$	92
	$\text{Bu}_3\text{Sn}-\text{CH}=\text{CH}-\text{C}_3\text{H}_7-\text{OTHP}$	71
	$\text{Sn}-\text{CH}=\text{CH}-\text{C}_7\text{H}_{15}$	59

THP = tetrahydropyranyl

As late as 2001, Fu *et al.* reported the first instance of alkyl-alkyl Suzuki coupling using  $\text{Pd}(\text{OAc})_2/\text{PCy}_3$  (where Cy = cyclohexyl) in the presence of  $\text{K}_3\text{PO}_4 \cdot \text{H}_2\text{O}$ .<sup>88</sup> The catalyst combination was found to bring about effective coupling of alkyl- and vinylboranes with alkyl bromides containing  $\beta$ -hydrogens.

In 2003, the same researchers reported the use of sterically large *N*-heterocyclic carbene ligands in Pd-catalyzed Sonogashira couplings of primary alkyl bromides and iodides (Scheme 1.15 for example).<sup>87</sup> The catalyst system was able to tolerate a range of functionalities on the alkyl halide, including olefins, esters, alcohols and others.



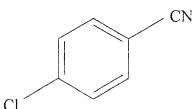
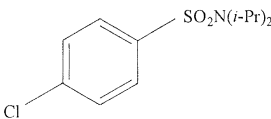
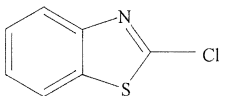
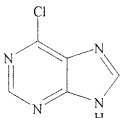
**Scheme 1.15**

## Other transition metal coupling catalysts

Some of the other later transition metals can also catalyze C-C cross-coupling of both  $C_{sp^2}$  and  $C_{sp^3}$  centres. There are numerous instances of nickel complexes that effect this type of reaction.<sup>81, 83</sup> Kambe *et al.* discovered that  $NiCl_2$ /butadiene was a proficient catalyst for the coupling of  $C_{sp^3}$  halides with alkyl or aryl Grignard reagents.<sup>81</sup> Good to excellent yields of alkyl-alkyl or alkyl-aryl product were obtained under mild conditions and with reasonably low catalyst loading.

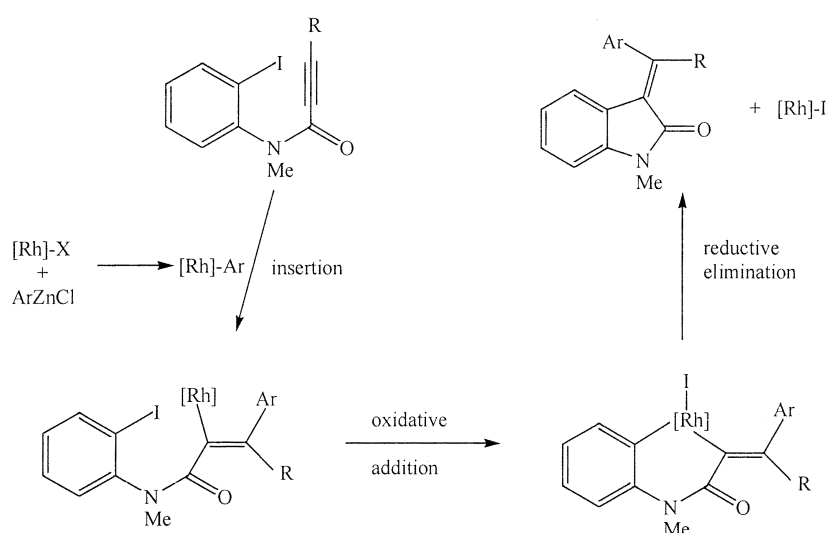
The use of iron cross-coupling catalysts as alternatives to Pd or Ni catalysts is attractive as iron complexes are inexpensive, readily available and environmentally friendly.<sup>78, 82</sup> The simple iron complex  $Fe(acac)_3$  is able to catalyze coupling of a wide range of aromatic and heteroaromatic halides with primary and secondary alkyl Grignard reagents in the presence of *N*-methylpyrrolidone, or NMP (Table 1.3 for example).<sup>78</sup>

**Table 1.3 Yields of products of cross-coupling reactions catalyzed by  $Fe(acac)_3$  (5 mol%) in THF/NMP**

Ar-X	R-MgBr	Yield (%)
	$n-C_{14}H_{29}-MgBr$	91
	$n-C_{14}H_{29}-MgBr$	94
	$n-C_{14}H_{29}-MgBr$	68
	$n-C_{14}H_{29}-MgBr$	85

A heterogenous, ligand-free ruthenium system was shown to catalyze a Suzuki-Miyaura-type coupling of aryl iodides and arylboron reagents.<sup>89</sup> Various diaryl products were obtained in high yields of, sometimes, close to 100%.

The development of rhodium cross-coupling catalysts has not been as extensive as for some of the other late transition metals. However,  $[\text{RhCl}(\text{C}_2\text{H}_4)_2]_2$  in the presence of phosphine ligand can bring about multicomponent coupling reactions<sup>90</sup> as depicted in Scheme 1.16.



**Scheme 1.16**

These are just a small selection of the many examples of useful carbon-carbon cross-coupling reactions catalyzed by the later transition metals. It is obvious, then, that the metals in groups 8 to 10 play a crucial role in organic synthesis, and especially in the preparation of biologically active molecules. The dialkyl complexes generated in the catalytic cycle are essential to the formation of the final products.

### 1.5.2 Cyclization and cyclooligomerization reactions

One challenge in organic synthesis is the formation of unsaturated cyclic moieties that are present in the backbones of many natural products.<sup>91, 92</sup> Complexes of late transition metals, and cobalt in particular,<sup>93</sup> are useful in this regard as they mediate the oligomerization of acetylene derivatives to form cyclic compounds.<sup>92</sup> The

reactions usually involve the formation of an unsaturated metallacyclic intermediate that can undergo reductive elimination to yield the product or undergo additional insertions to form larger metallacycles.<sup>93</sup>

Iridium and rhodium-containing metallacyclopentadiene complexes **17** and **18** (Figure 1.6) were shown to be isolable intermediates in the cyclotrimerization of substituted acetylenes.<sup>93, 94</sup>

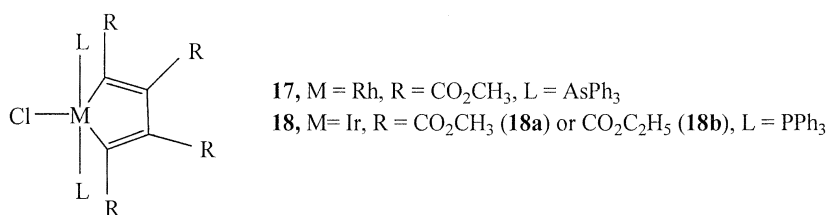


**Figure 1.6 Rhodium- and iridium-containing metallacyclopentadienes**

There are also numerous examples of dialkyl complexes that are themselves catalysts, not merely intermediates, in cyclooligomerization reactions. The dialkylcobalt complex Co(mes)<sub>2</sub>, where mes = mesityl, was found to catalyze the cyclic trimerization of 2-butyne to give hexamethylbenzene.<sup>95, 96</sup>

### 1.5.3 Other examples of applications of dialkyl complexes

- (Diolefin)platinum dialkyl complexes such as Pt(COD)(CH<sub>2</sub>C{CH<sub>3</sub>}<sub>2</sub>{CH<sub>2</sub>}<sub>n</sub>CD<sub>3</sub>)<sub>2</sub> (n = 1-3) catalyze the heterogeneous hydrogenation of olefins over a platinum metal support.<sup>97, 98</sup>
- The nickel complex Ni(bipy)Et<sub>2</sub>, as well as some other late transition metal dialkyl catalysts, facilitate the polymerization of acrylonitrile,<sup>99</sup> and both Ni(bipy)Et<sub>2</sub> and Fe(bipy)<sub>2</sub>Et<sub>2</sub> catalyze the cyclooligomerization of butadiene.<sup>100</sup>
- Metal dialkyl complexes also play a role in ethylene oligomerization and polymerization. The activation of nickel dialkyl complexes, for example, can lead to the formation of the active polymerization catalyst.<sup>64</sup> Certain nickel and

palladium complexes are useful precursors for other polymerization catalysts.<sup>101</sup> Recently, some iron dialkyl complexes,  $\text{Fe}_2\text{R}_2\text{py}_2$ , ( $\text{R} = \text{CH}_2\text{SiMe}_3, \text{CH}_2\text{Ph}, \text{CH}_2(\text{CMe}_2\text{Ph})$ ) were prepared and found to be useful as models for the investigation of iron-catalyzed ethylene oligomerization.<sup>102</sup>

- Palladium complexes **19** and **20**, of composition  $\text{PdR}_2(\text{PR}_3)_2$  (Figure 1.7), can catalyze the amination of olefins.<sup>103</sup>

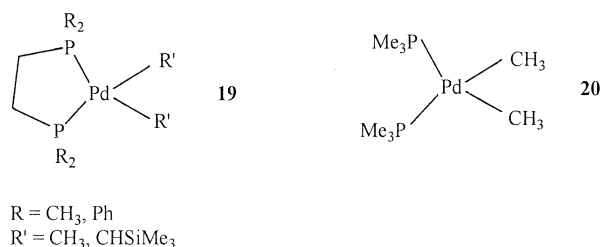


**Figure 1.7** These palladium complexes catalyze the addition of aniline to acrylonitrile.

- Dimethylcobalt complexes act as methylation agents for germanium, tin and lead compounds. They therefore play an important role in environmental chemistry.<sup>18, 104</sup>

It is clear that, whether as catalysts, catalytic intermediates, model complexes or other, the dialkyl complexes of the group 8 – 10 transition metals have application in many diverse areas of chemistry.

## 1.6 Summary of Chapter 1

Metal dialkyl complexes and metallacycloalkanes show many different and interesting reactivity patterns, such as  $\beta$ -H elimination, reductive elimination, alkyl migration, and others. It is due to this reactivity that such molecules are present as catalytic intermediates in many organic transformations. The transient species are often difficult or impossible to isolate. However, there are numerous examples of stable, known dialkyl complexes, and these have been discussed in the present review.

These isolable complexes provide useful models for the transient reaction intermediates, and the study of their reactivity patterns can help elucidate the exact mechanism of metal-catalyzed organic reactions.

## **1.7 Aims and objectives of this project**

### *1.7.1 The focus of this project*

In the above review metallacycloalkanes were discussed as a special class of dialkyl complex. These types of complexes are known to be intermediates in many important industrial catalytic reactions,<sup>5</sup> such as ethylene trimerization<sup>105, 106</sup> and olefin metathesis reactions.<sup>74 - 76</sup> These reactions produce, among other things, fuels and biologically active molecules, and are therefore highly significant in both industry and academia.

In order to optimize the efficiency of the reactions, it is necessary to have a very good understanding of the chemistry involved and of the catalytic cycle, during which non-isolable species may be formed. The use of model compounds is one way in which a catalytic step may be mimicked, allowing one to study indirectly the intermediates involved.

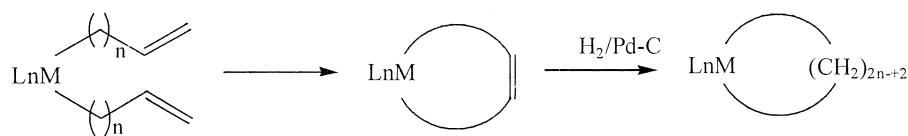
Therefore, the preparation of stable metallacycloalkanes, and the examination of their properties and reactivities, would be of inherent interest and would also provide a means of studying reactions in which metallacyclic intermediates are involved.

The aim of this project then, was to synthesize rhodium-containing metallacycloalkanes. There are few instances of rhodacycloalkanes in the literature and we hoped to expand on that particular area of chemistry.

### 1.7.2 Approaches to the synthesis of rhodacycloalkanes

The aim was to synthesize the rhodium complexes by two different methods:

1. The reaction of di-Grignard reagents with rhodium dihalides, according to Diversi's method.<sup>12, 13</sup>
2. A new route, involving the preparation of bis-alkenyl complexes, is shown in Scheme 1.17



**Scheme 1.17**

This method had been recently proven to be a highly successful one for the preparation of platinacycloalkanes.<sup>107</sup> It was hoped that similar success would be achieved in the case of rhodium.

Both of the aforementioned synthetic routes will be discussed in greater detail in the introductions to the relevant chapters in this thesis.

## 1.7 References

1. A. Yamamoto, *J. Organomet. Chem.*, 1995, **500**, 337.
2. F. Kawataka, Y. Kayaki, I. Shimizu and A. Yamamoto, *Organometallics*, 1994, **13**, 3517.
3. J. Cámpora, P. Palma and E. Carmona, *Coord. Chem. Rev.*, 1999, **193-195**, 207.
4. J. Cámpora, M. del Mar Conejo, K. Mereiter, P. Palma, C. Pérez, M. L. Reyes and C. Ruiz, *J. Organomet. Chem.*, 2003, **683**, 220.
5. B. Blom, H. Clayton, M. Kilkenny and J. R. Moss, *Adv. Organomet. Chem.*, 2006, **54**, 149.
6. (a) S. Komiya, S. Ozaki, I. Endo, K. Inoue, N. Kasuga and Y. Ishikazi, *J. Organomet. Chem.*, 1992, **433**, 337. (b) P. A. Shapley, J. J. Schwab and S. R. Wilson, *J. Coord. Chem.*, 1994, **32**, 213. (c) : S. H. L. Thoonen, M. Lutz, A. L. Spek, B-J. Deelman and G. van Koten, *Organometallics*, 2003, **22**, 1156.
7. I. J. Blackman, X. Jin and P. Legzdins, *Organometallics*, 2005, **24**, 4088.
8. S. Fokken, F. Reichwald, T. P. Spaniol and J. Okuda, *J. Organomet. Chem.*, 2002, **663**, 158.
9. S. Groysman, I. Goldberg, M. Kol, E. Genizi and Z. Goldschmidt, *Inorg. Chim. Acta*, 2003, **345**, 137.
10. B. Hessen, *J. Mol. Catal. A*, 2004, **213**, 129.
11. I. Haiduc and J. J. Zuckerman, *Basic Organometallic Chemistry*, Walter de Gruyter & Co., Berlin, 1985.

25. M. Ke, C. Sishta, B. R. James, D. Dolphin, J. W. Sparapany and J. A. Ibers, *Inorg. Chem.*, 1991, **30**, 4766.
26. J. P. Collman, L. McElwee-White, P. J. Brothers and E. Rose, *J. Am. Chem. Soc.*, 1986, **108**, 1332.
27. J. L. Kuiper and P. A. Shapley, *J. Organomet. Chem.*, 2007, in press.
28. P. A. Shapley, N. Zhang, J. L. Allen, D. H. Pool and H-C. Liang, *J. Am. Chem. Soc.*, 2000, **122**, 1079.
29. N. Zhang and P. A. Shapley, *Inorg. Chem.*, 1988, **27**, 976.
30. N. Zhang, C. M. Mann and P. A. Shapley, *J. Am. Chem. Soc.*, 1988, **110**, 6591.
31. S. Komiya, M. Bundo, T. Yamamoto and A. Yamamoto, *J. Organomet. Chem.*, 1979, **174**, 343.
32. M. Gómez, J. M. Kisenyi, G. J. Sunley and P. M. Maitlis, *J. Organomet. Chem.*, 1985, **296**, 197.
33. D. L. Thorn, *Organometallics*, 1986, **5**, 1897.
34. M. Gómez, P. I. W. Yarrow, D. J. Robinson and P. M. Maitlis, *J. Organomet. Chem.*, 1985, **279**, 115.
35. W-P. Leung, H-K. Lee, Z-Y. Zhou and T. C. W. Mack, *J. Organomet. Chem.*, 1998, **564**, 193.
36. Y-J. Kim, K. Osakada and A. Yamamoto, *Bull. Chem. Soc. Jpn*, 1989, **62**, 964.
37. J. Cámpora, J. A. López, C. Maya, P. Palma, E. Carmona and P. Valerga, *J. Organomet. Chem.*, 2002, **643-644**, 331.

38. Y. Pan and G. B. Young, *J. Organomet. Chem.*, 1999, **577**, 257.
39. A. Gille and J. K. Stille. *J. Am. Chem. Soc.*, 1980, **102**, 4933.
40. M. Heberhold, T. Schmalz, W. Milius and B. Wrackmeyer, *Inorg. Chim. Acta*, 2003, **352**, 51.
41. G. J. P. Britovsek, G. Y. Y. Woo and N. Assavathorn, *J. Organomet. Chem.*, 2003, **679**, 110.
42. M. J. Ingleson, M. Pink, J. C. Huffman, H. Fan and K. G. Caulton, *Organometallics*, 2006, **25**, 1112.
43. H. Shimakoshi, A. Goto, Y. Tachi, Y. Naruta and Y. Hisaeda, *Tetrahedron Lett.*, 2001, **42**, 1949.
44. Hua Zhu, Z. Hua Liu, H. Yan, J. Liu and H. Chen, *J. Inorg. Biochem.*, 1997, **65**, 45.
45. R. H. Crabtree, *The organometallic chemistry of the Transition metals*, 3<sup>rd</sup> ed. John Wiley and Sons, Inc., New York, 2001.
46. R. G. Nuzzo, T. J. McCarthy and G. M. Whitesides, *Inorg. Chem.*, 1981, **20**, 1312.
47. S. Komiya, Y. Morimoto, A. Yamamoto and T. Yamamoto, *Organometallics*, 1982, **1**, 1528.
48. A. Yamamoto, *Organotransition metal chemistry: Fundamental Concepts Applications*, John Wiley and Sons Inc., New York, 1986.
49. M. D. Fryzuk, P. A. MacNeil and S. J. Rettig, *J. Am. Chem. Soc.*, 1985, **107**, 6708.

50. M. Bochmann, *Organometallics 1: Complexes with transition metal-carbon  $\sigma$ -bonds*, Oxford University Press, New York, 1994.
51. M. P. Brown, R. J. Puddephatt and C. E. E. Upton, *J. Chem. Soc., Dalton Trans.*, 1974, 2457.
52. B. Åkermark and A. Ljungqvist, *J. Organomet. Chem.*, 1979, **182**, 47.
53. E. R. Evitt and R. G. Bergman, *J. Am. Chem. Soc.*, 1980, **102**, 7003.
54. F. Ozawa and A. Yamamoto, *Organometallics*, 1982, **1**, 1481.
55. J. von Slageren, A. L. Vermeer, D. J. Stufkens, M. Lutz and A. L. Spek. *J. Organomet. Chem.*, 2001, **626**, 118.
56. M. Gómez, P. I. W. Yarrow, A. Vásquez de Miguel and P. M. Maitlis, *J. Organomet. Chem.*, 1983, **259**, 237.
57. D. R. Saunders and R. J. Mawby, *J. Chem. Soc., Dalton Trans.*, 1984, 2133.
58. J. D. Ruddick and B. L. Shaw, *J. Chem. Soc. (A)*, 1969, 2969.
59. T. Ikariya and A. Yamamoto, *J. Organomet. Chem.*, 1976, **116**, 239.
60. A. Lei and X. Zhang, *Org. Lett.*, 2002, **4**, 2285.
61. L. S. Hegedus, P. M. Kendall, S. M. Lo and J. R. Sheats, *J. Am. Chem. Soc.*, 1975, **97**, 5448.
62. M. K. Loar and J. K. Stille, *J. Am. Chem. Soc.*, 1981, **103**, 4174.
63. K. Osakada, H. Onodera and Y. Nishihara, *Organometallics*, 2005, **24**, 190.

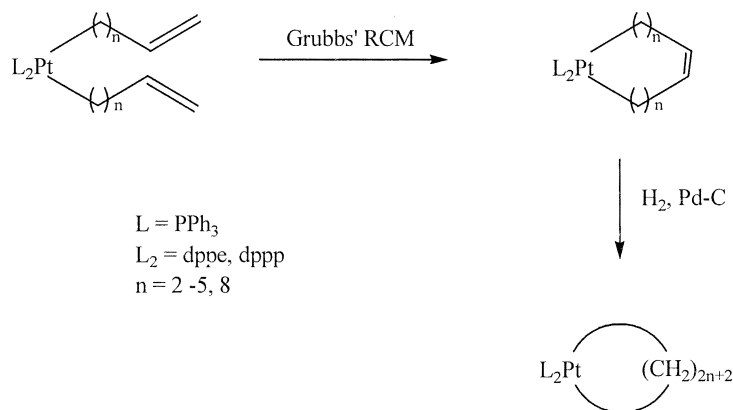
64. M. D. Leatherman, S. A. Svejda, L. K. Johnson and M. Brookhart, *J. Am. Chem. Soc.*, 2003, **125**, 3068.
65. T. Yamamoto, I. Yamaguchi and M. Abla, *J. Organomet. Chem.*, 2003, **671**, 179.
66. N. A. Grabowski, R. P. Hughes, B. S. Haynes and A. L. Rheingold, *J. Chem. Soc., Chem. Comm.*, 1986, 1694.
67. F. Calderazzo, S. Falaschi, F. Marchetti and G. Pampaloni, *J. Organomet. Chem.*, 2002, **662**, 137.
68. X. Li, H. Sun, A. Brand and H-F. Klein, *Inorg. Chim. Acta*, 2005, **358**, 3329.
69. E. G. Lindquist, K. Folting, J. C. Huffman and K. G. Caulton, *Organometallics*, 1990, **9**, 2254.
70. H. O. Frölich, R. Wyrwa, H. Görls and U. Pieper, *J. Organomet. Chem.*, 1994, **471**, 23.
71. K. R. Pörscke, *Angew. Chem. Int. Ed. Engl.*, 1987, **26**, 1288.
72. J. P. Collman, L. S. Hegedus, J. R. Norton and R. G. Finke, *Principles and applications of organotransition metal chemistry*, University Science Books, Mill Valley, 1987.
73. R. B. A. Pardy, *J. Organomet. Chem.*, 1981, **216**, C29.
74. W. H. Meyer, A. E. McConnell, G. S. Forman, C. L. Dwyer, M. M. Kirk, E. L. Ngidi, A. Blignaut, D. Saku and A. M. Z. Slawin, *Inorg. Chim. Acta*, 2006, **359**, 2910.
75. C. Adlhart and P. Chen, *J. Am. Chem. Soc.*, 2004, **126**, 3496.
76. R. C. Buijsman, E. Van Vuuren and J. G. Sterrenburg, *Org. Lett.*, 2001, **3**, 3785.

77. O. Navarro, R. A. Kelly, III, S. P. Nolan, *J. Am. Chem. Soc.*, 2003, **125**, 16194.
78. A. Fürstner, A. Leitner, M. Méndez and H. Krause, *J. Am. Chem. Soc.*, 2002, **124**, 13856.
79. H. Yasui, K. Mizutani, H. Yorimitsu and K. Oshima, *Tetrahedron*, 2006, **62**, 1410.
80. J. Clayden, N. Greeves, S. Warren and P. Wothers, *Organic Chemistry*, Oxford University Press, Oxford, 2001.
81. J. Terao, H. Watanabe, A. Ikumi, H. Kuniyasu and N. Kambe, *J. Am. Chem. Soc.*, 2002, **124**, 4222.
82. M. Nakamura, K. Matsuo, S. Ito and E. Nakamura, *J. Am. Chem. Soc.*, 2004, **126**, 3686.
83. G. D. Jones, J. L. Martin, C. McFarland, O. R. Allen, R. E. Hall, A. D. Haley, R. J. Brandon, T. Konovalova, P. J. Desrochers, P. Pulay and D. A. Vivic, *J. Am. Chem. Soc.*, 2006, **128**, 13175.
84. K. Menzel and G. C. Fu, *J. Am. Chem. Soc.*, 2003, **125**, 3718.
85. D. J. Koza, *Org. Lett.*, 2000, **2**, 815.
86. G. Altenhoff, R. Goddard, C. W. Lehmann and F. Glorius, *J. Am. Chem. Soc.*, 2004, **126**, 15195.
87. M. Eckhardt and G. C. Fu, *J. Am. Chem. Soc.*, 2003, **125**, 13642.
88. M. R. Netherton, C. Dai, K. Neuschütz and G. C. Fu, *J. Am. Chem. Soc.*, 2001, **123**, 10099.

89. Y. Na, S. Park, S. Bong Han, H. Han, S. Ko and S. Chang, *J. Am. Chem. Soc.*, 2004, **126**, 250.
90. R. Shintani, T. Yamagami and T. Hayashi, *Org. Lett.*, 2006, **8**, 4799.
91. C. Ho Oh, H. Rhyun Sung, S. Hyung Gung and Y. Mook Lim, *Tetrahedron Lett.*, 2001, **42**, 5493.
92. S. Saito, M. Masuda and S. Komagawa, *J. Am. Chem. Soc.*, 2004, **126**, 10540.
93. F. Mao, D. M. Schut and D. R. Tyler, *Organometallics*, 1996, **15**, 4770.
94. J. P. Collman, J. W. Kang, W. F. Little and M. F. Sullivan, *Inorg. Chem.*, 1968, **7**, 1298.
95. M. Tsutshui and H. Zeiss, *J. Am. Chem. Soc.*, 1981, **83**, 825.
96. O. Buriez, I. Kazmierski and J. Périchon, *J. Electroanalyt. Chem.*, 2002, **537**, 119.
97. T. M. Miller and G. M. Whitesides, *J. Am. Chem. Soc.*, 1988, **110**, 3164.
98. T. R. Lee and G. M. Whitesides, *Acc. Chem. Res.*, 1992, **25**, 266.
99. A. Yamamoto and S. Ikeda, *J. Am. Chem. Soc.*, 1967, **89**, 5989.
100. A. Yamamoto, K. Morifuji, S. Ikeda, T. Saito, Y. Uchida and A. Misono, *J. Am. Chem. Soc.*, 1965, **87**, 4652.
101. J. Cámpora, M. del Mar Conejo, K. Mereiter, P. Palma, C. Pérez, M. L. Reyes and C. Ruiz, *J. Organomet. Chem.*, 2003, **683**, 220.
102. J. Cámpora, A. M. Naz, P. Palma and E. Álvarez, *Organometallics*, 2005, **24**, 4878.

103. A. L. Seligson and W. C. Trogler, *Organometallics*, 1993, **12**, 744.
104. S. Rapsomanikis, J. J. Ciejka and J. H. Weber, *Inorg. Chim. Acta*, 1984, **89**, 179.
105. Y. Yang, H. Kim, J. Lee, H. Paik and H. G. Jang, *Applied Catalysis A*, 2000, **193**, 1929.
106. G. P. Chiusoli, *J. Mol. Catal.*, 1987, **41**, 75.
107. A. Sivaramakrishna, H. Su and J. R. Moss, *Angew. Chem. Int. Ed.*, 2007, in press.





**Scheme 2.1**

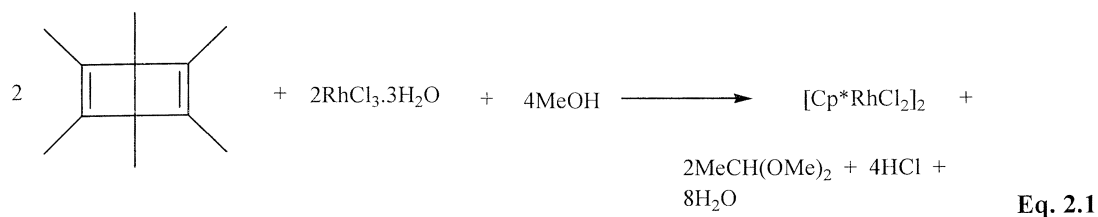
We have attempted to synthesize a series of rhodium bis-alkenyl complexes by the reaction of rhodium precursors with alkenyl-Grignard reagents. As with the platinum bis-alkenyl complexes, the rhodium complexes would be potential precursors in a new route to the preparation of rhodacycloalkanes.

## 2.2 Rhodium starting materials

The complexes  $[Cp^*RhCl_2]_2$  (**21**),  $Cp^*RhCl_2(PPh_3)$  (**22**),  $Cp^*RhCl_2(PMePh_2)$  (**23**),  $Cp^*RhCl_2(PMe_2Ph)$  (**24**),  $[Cp^*RhI_2]_2$  (**25**), and  $Cp^*RhI_2(PPh_3)$  (**26**) and  $[Cp^*RhBr_2]_2$  (**27**) were all synthesized according to literature methods.<sup>4-6</sup> Because these were all known compounds, they were characterized only by melting point,  $^1H$  NMR and, where applicable,  $^{31}P$  NMR spectroscopy.

### *2.2.1 Synthesis of rhodium chloride complexes*

The dimer  $[Cp^*RhCl_2]_2$  (**21**) is an air-stable deep red solid. It was synthesized by two different methods. The first was a simple addition of pentamethylcyclopentadiene ( $Cp^*H$ ) to an ethanol suspension of  $RhCl_3 \cdot 3H_2O$ . The reaction was refluxed with stirring for 2 days, and gave yields of over 90%. The second method was developed by Maitlis *et al.* in 1969,<sup>4</sup> and involves the addition of hexamethyldewarbenzene to the  $RhCl_3 \cdot 3H_2O$  methanol solution. The overall reaction is given by Equation 2.1.



Although the reaction mechanism appears quite complicated, a considerably shorter reaction time (15 hours) is required to obtain yields comparable to yields from the first method (between 85 and 95%). This makes the second method overall a rather more convenient one, even though it would appear that the first is the more obvious procedure for synthesizing complex **21**.

In all cases the product **21** was pure enough to be used without purification by recrystallization. We have found that the complex decomposes without melting above 310°C. This is consistent with the literature report, which states that the complex melts at a temperature above 230°C.<sup>4</sup>

Complex **22**,  $\text{Cp}^*\text{RhCl}_2(\text{PPh}_3)$ , was also prepared using two different methods, both of which gave high yields of the stable orange-red solid. In the first case, a quantity of **21** was refluxed with an excess of triphenylphosphine in methanol solvent for 5 hours. One of the advantages of this technique was that it did not require strict Schlenk reaction conditions and could, in fact, be carried out in air. At the end of the reaction the methanol-insoluble product was easily isolated by filtration and was washed thoroughly to remove any trace amount of  $\text{PPh}_3$  present.

In the second case, the reaction was carried out under nitrogen using strict Schlenk conditions according to the literature procedure. A 1:1 molar ratio of the rhodium dimer to phosphine was stirred at room temperature in dichloromethane during a 30-minute-long reaction. Isolation of the final product called for *in vacuo* removal of some DCM, addition of hexane, and cooling to encourage crystallization. Total removal of solvent immediately after reaction completion was attempted, but the  $\text{Cp}^*\text{RhCl}_2(\text{PPh}_3)$  was obtained as a wet, sticky mass that was difficult to work with. The time-consuming recrystallization step was, therefore, a necessary one.

$\text{Cp}^*\text{RhCl}_2(\text{PMePh}_2)$  and  $\text{Cp}^*\text{RhCl}_2(\text{PMe}_2\text{Ph})$ , **23** and **24**, were synthesized by the dichloromethane method as the phosphine starting materials for these complexes are air- and moisture-sensitive. Good yields of both complexes were obtained, and the recrystallized products were of high purity.

### 2.2.2 Characterization of rhodium chloride complexes

The phosphine complexes all have fairly high melting or decomposition points.  $\text{Cp}^*\text{RhCl}_2(\text{PPh}_3)$  was found to decompose above 248 °C, which is consistent with the literature report that states that the melting point occurs at some temperature above 230°C.<sup>4</sup>  $\text{Cp}^*\text{RhCl}_2(\text{PMePh}_2)$  and  $\text{Cp}^*\text{RhCl}_2(\text{PMe}_2\text{Ph})$  melt at 257 and 229°C respectively. No literature melting points for the two complexes were found.

Chemical shifts and  $J$ -values obtained from the  $^1\text{H}$  NMR spectra of **22-24** agree with the literature reports.  $\text{Cp}^*$  signals are observed as doublets due to coupling with the phosphorus atom of the phosphine ligand. It may seem strange that the protons on the  $\text{Cp}^*$  ring would couple with the phosphorus rather than the rhodium atom, which is in closer proximity. However most of the  $[\text{Cp}^*\text{RhL}_n]$  complexes reported by Maitlis in 1969 showed Me-P coupling, but no Me-Rh coupling.<sup>4</sup> The few complexes that did have Me-Rh coupling ( $\text{Cp}^*\text{RhMe}_2(\text{PPh}_3)$ , for example) had very small  $J_{\text{Me-Rh}}$  coupling constants compared to the  $J_{\text{Me-P}}$  values. In other instances it has also been found that where a  $[\text{Cp}^*\text{RhL}_n]$  complex exhibits any Me-Rh coupling at all, the  $J$ -value is very small with a value less than 1Hz.<sup>7, 8</sup>

The  $\text{Cp}^*$  signal in each phosphine complex is noticeably upfield compared to the  $\text{Cp}^*$  signal of the chloride dimer **21**. This probably arises as a result of the  $\sigma$ -donor ability of the phosphine ligand. When it coordinates to the rhodium atom it increases electron density on the metal centre. This would have an overall shielding effect on the protons of the other ligands present: in this case, the methyl protons of the pentamethylcyclopentadienyl ligand. Consequently, each of the complexes **22**, **23**, and **24** exhibit  $\text{Cp}^*$  peaks at around 1.4 ppm compared to the peak at 1.6 ppm in **21**.

For each complex the phosphorus spectrum shows one doublet with a  $J$ -value of approximately 140 Hz, in accordance with the literature values. The signals for

$\text{Cp}^*\text{RhCl}_2(\text{PPh}_3)$ ,  $\text{Cp}^*\text{RhCl}_2(\text{PMePh}_2)$  and  $\text{Cp}^*\text{RhCl}_2(\text{PMe}_2\text{Ph})$  were found at 30.28, 24.31 and 13.26 ppm respectively. Each of these values differs by about 2 ppm from the corresponding literature value. These discrepancies are not significant and probably arise from the inherent differences between individual NMR analysis instruments.

From the figures above we can see that the  $^{31}\text{P}$  chemical shifts decrease quite dramatically from **22** to **23** to **24**. This is expected: as electron-withdrawing groups (phenyls) on the phosphine are replaced with electron-donating groups (methyls), the phosphorus atom becomes more shielded, and exhibits a lower NMR chemical shift.

### 2.2.3 Synthesis and characterization of rhodium iodide complexes

The iodide complexes **25** and **26** were synthesized as alternatives to the chloride analogues. The dark purple iodide dimer was prepared via a halide-exchange reaction in which  $[\text{Cp}^*\text{RhCl}_2]_2$  was refluxed with a considerable excess of sodium iodide in acetone. Addition of triphenylphosphine to  $[\text{Cp}^*\text{RhI}_2]_2$  produced a high yield of the purple solid  $\text{Cp}^*\text{RhI}_2(\text{PPh}_3)$ .

The single proton NMR shift of  $[\text{Cp}^*\text{RhI}_2]_2$  is somewhat more downfield than that of the chloride analogue. This indicates that the iodide ligand is less able to contribute to the electron density on the metal centre, a consequence of the greater size of the iodide. Likewise, the  $\text{Cp}^*$  signal of iodide complex **26** occurs at a higher frequency than that of chloride complex **22**. And, as in the case of the chloride complexes **21** and **22**, the  $\text{Cp}^*$  proton NMR chemical shift of the phosphine **26** is approximately 0.2 ppm upfield from that of the dimer **25**.

### 2.2.4 Synthesis and characterization of rhodium bromide complex

The rhodium bromide dimer **7** was prepared in a similar manner to **25**, in a halide-exchange reaction between **21** and sodium bromide. It exists as a stable orange-brown solid that decomposes slowly from 285°C. As expected, its  $^1\text{H}$  NMR signal occurs at an intermediate value between those of **21** and **25**, at 1.73 ppm.

These seven known starting materials were therefore synthesized and characterized without difficulty. Each was used in further reactions carried out during the project, with varying degrees of success, as will be discussed below.

### **2.3 Reactions of alkenyl Grignard reagents with rhodium precursors**

The synthesis of complexes of the type  $\text{Cp}^*\text{Rh}(\text{PPh}_3)(\{\text{CH}_2\}_n\text{CH}=\text{CH}_2)_2$  was attempted by reacting alkenyl Grignard reagents with  $\text{Cp}^*\text{RhCl}_2(\text{PPh}_3)$  at  $-78^\circ\text{C}$  in diethyl ether. This method was fraught with difficulties. Not only did the reaction yield a complex mixture of products that was difficult to separate, but it also appeared that the bulky  $\text{PPh}_3$  ligand was dissociating itself from the rhodium centre. This was evident from  $^1\text{H}$  NMR of the products, which showed a weak phenyl proton signal relative to the other signals.  $^{31}\text{P}$  NMR likewise revealed a weaker-than-expected phosphorus peak, together with a signal at approximately  $-5\text{ppm}$ , indicative of free triphenylphosphine that could only have come from dissociation of the ligand from the complex.

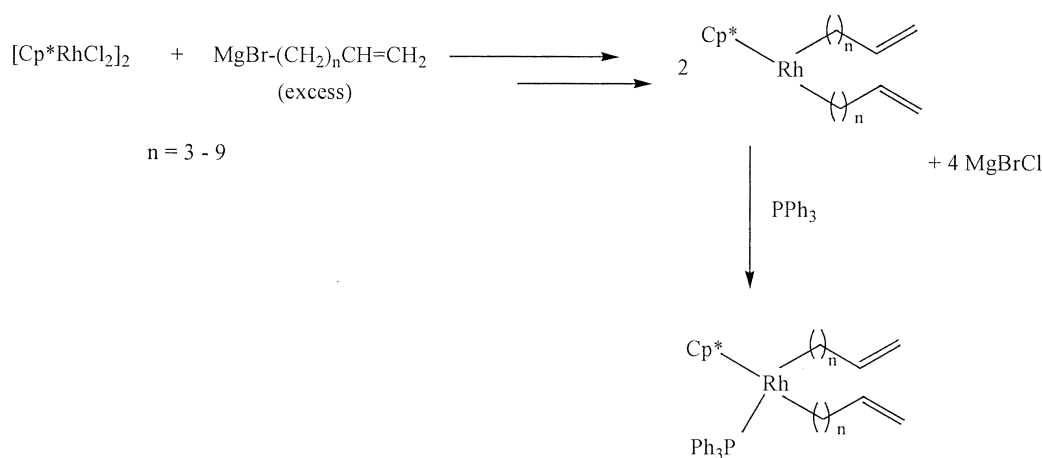
Following the belief that a more labile halide leaving group might facilitate the reaction, the chloride starting material was converted to the iodide analogue,  $\text{Cp}^*\text{RhI}_2(\text{PPh}_3)$ , by refluxing in excess  $\text{NaI}$ . The product was then used in the Grignard reaction. This time, the conversion of precursor (a purple suspension) to product (an orange-brown solution) occurred rapidly. However, as soon as the reaction mixture was removed from the nitrogen atmosphere, the product was seen to decompose to a purplish solid. NMR analysis confirmed that the solid constituted starting material. We did manage to obtain NMR confirmation that showed that the desired bis-alkene was present, although already degenerating. In the phosphorus spectrum, the product signal was very weak compared to that of the precursor.

The same phenomenon was observed in analogous reactions involving the iridium analogue  $\text{Cp}^*\text{IrI}_2(\text{PPh}_3)$ .<sup>9</sup> The newly-formed product decomposed immediately on exposure to air. This did not happen when the iridium *chloride* complex was used.

The question posed was why the product of the iodide reaction decomposed so rapidly while the product of the chloride reaction did not appear to do so. One possible explanation is that the iodide ion is a better nucleophile than the chloride ion. Therefore, the MgBrI by-product from the iodide reaction would be more likely to attack the newly-formed bis-alkenyl complex, converting it back to the iodide starting material.

We then attempted to isolate our metal bis-alkenyl complexes as follows: after the reaction was complete, there was direct removal of the ether solvent from the reaction vessel, *in vacuo*. The residue was dissolved in benzene, a non-polar solvent in which the MgBrI by-product was not expected to be soluble; we assumed, therefore, that there was little threat of dissolved MgBrI particles attacking the bis-alkenyl complex. The benzene solution was separated from the solid phase, and the products isolated. The technique proved not to be very efficient. In the case of iridium, a very small amount of product material was successfully isolated. With rhodium however, decomposition was still rapid and complete.

Therefore neither  $\text{Cp}^*\text{RhI}_2(\text{PPh}_3)$  nor  $\text{Cp}^*\text{RhCl}_2(\text{PPh}_3)$  gave satisfactory results, and this compelled us to formulate a new approach. The new strategy was based on the formation of a phosphine-free bis-alkene directly from the  $[\text{Cp}^*\text{RhCl}_2]_2$  dimer as depicted in Scheme 2.2.



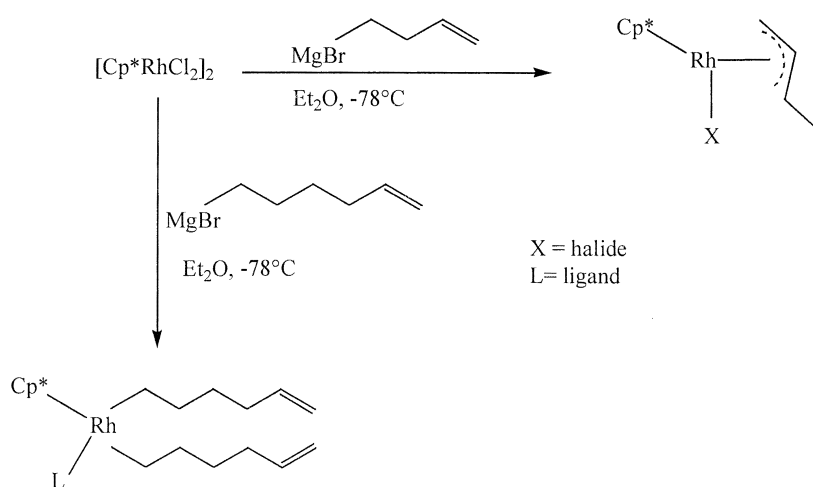
Scheme 2.2

In the first step, the rhodium dimer is cleaved by the substitution of the chloride ligands (both terminal and bridging) with the alkenyl chains. The phosphine ligand is then added to the complex in what would be, it was presumed, a facile reaction to give an 18e<sup>-</sup> complex. Thus a host of different alkenyl Grignard reagents, with increasing carbon chain lengths, was used in the series of reactions involving the addition of Grignard to (pentamethylcyclopentadienyl)dichlororhodium dimer. Alkenyl Grignard reagents of the type MgBr-(CH<sub>2</sub>)<sub>n</sub>CH=CH<sub>2</sub> were used.

## 2.4 Reactions of rhodium complexes with short-chain versus long-chain alkenyl Grignard reagents

The first two experiments were carried out using 1-butenyl- and 1-hexenyl Grignard reagents. Surprisingly, the reactions gave different types of products (Scheme 2.3). The butenyl reaction yielded an orange crystalline solid. The proton NMR spectrum (discussed later) showed a pattern of peaks indicative of an η<sup>3</sup>-allylic complex.

The analogous hexenyl-Grignard reaction gave an orange-red oily residue that proved to be a mixture of products. <sup>1</sup>H NMR analysis showed two multiplets at 5.0 and 5.8ppm characteristic of the bis-alkenyl terminal and internal olefinic protons respectively. Chromatography on a short alumina column yielded the purified bis-alkene as a yellow oil in low yield (ca 40%).



Scheme 2.3

So, two similar Grignard reagents, differing only by two CH<sub>2</sub> groups, used in the same reaction gave widely different results. The only influencing factor could be the length of the alkenyl chain. The reaction using the pentenyl-Grignard, with chain length intermediate to the butenyl and hexenyl chains, was carried out to see what the result would be. After three hours' reaction time the major product was a yellow oil, but a small amount of the orange crystals was also isolated. <sup>1</sup>H NMR proved that these were the rhodium bis-alkenyl and allylic complexes respectively.

These observations led to the hypothesis that shorter-chain Grignard reagents bring about the formation of allylic complexes, while longer-chain reagents lead to bis-alkenyl complexes. This suggestion was validated when using Grignard reagents of other carbon chain lengths in the Grignard/rhodium dimer reaction. The reaction involving the short carbon-backbone reagent, allylmagnesium bromide, gave a reasonably high yield of the crystalline allylic complex. On the other hand, all alkenyl Grignards with a carbon number of 6 or greater yielded the bis-alkenyl products, Cp\*Rh(L)((CH<sub>2</sub>)<sub>n</sub>CH=CH<sub>2</sub>)<sub>2</sub>, exclusively.

## **2.5 Allyl complexes**

### *2.5.1 Synthesis of allyl complexes*

There are several examples of stable rhodium allyl complexes in the literature.<sup>7, 10 - 12</sup> It appeared that we had unintentionally added to that number in the reaction of our butenyl Grignard reagent with a rhodium precursor. Although this type of complex was not immediately relevant to the project, we found it interesting enough to explore further. Allylic species are believed to occur in many metal-catalyzed reactions,<sup>13 -16</sup> and isolated allylic complexes are therefore potentially useful as model compounds for the investigation of catalytic cycles.

During this project, three different rhodium allylic complexes were prepared: an allyl, a 1-methylallyl and 1-ethylallyl complex (Scheme 2.4).



only one type of halide was present in the reaction system, either chloride or bromide, to prevent the formation of a mixture of products. There were two options: to use chloride-containing Grignard reagents with our  $[\text{Cp}^*\text{RhCl}_2]_2$  precursor, or to use the more conventional bromide-containing Grignard reagents with the  $[\text{Cp}^*\text{RhBr}_2]_2$  analogue. We decided on the latter method, and synthesized the rhodium bromide complex from literature methods. The complex was then reacted with the allyl-, butenyl- and pentenyl-Grignard reagents, and the familiar orange-red crystals were obtained, and recrystallized from diethyl ether/hexane. This time, the characterization data were satisfactory. The microanalysis results were in good agreement with the calculated values, proving that our proposal of halide-exchange had been correct.

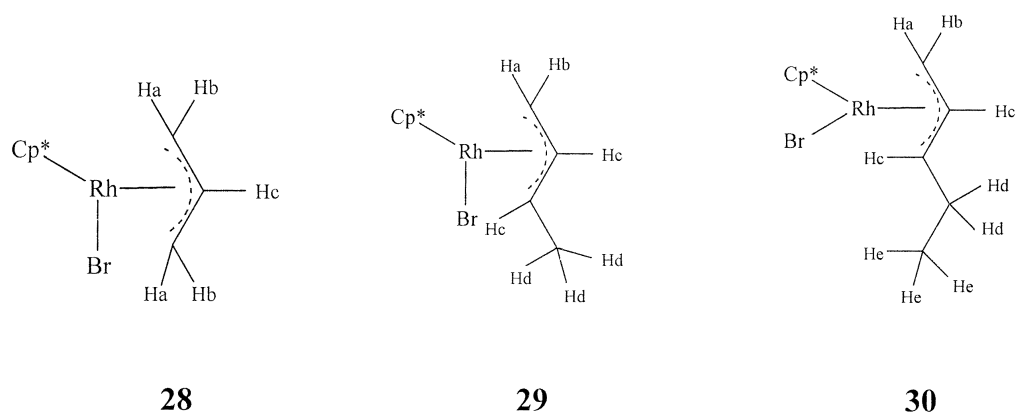


**Figure 2.2 Complexes 28 – 30 with individual hydrogen atoms labelled**

Complex **29** is a known compound, reported by Maitlis *et al* in 1995,<sup>17</sup> although it was prepared by a different method to the one described here. The chloride analogue is also known.<sup>11, 12</sup> **28** and **30** are, however, new complexes (Figure 2.2).

All three complexes are stable in solution, with no decomposition observed in any organic solvent. All are thermally stable above 100°C. Product **28** decomposes at 120°C, **29** decomposes with some melting, also at 120°C and **30** melts at 118°C.

### 2.5.2 NMR spectra of allyl complexes

$^1\text{H}$  NMR assignments for the allylic complexes can be found in Table 2.1. Figure 2.2 shows the labelling of the individual hydrogen atoms.

The spectrum of complex **28** shows two doublets, each integrating for two protons. Each terminal carbon carries two protons that are not chemically equivalent to each other. However, because the allyl moiety is symmetrical, the two terminal carbons are identical to each other and each carries a set of protons ( $\text{H}_a$  and  $\text{H}_b$ ) that is identical to the set on the other.  $\text{H}_a$  and  $\text{H}_b$  have significantly different coupling constants, and their values appear to indicate, respectively, *cis*- and *trans*-coupling between the terminal and internal hydrogen atoms.

**Table 2.1**  $^1\text{H}$  NMR values for complexes **28** – **30**

Type of proton	Complex		
	<b>28</b>	<b>29</b>	<b>30</b>
Cp*	1.78 (s, 15H)	1.76 (s, 15H)	1.77 (s, 15H)
Terminal allyl	3.14 (d, 2 $\text{H}_a$ , $J = 11.7\text{Hz}$ )	3.11 (d, 1 $\text{H}_a$ , $J = 11.2\text{Hz}$ )	3.11 (d, 1 $\text{H}_a$ , $J = 10.1\text{Hz}$ )
Terminal allyl	3.33 (d, 2 $\text{H}_b$ , $J = 6.8\text{Hz}$ )	3.14 (d, 1 $\text{H}_b$ , $J = 6.3\text{Hz}$ )	3.14 (d, 1 $\text{H}_b$ , $J = 6.4\text{Hz}$ )
Internal allyl	3.95 (m, 1 $\text{H}_c$ )	3.76 <sub>c</sub> (m, 2H)	3.74 (m, 2 $\text{H}_c$ )
Methylene	-	-	1.93 (m, 2 $\text{H}_d$ )
Methyl	-	1.56, d, 3 $\text{H}_d$ ( $J = 5.4\text{Hz}$ )	1.16 (t, 3 $\text{H}_e$ , $J = 7.3\text{Hz}$ )

Compound **29** displays a similar  $^1\text{H}$  NMR pattern, but in this case each doublet corresponds to only a single proton,  $\text{H}_a$  or  $\text{H}_b$ . The two internal allyl protons are situated on non-equivalent carbon atoms, but are sufficiently chemically alike to

exhibit the same NMR signal. Thus the multiplet in **29** integrates for *two* H<sub>c</sub> nuclei. These results match the literature values reported by Maitlis and co-workers, and indicate the formation of a *syn*- versus an *anti*-1-methylallyl complex.<sup>17</sup>

The NMR spectrum of **30** has an additional multiplet due to the methylene protons, H<sub>d</sub>. The methyl group, now adjacent to a methylene rather than an allyl group, shows a triplet at just above 1 ppm, significantly upfield from the methyl peak in **29**.

The <sup>13</sup>C NMR spectra of **28**, **29**, and **30** can be fully assigned. The Cp\* methyl carbons occur most upfield, between 9 and 10ppm. The aromatic Cp\* carbons are most downfield near 100ppm, with the internal allylic carbon(s) at a slightly lower chemical shift, around 95ppm. Terminal allylic shifts occur around 55 – 60ppm, and allylic carbons attached to methyl or ethyl groups resonate between 70 and 80ppm. It is interesting to note that the carbons directly bonded to the rhodium centre (aromatic Cp\* carbons, allylic carbons) give doublets while those that are not directly bonded (methyl Cp\*, non-allylic carbons) give singlets. This is a consequence of rhodium-carbon (<sup>103</sup>Rh-<sup>12</sup>C) coupling. Any carbon atom bonded to the rhodium centre will couple with the metal, resulting in a doublet in the NMR spectrum.

### 2.5.3 The effect of different solvents on the complex

Figure 2.3 shows the effect of two solvents on the proton spectrum of complex **30**. The region displayed is that between 2.7 and 3.7 ppm, the region in which the two doublets of the terminal allylic protons occur. While one would expect that the chemical shifts of the doublets would differ somewhat between solvents, it is perhaps surprising that the separation between the two doublets is so vastly different in the two cases.

In Figure 2.3a, the spectrum of **30** in deuterated chloroform, the peaks are so close to each other that they are overlapping. Meanwhile, Figure 2.3b shows how widely the doublets are separated when deuterated benzene is used as solvent.

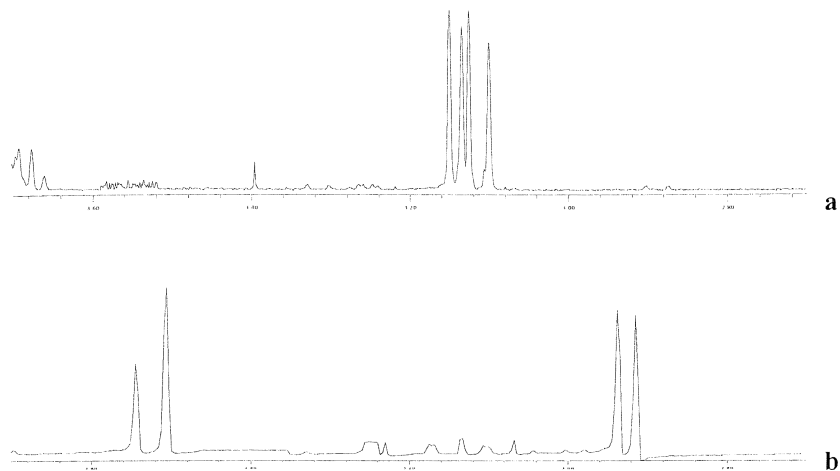
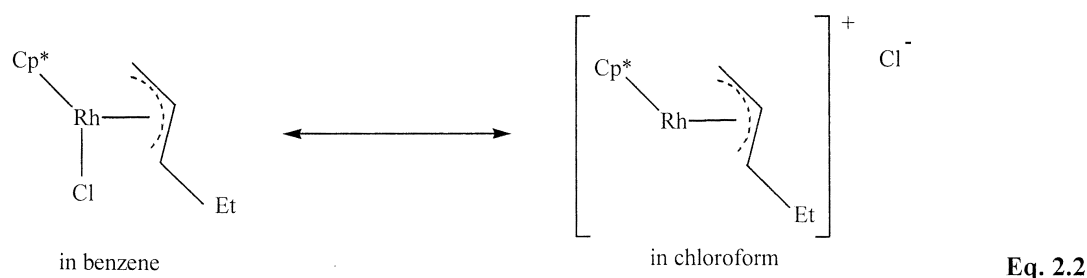


**Figure 2.3** The  $^1\text{H}$  NMR spectra (region 2.7 – 3.7 ppm) for  $\text{Cp}^*\text{RhBr}(\eta^3\text{-ethylallyl})$  in (a)  $\text{CDCl}_3$  and (b)  $\text{C}_6\text{D}_6$

This is interesting because the same experiment using a related iridium complex,  $(\eta^5\text{-C}_5\text{Me}_4\text{H})\text{IrCl}(\eta^3\text{-allyl-R})$ , gives the opposite result.<sup>9</sup> In chloroform the distance between doublets is large, while in benzene the peaks overlap. In that case, it was suggested that the complex became ionized in chlorinated solvents whereas it remained neutral in non-chlorinated solvents. This change in the nature of the complex would affect the chemical shifts of the various protons by different degrees. It is possible that we are seeing a similar effect with rhodium, where ionization of the complex occurs in more polar solvents (Equation 2.2). This would account for the major differences in the NMR spectra of the same complex in different solvents.



#### 2.5.4 Mass spectrometry of allyl complexes

The mass spectrometric data were fairly routine. Complexes **28** and **29** showed two parent ion peaks (resulting from the existence of two main isotopes of bromine,  $^{79}\text{Br}$  or  $^{81}\text{Br}$ ) at 358/360 and 372/374 respectively. This proves that the complexes synthesized were of the proposed compositions. In the case of **30** the signals at 385/387, indicative of  $[\text{M}-\text{H}]^+$  fragments, were somewhat more intense than the expected parent ion peaks at 386/388.

In each case there is a peak, equivalent to the fragment  $[\text{M} - \text{Br}]^+$ , occurring at 279, 293 and 307 for **28**, **29** and **30**. Also present in each case is a peak at 237, corresponding to the fragment  $[\text{RhC}_5\text{Me}_4\text{CH}_2]^+$ , where a hydrogen has been lost from the pentamethylcyclopentadienyl ligand. Maitlis and co-workers had previously observed this particular fragment in the mass spectrum of  $[\text{Cp}^*\text{RhCl}_2]_2$ .<sup>4</sup>

#### 2.5.5 X-ray crystal structure of $\text{Cp}^*\text{RhBr}(\eta^3\text{-1-ethylallyl})$

The X-ray crystal structure for **30** is shown below in figure 2.4. The structure confirms the proposed formulation of a neutral ethylallyl complex. Selected bond lengths and angles are given in Table 2.2.

As expected for an allylic complex, the structure shows bonding of the rhodium to three carbon atoms on the allyl chain. The Rh-Br bond distance of 2.53 Å is similar to other, known Rh-Br bond distances occurring at approximately 2.5 Å<sup>18, 19</sup>. The distance between C12 and C13 is intermediate between the average values for C-C single bonds and C=C double bonds. The pentamethylcyclopentadienyl ring is almost planar. The C13-C14-C15 bond angle of 110.9 ° is typical of a tetrahedral,  $\text{sp}^3$ -hybridized carbon, while the C11-C12-C13 bond angle between the allylic carbons is close to that of an  $\text{sp}^2$ -hybridized carbon atom.<sup>20, 21</sup>

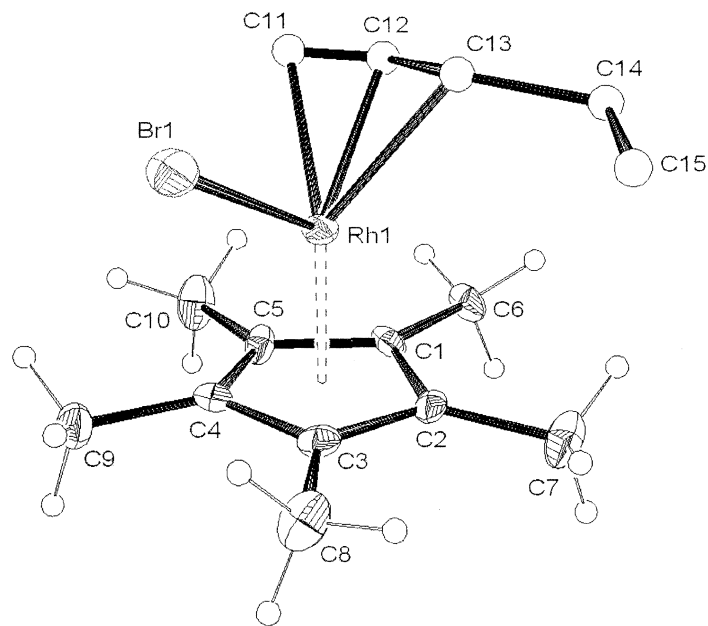


Figure 2.4 Crystal structure of 30, Cp\*RhBr( $\eta^3$ -1-ethylallyl)

Table 2.2 Selected bond lengths (Å) and angles (°) for complex 30

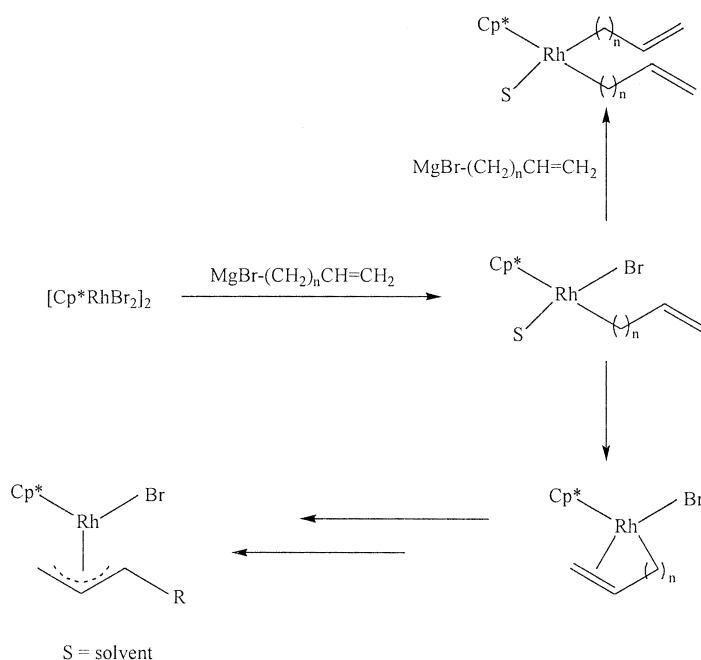
Bond lengths (Å)		Bond angles (°)	
Rh1 – C11	2.179 (12)	C12 – Rh1 – Br	106.3 (6)
Rh1 – C12	2.09 (2)	C1 – Rh1 – Br1	155.3 (3)
Rh1 – C3	2.234 (11)	C4 – Rh1 – Br1	92.9 (3)
C1 – C5	1.439 (16)	C12 – C11 – Rh1	70.1 (13)
C4 – C9	1.515 (17)	C14 – C13 – Rh1	121.9 (10)
C12 – C13	1.41 (3)	C5 – C4 – C9	123.8 (11)
C14 – C15	1.48 (3)	C2 – C1 – C6	127.4 (16)

### 2.5.6 Mechanism of formation of the allyl complex

In order to gain some insight into the question of why the allylic complex formed, we returned to the reaction involving the pentenyl-Grignard reagent, the only carbon chain length that had yielded both bis-alkenyl and allylic products. The reaction was repeated several times, with the only variable being the length of reaction time. It was found that a reaction of short duration (three hours or less) gave principally the bis-

alkenyl product, with perhaps a very small quantity of the allylic complex. With longer reaction times, the proportion of allylic complex increased significantly, and when the mixture was stirred for a day or more it was the sole product formed. These results suggest that the bis-alkenyl product, the first-formed product, is converted to the allylic complex.

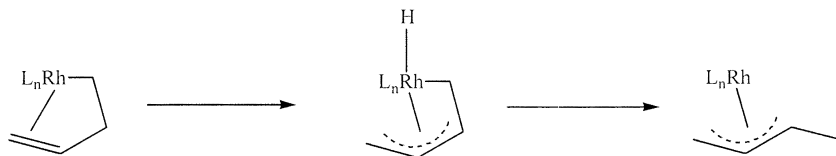
Scheme 2.6 outlines a possible reaction mechanism for the formation of the allylic complex. The scheme indicates that the rhodium dimer is cleaved when one of the chlorides is substituted by an alkenyl chain. There is possible coordination of a solvent molecule to stabilize what would otherwise be a  $16e^-$  complex. If the chain is of an appropriate length (as in the case of the propenyl, butenyl and pentenyl molecules) it can bend back, allowing  $\eta^2$ -coordination of the alkene and displacing the solvent molecule. The system eventually rearranges to form the  $\eta^3$ -coordinated allyl complex.



**Scheme 2.6**

The final step in the process, the conversion of  $\eta^2$ -olefin complex to  $\eta^3$ -allyl complex, can occur via migration of a hydrogen atom from the carbon adjacent to the double bond, to the rhodium centre (Scheme 2.7). The hydride and the  $\sigma$ -bonded alkyl group

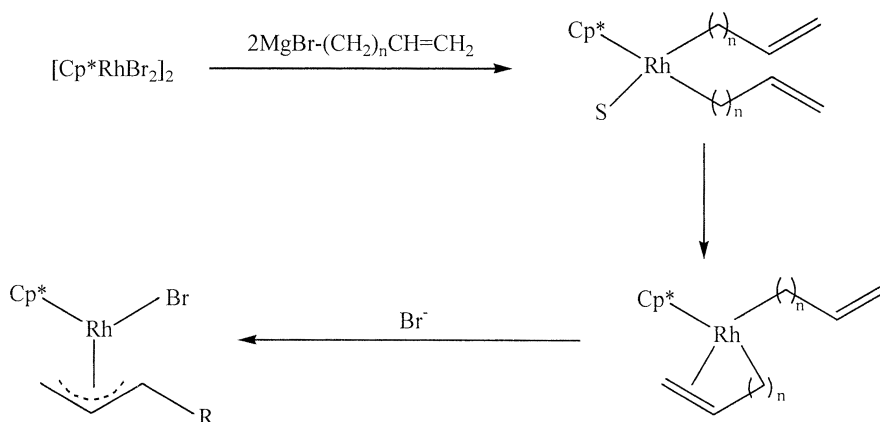
can then undergo coupling, freeing that end of the alkyl chain from the metal centre, so that bonding to the metal occurs only through the allyl moiety.



**Scheme 2.7**

The problem with Scheme 2.6 as shown is that it does not account for the formation of the bis-pentenyl complex. We know that the bis-alkenyl complex *does* form. The integration of the signals in the  $^1\text{H}$  NMR spectrum indicates the presence of a bis-alkenyl, not a monoalkenyl, complex.

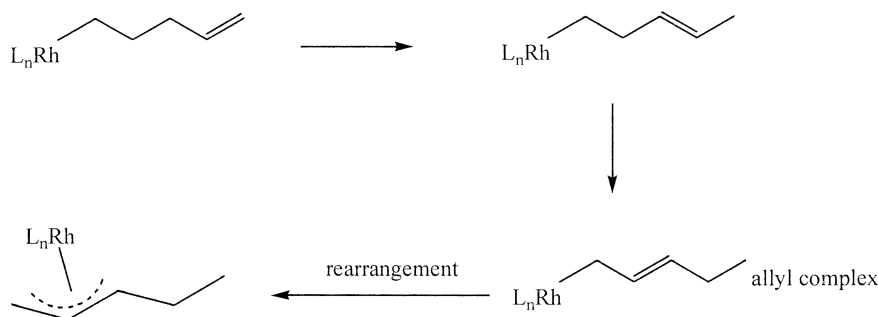
Scheme 2.8 gives another possible scenario, and also accounts for the formation of the bis-alkenyl complex. The final step requires that the alkenyl chain be replaced by an attacking bromide ligand. Since there is an excess of bromide in the reaction mixture, it is not hard to imagine that this might occur.



**Scheme 2.8**

Another possible mechanism for the formation of the allylic complex is  $\sigma$ - $\pi$  allyl rearrangement, which is quite a common method for the preparation of allylic complexes.<sup>22</sup> This means that the rearrangement would take place from the  $\sigma$ -alkenyl complex rather than the  $\pi$ -bonded complex (Scheme 2.9). For terminal alkene chains

longer than three carbons (for example, as in the case of **30**), the process would require isomerization of the double bond to form a  $\sigma$ -allyl intermediate (Scheme 2.9).



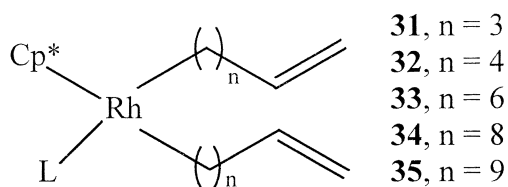
**Scheme 2.9**

If this was indeed the reaction mechanism, it should be possible to obtain evidence of the isomerization reaction, which is a stepwise process. The intermediates (internal alkenes) would be detected in the NMR spectra. However, no such evidence has been observed here, and the mechanism shown in Scheme 2.9 is therefore unlikely to be the one occurring in this case. We believe the mechanism in Scheme 2.8 to be the most likely one for the formation of the  $\pi$ -allyl complex.

## **2.6 Bis-alkenyl complexes**

### *2.6.1 Synthesis of bis-alkenyl complexes*

A series of complexes (**31** – **35**) of proposed composition  $Cp^*Rh(\{CH_2\}_nCH=CH_2)_2L$  was prepared. The synthetic procedure was as follows: A suspension of  $[Cp^*RhCl_2]_2$  was cooled to  $-78^\circ C$  and approximately 5 molar equivalents of the relevant alkenyl Grignard reagent was added. The reaction mixture was stirred for 3 – 4 hours during which time the solution turned a brownish-green colour. The reaction was quenched with saturated  $NH_4Cl(aq)$  solution and the reaction mixture turned orange-red. The organic layer was separated, dried over anhydrous magnesium sulphate and filtered through a glass funnel; the solvent was then removed *in vacuo*, leaving behind a red oily residue.



L = ligand (H<sub>2</sub>O)

**Figure 2.5 Structure of the bis-alkenyl complexes synthesized**

The red residue turned out to be a mixture of products that required separation by column chromatography. After testing several different solvents, we found that benzene worked best as an eluent, as it dissolved the bis-alkenyl very well, and the other products less so. The red residue was dissolved in a little benzene, applied to the column, and eluted with benzene. A bright yellow band was the first to elute, and was collected. The other bands, orange, orange-red and crimson, moved extremely slowly and eventually remained stationary near the top of the column. Despite the use of more polar solvents, these bands could not be eluted. It was suspected that the deep red band constituted some starting material that had, perhaps, been generated by some of the product decomposing on the column. The other bands were likely due to side-products formed in the reaction.

In all cases the yield of the bis-alkenyl complex (yellow band) was low, approximately 40%. These disappointing yields were probably a result of the inefficiency of the reaction that generated several side-products, and/or the relative instability of the complex. The bis-alkenyl complexes have been shown to be fairly stable in non-chlorinated solvents. They are stable in chlorinated solvents for a short time, and were submitted for NMR analysis in deuterated chloroform. However, upon prolonged exposure to the chlorine-containing solvent, the complex would decompose. It was seen that a yellow solution of the product in dichloromethane or chloroform turned red after some hours. Dark red crystals began to form as the solvent evaporated. The crystals were analyzed and were shown to be [Cp\*RhCl<sub>2</sub>]<sub>2</sub>, the starting material. Presumably, the degeneration of the product to the rhodium dimer occurs as a result of the chlorine radicals that are generated from the solvent.

These reactive radicals can attack the bis-alkenyl compound, converting it to the chloride complex. Another possibility is that there are trace amounts of HCl present in the chlorinated solvent, causing decomposition of the bis-alkenyl complex.

### 2.6.2 Microanalysis results for bis-alkenyl complexes

Initially we had assumed that the bis-alkenyl complex consisted of one Cp\* ligand and two alkenyl chains bonded to the rhodium centre, and no other ligands were present. <sup>1</sup>H NMR seemed to support the belief, as did mass-spectrometry.

However, further analysis highlighted a problem. The microanalysis results for carbon composition (Table 2.3) were not within the acceptable range.

We deduced that there were two potential reasons for the discrepancies. Firstly, it was possible that the samples were contaminated with solvent or with other impurities. Alternatively, there could be coordination of a solvent molecule such as ether to the rhodium centre. However, despite numerous attempts at purification, thorough drying and recalculation of the expected values, the calculated and found microanalysis figures remained dissimilar.

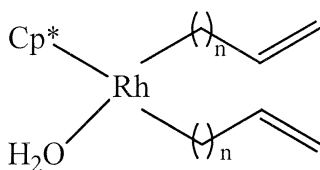
**Table 2.3 Microanalysis values for the proposed rhodium bis-alkenyl complexes**

Complex	C% (Calc)	C% (found)	H% (calc)	H% (found)
11	63.8	60.9	8.8	8.1
12	65.4	63.0	9.2	9.4
13	67.8	65.4	9.8	9.9
14	69.8	67.8	9.7	10.4
15	70.6	76.7	10.5	11.5

Since the excess Grignard reagent had been hydrolyzed with a saturated, *aqueous* solution of ammonium chloride, water could also have been present. Once again, the expected elemental analysis values were recalculated using H<sub>2</sub>O in place of X. The results can be found in Table 2.4.

It is quite clear that, for complexes **31** – **34**, the new calculated figures are in excellent agreement with the experimentally determined values. They indicate that water is present in the sample in a ratio of 1:1 to the bis-alkenyl complex. It is thus probable that a water molecule is coordinated to the metal centre, so making up the full complement of 18 electrons. It is also *possible*, though not likely, that the water is merely trapped within the sample, and that its lack of volatility prevents its being removed by drying under vacuum. However, this would not account for why there is only ever a 1:1 ratio of rhodium to water molecule in each of the samples.

**Table 2.4 Calculated microanalysis values for rhodium bis-alkenyl complexes containing H<sub>2</sub>O ligand**



Complex	C% (Calc)	C% (found)	H% (calc)	H% (found)
<b>11</b>	60.9	60.9	8.9	8.1
<b>12</b>	62.6	63.0	9.2	9.4
<b>13</b>	65.3	65.4	9.8	9.9
<b>14</b>	67.4	67.8	10.3	10.4

One would expect that a signal for water would be present in the  $^1\text{H}$  NMR spectrum. Due to the poor resolution of the spectra, however, many of the proton signals, including that of water, are not clearly defined. It is likely that the  $\text{H}_2\text{O}$  peak is hidden under, or overlapping with, one or more of the other peaks.

As mentioned previously, the mass spectrum parent ion peaks occurred at values corresponding to complexes of composition  $\text{Cp}^*\text{Rh}(\{\text{CH}_2\}_n\text{CH}=\text{CH}_2)_2$ , ie. with no water molecule present. However, this does not necessarily refute the possibility of an  $\text{H}_2\text{O}$  ligand. It could be that dissociation of the water molecule occurred when the sample was dissolved in the solvent in which the analysis was to be performed. The mass spectrum results would therefore reflect the remaining fragment of the bis-alkene complex, and not the entire, isolated complex.

Infrared spectra were obtained for two of the complexes (**33** and **35**). These show broad peaks at  $3420\text{ cm}^{-1}$ . This is within the correct range for the stretching frequency of a water molecule, and is further argument for the presence of water in the complex.

### 2.6.3 NMR spectra of the bis-alkenyl complexes

Each bis-alkenyl complex contains, in the alkenyl chains, a number of methylene groups that are in similar chemical environments. These methylene protons exhibit similar, overlapping chemical shifts in the  $^1\text{H}$  NMR spectrum, which is thus poorly resolved. However, there are several other distinguishable features in the  $^1\text{H}$  spectrum. A sample spectrum, belonging to **35**, is shown in Figure 2.6.

The most obvious NMR peaks are the two multiplets belonging to the terminal and internal olefinic protons. These appear at 5.0 and 5.8ppm respectively, in all of the bis-alkenyl complexes. The chemical shifts of several other proton groups in the complex are found in Table 2.5.

The  $\text{Cp}^*$  signal is a singlet, integrating for 15 protons, between 1.2 and 1.3 ppm. A triplet at about 1ppm can be assigned to the protons of the methylene positioned  $\alpha$  to

the rhodium atom. These hydrogen atoms couple only with those immediately adjacent to it, and not with the metal atom, and the triplet is therefore quite distinct.

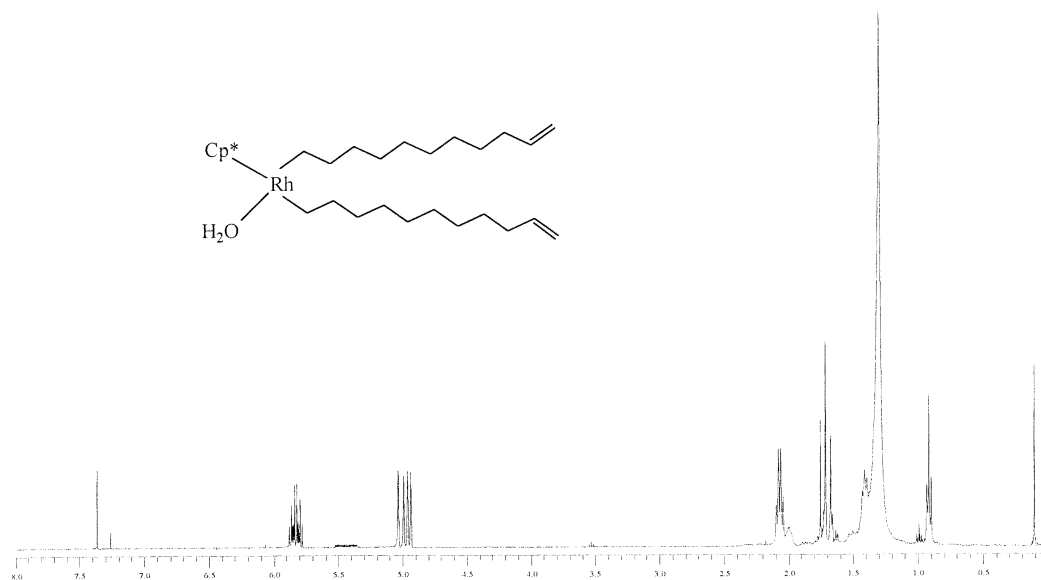
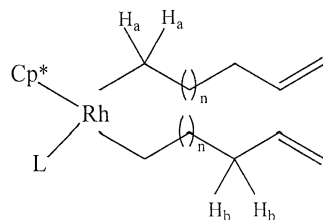


Figure 2.6  $^1\text{H}$  NMR spectrum ( $\text{CDCl}_3$ ) of bis-undecenyl rhodium complex 35

Table 2.5 Some  $^1\text{H}$  NMR assignments of rhodium bis-alkenyl complexes



Complex	$\text{Cp}^*$	Proton $\text{H}_a$ (adjacent to rhodium)	Proton $\text{H}_b$ (adjacent to double bond)
31	1.26 (s, 15H)	0.91 (t, 4H, $J = 7.4$ Hz)	2.05 (q, 4H, $J = 7.3$ Hz)
32	1.29 (s, 15H)	0.90 (t, 4H, $J = 6.9$ Hz)	2.04 (q, 4H, $J = 7.1$ Hz)
33	1.28 (s, 15H)	0.89 (t, 4H, $J = 7.8$ Hz)	2.05 (q, 4H, $J = 7.1$ Hz)
34	1.26 (s, 15H)	0.89 (t, 4H, $J = 7.4$ Hz)	2.04 (q, 4H, $J = 7.1$ Hz)
35	1.29 (s, 15H)	0.91 (t, 4H, $J = 7.0$ Hz)	2.07 (q, 4H, $J = 7.1$ Hz)

The last feature in the spectrum is the peak belonging to the protons adjacent to the alkene group. Coupling with a single olefinic proton on one side, and a pair of methylene protons on the other, they show a noticeable quartet at 2ppm. The peaks belonging to the other protons in the complex could not be resolved but are reported as a “broad multiplet”. These values can be found in Chapter 4 (Experimental Details).

Samples were submitted for  $^{13}\text{C}$  NMR analysis; however, the spectra were very complicated and difficult to assign.

#### *2.6.4 The absence of allylic product with long-chain alkenyl Grignard reagents*

It was previously observed that the reaction between  $[\text{Cp}^*\text{RhCl}_2]_2$  and the pentenyl-Grignard reagent gave two different products depending on the reaction time. When the reaction mixture was stirred for three hours the product was primarily bis-alkenyl product, whereas a reaction time of a day or more ensured that only the allylic complex was obtained. It was thought that it might be possible to isolate longer-chain rhodium allylic complexes if the reaction mixtures were left to stir for long enough periods.

We attempted the preparation of a (1-propylallyl)rhodium complex. The procedure was similar to the one used for the preparation of the bis-hexenyl complex, but the reaction was left for 2 days instead of 3 hours. At the end of the allocated time period, a  $^1\text{H}$  NMR spectrum was obtained for the crude, bulk product. The results were clear. The mixture consisted of the bis-alkenyl complex and side-products, with no trace of any allylic complex. Repeat experiments of this nature had similar outcomes: the longer-chain alkenyl Grignards did not form any allylic complex even with prolonged reaction times.

Possible explanations for these observations are suggested here. The formation of a  $16e^-$  bis-alkenyl complex in the reaction mixture (prior to hydrolysis) has previously been discussed. In the case of the short-chain alkenyl complexes, it was thought that the conversion of bis-alkene to allylic complex was the most convenient way of attaining a stable  $18e^-$  configuration, if the carbon chain was of a length sufficient to

allow both  $\eta^2$  alkene-metal contact through back-bending, and subsequent isomerization to form the allyl complex.

The long-chain alkenyl complexes could also be stabilized by intramolecular  $\eta^2$ -coordination, as shown in Figure 2.7. The flexibility of the long chain would allow the chain to swing back and coordinate to the metal centre, as in the case of the short-chain complexes. However, in order for an allylic complex to form there must be transfer of a hydrogen atom from the carbon adjacent to the alkene to the metal centre. This would be considerably more difficult in the case of the long-chain alkenyl complexes, due to the distance between rhodium atom and the carbon atom concerned. This would prevent the conversion of the  $\sigma$ -alkenyl complex to a  $\pi$ -allyl complex.

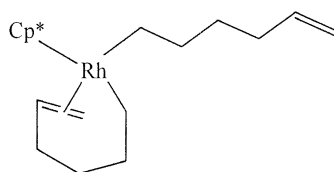


**Figure 2.7 Intramolecular  $\eta^2$ -coordination by the pendant alkene**

Another possibility is that the  $16e^-$  complexes are stabilized by intermolecular rhodium-alkene coordination (Figure 2.8).

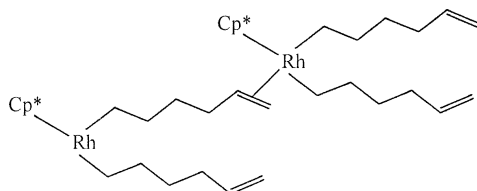


**Figure 2.8 Intermolecular coordination of pendant alkene to external rhodium centre**

This would be more likely to occur with the long-chain alkenyl complexes, as the length of the chain would prevent the rhodium centres from getting too close to each other. Steric interference from pentamethylcyclopentadienyl rings would be minimized. Therefore there would not be intramolecular  $\eta^2$ -coordination, a prerequisite for the formation of the allyl complex as indicated by the proposed mechanism (Scheme 2.7), and no allyl complex would be produced.

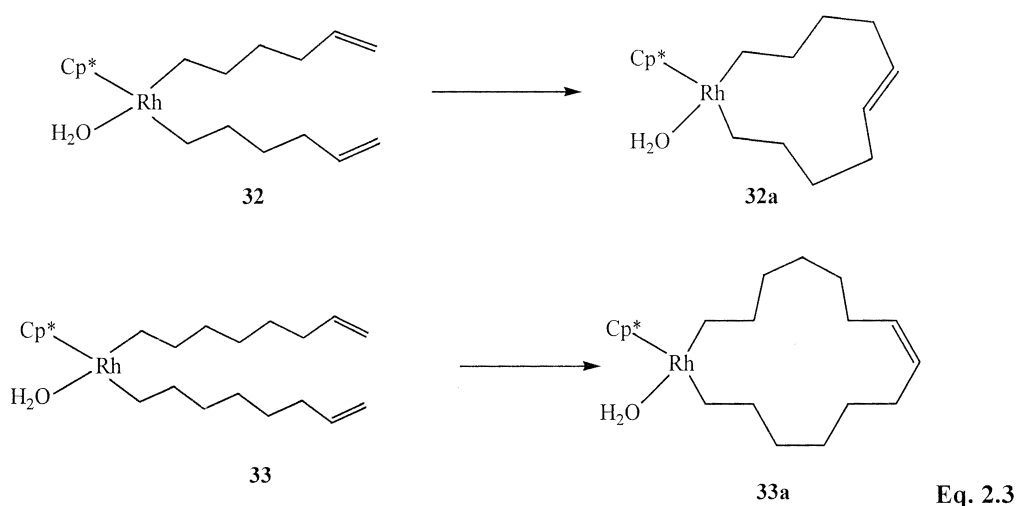
### 2.6.5 Reaction mechanism for formation of the complex

We can now suggest a possible sequence of events that occurs during the course of the reaction.

- The Grignard reagent attacks the rhodium dimer, which is cleaved. The alkenyl chains replace the chlorides, two on each rhodium atom. The ether-insoluble dimer has been transformed into a soluble bis-alkenyl complex.
- The newly-formed bis-alkene is stabilized either by intramolecular alkene coordination, or by intermolecular  $\eta^2$ -coordination of a double bond to an external metal centre. This effectively converts the complex to an 18-electron system. It is at this point that we observe the greenish-brown colour that persists as long as the reaction is kept stirring under nitrogen.
- When the Schlenk tube is opened, and the  $\text{NH}_4\text{Cl}$  solution added, the colour changes rapidly to orange-red. The green-brown product has disappeared, and this implies that the bis-alkenyl product as described in the previous paragraph is no longer there. This change is possibly due to the coordination of a water molecule, introduced with the addition of the aqueous  $\text{NH}_4\text{Cl}$  solution. This disrupts the intermolecular structure described in the previous paragraph.
- We know that the final product is a yellow oil, yet the crude product is red. This shows that other complexes, side-products, are present. These complexes were probably not in solution during the actual reaction, or some red colour would have been observed. A potential scenario is this: upon exposure to air, some of the bis-alkene decomposed back to starting material and other rhodium species. The nature of these other species is not known. We do know that they are not very soluble in benzene (and are not eluted on a chromatography column when benzene is used as an eluent) and are probably quite polar, or even ionic, complexes. These insoluble complexes are therefore left behind on the chromatography column, and only the bis-alkenyl product is eluted in the benzene.

## 2.7 Ring-closing reactions

Complexes **32** and **33** were subjected to Grubbs' ring-closing metathesis conditions in test reactions on an NMR scale to determine whether ring-closing would occur (Equation 2.3). About 20 mg of complex **32** or **33** was dissolved in deuterated benzene; the solution was then placed in an NMR tube. Grubbs' first-generation catalyst,  $\text{RuCl}_2(\text{PCy}_3)_2(=\text{CHPh})$ , (*ca* 5 mol % with respect to rhodium) was added. The tube was heated and the  $^1\text{H}$  NMR spectra were recorded at intervals of 2 or 3 hours.



Initially, the solution inside the NMR tube was yellow, the colour of the bis-alkenyl complex. As heating continued, the colour changed to a darker orange. At this point, the  $^1\text{H}$  NMR revealed the presence of a new peak at 5.4ppm, in between the signals for the terminal and internal olefinic protons. This signal is believed to represent the protons of the new, ring-closed metallacycloalkenes, **32a** or **33a** (see comparison with palladacycloalkene later). Figure 2.9 shows the growth of the signal for **33** as the Grubbs' reaction progresses.

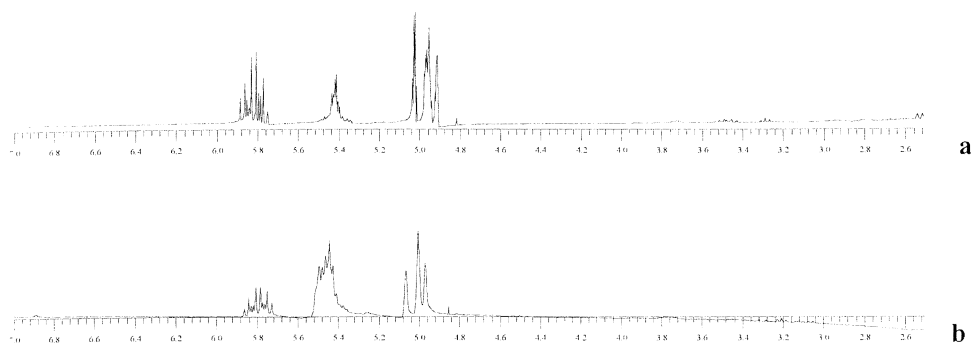


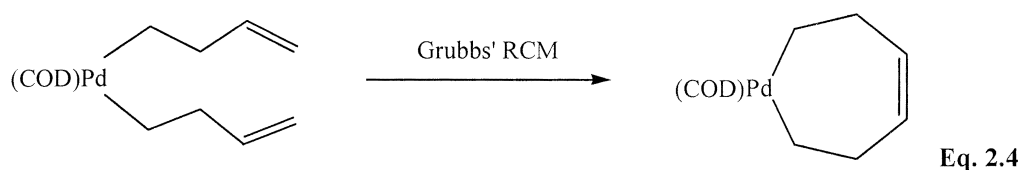
**Figure 2.9** NMR spectrum (region 2.5 – 7 ppm) for reaction of **33** with Grubbs' catalyst (a) immediately after addition of catalyst (b) after 9 hours' heating with catalyst

The colour of the reaction solution continued to darken, eventually attaining a dark-brown colour after 10 hours. NMR spectra obtained periodically during this time showed the reaction progression. The bis-alkenyl signals at 5.0 and 5.8 ppm steadily decreased in intensity, compared to that of the ring-closed product at 5.4 ppm, which grew in intensity. After about ten hours there were no further changes; the peak at 5.4 ppm reached a maximum and the bis-alkene peaks reached minimum intensities. By comparing the relative intensities of the two complexes' alkene signals, it was judged that the ring-closing reaction was approximately 75% complete. Further addition of Grubbs' first-generation catalyst did not affect this distribution. We attempted to separate the two complexes by column chromatography. A short, narrow column of deactivated alumina was used, with benzene as eluent. However, it appeared that the decomposition occurred on the column, and nothing was eluted.

Our initial explanation of the appearance of the NMR signal at 5.4 ppm was that it was due to ring-closing of the bis-alkenyl complex to form a metallacycloalkene. However, another explanation of the signal could be that it was due to isomerization of the terminal olefin to an internal olefin. Isomerization can be expected to take place upon heating, as has been observed with some platinum bis-alkenyl complexes.<sup>23</sup> This possibility was investigated during one further experiment. The rhodium bis-alkenyl complex **35** was heated in benzene for 10 hours *without* Grubbs' catalyst. The solution colour and the NMR spectrum remained unchanged after 10 hours. This is indirect evidence that the changes observed previously were due to the action of Grubbs' catalyst. More specifically, the changes were likely due to ring-closing

metathesis in the presence of Grubbs' catalyst, and the respective rhodacycloalkenes were formed.

Grubbs' RCM experiments carried out on palladium bis-alkenyl complexes (Equation 2.4) has shown similar results to what has been shown here: the disappearance of the terminal protons at 5.0 and 5.8 ppm in the NMR spectrum to give rise to the new peak at 5.4 ppm.<sup>24</sup> In that case, the reaction product was isolated and characterized and shown to be the palladacycloalkene complex. The parallels between the results and those presented here gives yet further evidence that the rhodacycloalkene was formed during our reaction, even though it could not be isolated after its completion.



Therefore, at present we have only <sup>1</sup>H NMR evidence that the ring-closed products of **32** and **33** (respectively, an 11-membered and a 15-membered rhodacycloalkene) were formed. Although the results thus far appear promising, further experiments must be done in order to prove that ring-closing occurs under Grubbs' metathesis conditions, and to isolate the products themselves.

## 2.8 Summary of Chapter 2

In Chapter 2 we have discussed the synthesis of several known rhodium complexes. After reacting some of the complexes with various alkenyl Grignard reagents, it was found that only one, [Cp\**RhCl*<sub>2</sub>]<sub>2</sub>, gave stable, isolable products. The rhodium dimer was then reacted with a series of alkenyl Grignard reagents of increasing chain length. Interestingly, it was found that the type of product formed in each case was dependent on the length of the alkenyl chain. Rhodium allylic complexes of the type Cp\**RhBr*(η<sup>3</sup>-allyl-R) where R = H, CH<sub>3</sub>, CH<sub>2</sub>CH<sub>3</sub>, were formed from reactions involving short-chain alkenyls. Reactions involving longer carbon chain reagents

resulted in the formation of the bis-alkenyl complexes,  $\text{Cp}^*\text{Rh}(\{\text{CH}_2\}_n\text{CH}=\text{CH}_2)_2(\text{H}_2\text{O})$ , where  $n = 3, 4, 6, 8, 9$ .

The allylic and bis-alkenyl complexes were characterized by various methods. In most cases they were found to be novel rhodium complexes. Ring-closing reactions were carried out on the bis-alkenyl complexes.  $^1\text{H}$  NMR indicates that ring-closing has occurred although pure rhodacycloalkenes were not isolated.

## 2.9 References

1. A. Sivaramakrishna, H. S. Clayton, C. Kaschula and J. R. Moss, *Coord. Chem. Rev.*, 2007, in press.
2. R. Benn, R-D. Reinhardt and A. Rufinska, *J. Organomet. Chem.*, 1985, **282**, 291.
3. A. Sivaramakrishna, H. Su and J. R. Moss, *Angew. Chem. Int. Ed.*, 2007, in press.
4. J. W. Kang, K. Moseley and P. M. Maitlis, *J. Am. Chem. Soc.*, 1969, **91**, 5970.
5. W. D. Jones and V. L. Kuykendall, *Inorg. Chem.*, 1991, **30**, 2615.
6. W. D. Jones and F. J. Fehrer, *Inorg. Chem.*, 1984, **23**, 2376.
7. J. Powell and B. L. Shaw, *J. Chem. Soc. (A)*, 1968, 583
8. S. M. Nelson, M. Sloan and M. G. B. Drew, *J. Chem. Soc., Dalton Trans.*, 1973, 2195.
9. A. Sivaramakrishna, unpublished results.
10. K. Moseley, J. W. Kang and P. M. Maitlis, *J. Chem. Soc. (A)*, 1970, 2875.
11. P. Powell and L. J. Russell, *J. Organomet. Chem.*, 1977, **129**, 415.
12. A. Vásquez de Miguel and P. M. Maitlis, *J. Organomet. Chem.*, 1983, **244**, C35.
13. A. M. Johns, J. W. Tye and J. F. Hartwig, *J. Am. Chem. Soc.*, 2006, **128**, 16010.
14. R. Kuwano, Y. Kondo, *Org. Lett.*, 2004, **6**, 3545.

15. T. Nishimura, S. Hirabayashi, Y. Yashura and T. Hayashi, *J. Am. Chem. Soc.*, 2006, **128**, 2557.
16. C. Wang and J. A. Tunge, *Org. Lett.*, 2005, **7**, 2137.
17. Z-Q. Wang, M. L. Turner, A. R. Kunicki and P. M. Maitlis, *J. Organomet. Chem.*, 1995, **488**, C11.
18. J. Reed and P. Eisenberger, *Acta Crystallographica, B*, 1978, **B34**, 344.
19. M. M. Muir, G. M. Gomez, J.A Muir and S. Sanchez, *Acta Crystallographica, C*, 1987, **C43**, 839.
20. E. V. Anslyn and D. A. Dougherty, *Modern Physical Organic Chemistry*, University Science Books, Sausalito, 2006.
21. E. L. Eliel, S. H. Wilen and M. P. Doyle, *Basic Organic Stereochemistry*, John Wiley and Sons, Inc., New York, 2001.
22. J. P. Collman, L. S. Hegedus, J. R. Norton and R. G. Finke, *Principles and applications of organotransition metal chemistry*, University Science Books, 1987.
23. A. Sivaramakrishna, H. Su and J. R. Moss, *Organometallics*, 2007, under revision.
24. T. Mahamo, 2007, unpublished results.

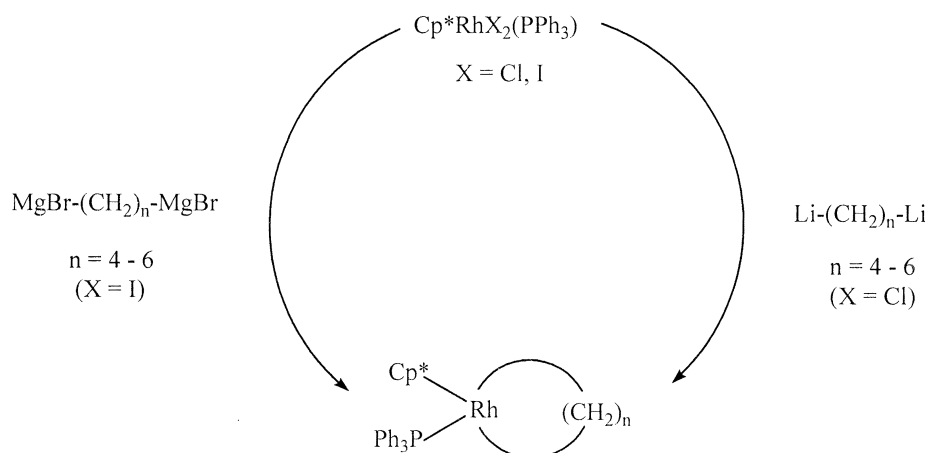
## Chapter 3

# Results and Discussion: Reactions of rhodium precursors with di-Grignard reagents

### 3.1 Introduction

In order to gain a more in-depth knowledge of the metallocycloalkanes we were attempting to obtain via the bis-alkenyl route (see Chapter 2), we decided to prepare some rhodacycloalkanes by the reported literature method. It would thus be possible to attain a better understanding of the stability and properties of these types of complexes. An even more pertinent advantage would be the comparison of the spectroscopic data of metallocycloalkanes with that of the various species obtained along the bis-alkenyl route.

The research group headed by Pietro Diversi had, in the late 1970's and early 1980's, described synthetic procedures for a series of rhodium and iridium metallocycloalkanes.<sup>1,2</sup> Their method involved the addition of di-Grignard or di-lithium reagent to a metal dihalide, as shown in Scheme 3.1.



Scheme 3.1

We now report the use of this method to prepare some new rhodium-containing metallocycloalkanes. According to the literature, the largest rhodacycloalkane previously synthesized was a 7-membered metallacycle.<sup>2</sup> It would be interesting to

see if Diversi's method could be employed to prepare larger-ring compounds, with 8 or more members. In addition, we wished to extend the series of known rhodacycloalkanes of the type  $\text{Cp}^*\text{Rh}(\text{CH}_2)_n\text{L}$  by preparing complexes with other phosphine ligands, as Diversi's group had only prepared triphenylphosphine derivatives.

## **3.2 Reactions of rhodium complexes with di-Grignard reagents**

### *3.2.1 Di-Grignard reagents*

The preparation and properties of di-Grignard reagents<sup>3,4</sup> are somewhat different to their more common mono-Grignard relatives. The initial part of the synthesis is similar, with the addition of the appropriate dibromoalkane to dried magnesium turnings, and subsequent refluxing of the reaction mixture. However, once the reaction is complete, the resultant di-Grignard compound is not soluble in ether. It forms a clear, viscous liquid layer that lies below the ethereal layer. In order to use the compound, the ether layer must be *completely* removed from the reaction vessel. The di-Grignard can then be dissolved in a quantity of THF and that solution may then be added to ethereal solutions or suspensions of a metal complex.

We found that addition of THF when even minute traces of ether remained in the reaction vessel caused solidification of the reagent. The di-Grignard reagent then formed thick white clumps that could not be dissolved, and could therefore not be used. It is possible to use the pure, concentrated liquid reagent without dissolution in THF. The high viscosity of the liquid, however, can make handling of the compound slightly more difficult.

For our experiments, the di-Grignard reagents used were either bromo- or iodomagnesium compounds, as the starting materials (diiodo- or dibromoalkanes) were most readily available. The reagents we used were either the pure di-Grignard in the liquid form, or as a THF solution, as was convenient.

### 3.2.2 The di-Grignard reaction: chloride versus iodide starting materials

Large quantities of the starting material, Cp\*RhI<sub>2</sub>(PPh<sub>3</sub>) were prepared, recrystallized and dried. It was desirable that the diiodide complex be as pure and as dry as possible, so there could be nothing present that could interfere with the reaction once it was started. Despite our precautions, our initial attempts to prepare the metallacycles were unsuccessful.

The reaction itself seemed to proceed without difficulty. Three equivalents of the di-Grignard were added at -78 °C. The reaction mixture was then allowed to warm to room temperature. An almost-immediate reaction was observed; the quantity of dark, insoluble starting complex appeared to lessen, while the solution took on an orange hue that intensified as time progressed. This indicated the formation of the soluble metallocycloalkane species.

After completion of the reaction, which was signalled by the disappearance of insoluble starting material and the translucent orange solution colour, the solution was *not* hydrolyzed with water or saturated NH<sub>4</sub>Cl solution. The execution of this step, required after typical Grignard reactions, is made unnecessary by the fact that the excess di-Grignard would be insoluble in the extracting solvent. There would thus be no need remove the excess reagent by hydrolysis with an aqueous medium.

The metallacycles themselves were obtained as yellow to orange oils. Chromatographic techniques proved insufficient to completely separate the desired product from unwanted products. Following repeated fractional crystallizations the pure form of products were obtained. <sup>31</sup>P NMR spectroscopy, while highlighting the metallocycloalkane as the major product, also indicated the presence of some relatively small signals with low intensity. The similarity of some of these peaks to the product suggested a close similarity between the complexes, or perhaps indicated some conformational variation within the metallocycloalkane complex, for example, different conformations adopted by the cycloalkane ring.

Figure 3.1 shows the rhodacycloalkanes that were synthesized, albeit in impure form.

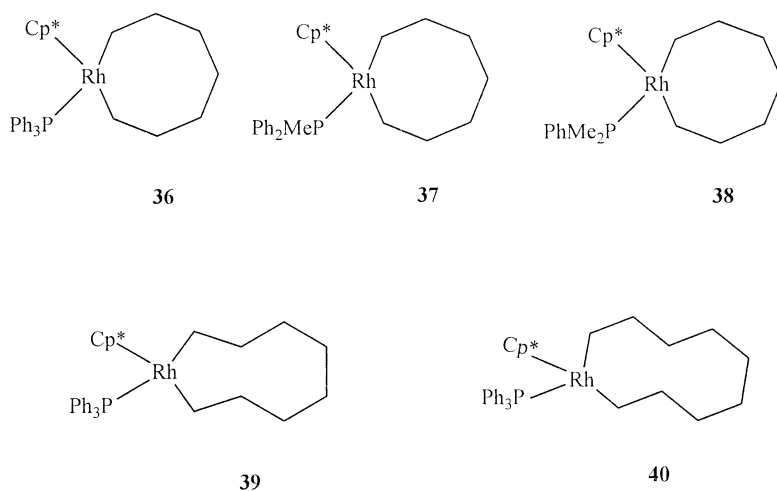


**Figure 3.1** A series of medium-sized rhodacycloalkanes

### 3.2.3 NMR characterization of rhodacycloalkanes

Although the rhodacycloalkanes were isolated as bright yellow oils, it was observed that the colour would darken over several hours, presumably due to decomposition. They are more stable when stored under nitrogen at low temperatures, below 0 °C. The complexes appeared to be particularly unstable in solution, and especially with chlorinated solvents. Therefore NMR spectra were recorded in C<sub>6</sub>D<sub>6</sub> instead of CDCl<sub>3</sub>. The proton and phosphorus NMR data are summarized in Tables 3.1 and 3.2.

**Table 3.1** <sup>1</sup>H NMR data (ppm) in C<sub>6</sub>D<sub>6</sub> for the rhodacycloalkanes

Complex	Cp*	Phenyl	Ring methylene
<b>36</b>	1.53 (d, 15H <i>J</i> = 2.0 Hz)	7.22 – 7.37 (m, 15H)	0.83 – 1.38 (br m, 14H)
<b>37</b>	1.57 (d, 15H, <i>J</i> = 2.4 Hz)	6.99 – 7.36 (m, 10H)	0.85 -1.34 (br m, 17H)*
<b>38</b>	1.55 (d, 15H, <i>J</i> = 2.4 Hz)	6.89 – 7.38 (m, 5H)	0.85 – 1.34 (br m, 20H)*
<b>39</b>	1.59 (d, 15H, <i>J</i> = 2.0 Hz)	7.10 – 7.45 (m, 15H)	0.88 – 1.37 (m, 16H)
<b>40</b>	1.59 (d, 15H, <i>J</i> = 2.0 Hz)	7.07 – 7.45 (m, 15H)	0.87 – 1.35 (m, 18H)

\* These signals include the methyl protons of the phosphorus ligand

The  $^1\text{H}$  NMR spectra in  $\text{C}_6\text{D}_6$  yielded only clearly-defined phenyl and  $\text{Cp}^*$  signals; those of the ring methylene and phosphorus methyl protons were broad and overlapping, and could not be resolved, but were rather recorded as broad multiplets. The  $\text{Cp}^*$  signal appears as a doublet, due to  $^{31}\text{P} - ^1\text{H}$  coupling ( $J = 2.0\text{Hz}$ ). This is consistent with the literature values for the previously-synthesized rhodacycloalkanes.<sup>2</sup>

**Table 3.2**  $^{31}\text{P}$  NMR data in  $\text{C}_6\text{D}_6$  for rhodacycloalkanes

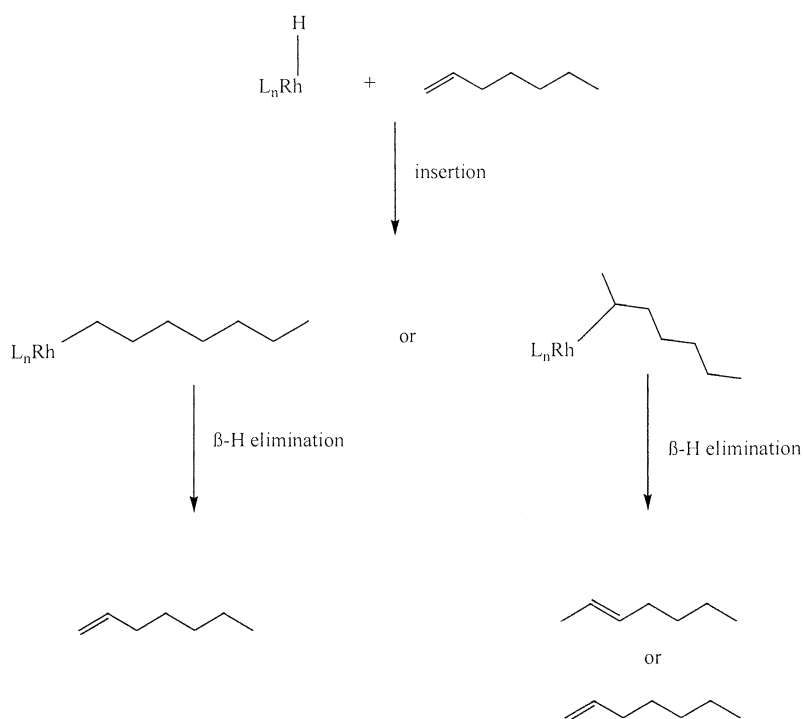
Complex	$^{31}\text{P}$ NMR signal (ppm)
<b>36</b>	56. 15 (d, $J = 186.4$ Hz)
<b>37</b>	38. 77 (d, $J = 185.4$ Hz)
<b>38</b>	20. 96 (d, $J = 183.1$ Hz)
<b>39</b>	56.33 (d, $J = 185.4$ Hz)
<b>40</b>	56. 34 (d, $J = 185.4$ Hz)

The phosphorus NMR peaks appear as doublets, with large Rh-P coupling constants of about 185 Hz. These  $^{103}\text{Rh}-^{31}\text{P}$  coupling constants occur within the same range as those of other Rh(III) complexes containing tertiary phosphine ligands.<sup>5-7</sup>

### 3.2.4 Other characterization methods

On long standing, even at room temperature, it was observed that the products turned a darker orange colour from the original bright yellow, indicating decomposition of the complex. This is a probable explanation for why good elemental analysis results could not be obtained.

Mass-spectra were obtained for some of the samples. Complex **36** gave the best results: the complex, with a calculated mass of 598, showed a somewhat weak parent ion peak at 597. None of the other complexes showed peaks close to the individual calculated values for molecular ion values. However, fragmentation patterns of the

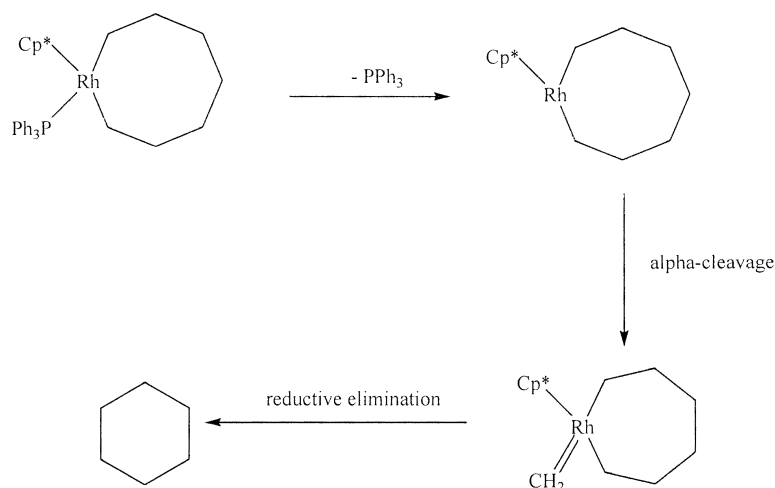


**Scheme 3.3**

The major and minor decomposition products for **37** and **38** are all 7-carbon organic compounds, as would be expected. However, in the case of the triphenylphosphine derivative **36**, the product profile is quite different. Now, heptane and heptene are obtained in equal quantities, but the main product is cyclohexane.

C-C fission reactions of metallacycloalkanes are known.<sup>11, 12, 13</sup> An  $\alpha$ -C-C cleavage would result in the reduction of the ring size by one carbon atom (Scheme 3.4). The triphenylphosphine molecule can dissociate from the metal centre, resulting in a  $16e^-$  complex with a vacant coordination site. This less stable complex could regain its full complement of 18 electrons by abstracting a methylene from the metallacarbon ring in an  $\alpha$ -C-C cleavage reaction. There would now be only six carbon atoms in the ring and if an intramolecular reductive elimination were to occur, cyclohexane would be produced.<sup>12, 13</sup>

There are several examples of decomposition by carbon-carbon fission in the case of nickela- and platinacycloalkanes.<sup>11</sup> It is therefore very possible that the same type of reactivity could be observed with rhodium-containing metallacycloalkanes.



**Scheme 3.4**

There are no six-carbon decomposition products in the case of the PMePh<sub>2</sub> and PMe<sub>2</sub>Ph derivatives. These phosphines are more basic than PPh<sub>3</sub>, and therefore bind more strongly to the rhodium centre. With fewer phenyl rings they are also less sterically demanding. This might prevent the molecules from dissociating from the complex, and thus the abstraction of a methylene carbon from the alkane ring would not occur.

### **3.4 Summary of Chapter 3**

Five novel rhodium-containing metallacycloalkanes were synthesized. The complexes, with ring sizes of 8 – 10 members, were the largest known rhodacycloalkanes. These were characterized by <sup>1</sup>H and <sup>31</sup>P NMR spectroscopy. Owing to the unstable nature of these complexes, further characterization such as elemental analysis was not successfully achieved. Further work would be necessary to fully characterize these compounds.

Thermal decomposition studies were carried out on four of the five rhodacycles. The distribution of the decomposition products appeared to be influenced by the nature of the phosphine ligand.

### **3.5 References**

1. P. Diversi, G. Ingrosso, A. Lucherini, P. Martinelli, M. Benetti and S. Pucci, *J. Organomet. Chem.*, 1979, **165**, 253.
2. P. Diversi, G. Ingrosso, A. Lucherini, W. Porzio and M. Zocchi, *Inorg. Chem.*, 1980, **19**, 3590.
3. J. X. McDermott, J. F. White and G. M. Whitesides, *J. Am. Chem. Soc.*, 1976, **98**, 6521.
4. G. S. Silverman, in *Handbook of Grignard reagents*, G. S. Silverman and P. E. Rakita (eds.), Marcel Dekker, Inc., New York, 1996.
5. W. D. Jones and V. L. Kuykendall, *Inorg. Chem.*, 1991, **30**, 2615.
6. J. Conradie, G. J. Lamprecht, S. Otto and J. C. Swarts. *Inorg. Chim. Acta*, 2002, **328**, 191.
7. L. A. Van ver Veen, P. H. Keeven, G. C. Schoemaker, J. N. H. Reek, P. C. J Kamer, P. W. N. M. van Leeuwen, M. Lutz and A. L. Spek, *Organometallics*, 2000, **19**, 872.
8. J. P. Collman and L. S. Hegedus, *Principles and applications of organotransition metal chemistry*, University Science Books, 1980.
9. C. Elschenbroich and A. Salzer, *Organometallics: A concise introduction*, VCH Verlagsgesellschaft, 1989.
10. M. Bochmann, *Organometallics 1: Complexes with transition metal-carbon  $\sigma$ -bonds*, Oxford University Press, 1994.
11. J. Cámpora, P. Palma and E. Carmona, *Coord. Chem. Rev.*, 1999, **193-195**, 207.

12. R. H. Grubbs and A. Miyashita, *J. Am. Chem. Soc.*, 1978, **100**, 7418.
13. A. Miyashita, M. Ohyoshi, H. Shitara and H. Nohira, *J. Organomet. Chem.*, 1988, **338**, 103.

## Chapter 4

### Experimental Details

#### 4.1 General

All reactions were carried out under a nitrogen atmosphere using standard Schlenk techniques. Solvents were distilled under N<sub>2</sub> immediately prior to use unless otherwise stated. Diethyl ether and tetrahydrofuran were dried over sodium wire/benzophenone and dichloromethane over calcium hydride. Rhodium chloride trihydrate was obtained from Johnson Matthey. Chemicals were purchased from Sigma Aldrich. Melting points were recorded using a Kofler hot stage microscope (Reichert Thermovar) and are uncorrected. <sup>1</sup>H, <sup>13</sup>C and <sup>31</sup>P NMR spectra were recorded on Varian XR300 MHz or XR400 MHz spectrometers using tetramethylsilane (TMS) as the internal standard. The IR instrument was a Perkin-Elmer FT-IR machine. Microanalyses were carried out at the University of Cape Town, using a Fisons EA 1108 CHNS Elemental Analysis instrument. Mass spectral analyses were carried out at the University of Witwatersrand.

Thermal decomposition studies were carried out at the University of Cape Town; the decomposition products were analyzed using a Varian 3900 GC equipped with FID and a 30m x 0.32mm CP-Wax 52 CB column (0.25 μm film thickness), and an Agilent 5973 GC equipped with MSD and 60 m x 0.25 mm column (0.5 μm film thickness).

#### 4.2 Synthesis of Grignard reagents<sup>1</sup>

Strict Schlenk conditions were observed in the preparation of Grignard reagents and solvents were distilled prior to the reaction.

Freshly-distilled diethyl ether and an excess of dried magnesium turnings were placed in a two- or three-necked flask equipped with stirrer and reflux condenser. The flask was cooled to -78 °C and the appropriate bromoalkene was added. The reaction was then refluxed for several hours until the solution attained a distinctive grey hue.

Molarities of the Grignard reagents were determined by hydrolyzing small aliquots in distilled water, adding excess hydrochloric acid (standard solution) and back-titrating against sodium hydroxide solution using phenolphthalein indicator.

### **4.3 Di-Grignard reagents**<sup>2</sup>

The di-Grignard reagents were synthesized using a method slightly modified from that reported by Whitesides *et al.* Strict Schlenk conditions were observed and solvents were distilled prior to the reaction.

Magnesium turnings were dried *in vacuo* in a three-necked round-bottomed flask equipped with reflux condenser, magnetic stirrer and hot plate. Diethyl ether was transferred, under nitrogen, to the flask, which was then cooled to  $-78^{\circ}\text{C}$ . The appropriate dibromoalkane (0.25 molar equivalents with respect to Mg) was added; the reaction vessel was removed from the cold bath. As it warmed up, the mixture began to boil. After it stopped boiling on its own, the reaction was refluxed for several hours more. The mixture separated into two layers: an ethereal upper layer and a viscous di-Grignard lower layer. The ether was carefully and completely removed using a syringe, and the remaining di-Grignard was dissolved in dry THF.

Molarities of the solutions were determined by quenching  $1\text{cm}^3$  of the di-Grignard with a small quantity of distilled water, adding excess  $\text{HCl}_{(\text{aq})}$  and back-titrating against  $\text{NaOH}_{(\text{aq})}$  with phenolphthalein indicator.

### **4.4 Synthesis of rhodium starting materials**

#### **4.4.1 $[\text{Cp}^*\text{RhCl}_2]_2$ (21)**

This complex has been prepared using two different methods.

##### *Reaction with hexamethyldewarbenzene*<sup>3</sup>

A round-bottomed flask fitted with reflux condenser was charged with  $20\text{cm}^3$  reagent-grade methanol and  $\text{RhCl}_3 \cdot 3\text{H}_2\text{O}$  (0.5 g, 1.9 mmol). Hexamethyldewarbenzene, or

HMDB, (1 g, 6.16 mmol) was added, and the mixture refluxed at 65 °C for 21 hrs. Solvent was removed *in vacuo* and the red residue was washed with ether (3 x 5 cm<sup>3</sup>) to remove traces of HMDB, and dried under vacuum. The product was isolated as dark red crystals (523mg, 89%). Mp. = 310°C (slow decomp) (lit. mp. > 230 °C). NMR (CDCl<sub>3</sub>)  $\delta$ (<sup>1</sup>H) = 1.61 (s). The NMR results are in agreement with the literature values.

#### *Reaction with pentamethylcyclopentadiene*<sup>4</sup>

RhCl<sub>3</sub>.3H<sub>2</sub>O (1 g, 3.80 mmol) and pentamethylcyclopentadiene (0.6 g, 4.40 mmol) were refluxed under nitrogen for 48 hours. The red solid product was isolated by suction filtration and washed with ethanol and washed with portions of ether (3 x 5 cm<sup>3</sup>). The mother liquor was reduced *in vacuo* to give more crystals that was combined with the first crop. The final percentage yield was 92 %.

Characterization data are similar to those obtained for the reaction with HMDB.

#### 4.4.2 Cp\*RhCl<sub>2</sub>(PPh<sub>3</sub>) (22)

This complex has been prepared using two different methods.

#### *Reaction in ethanol*<sup>3</sup>

[Cp\*RhCl<sub>2</sub>]<sub>2</sub> (300 mg, 0.48 mmol) and PPh<sub>3</sub> (300 mg, 1.14 mmol) were refluxed in ethanol for 5 hours. The reaction mixture was cooled, and the reddish-gold crystals were filtered and washed with ethanol and water. Yield was 463mg (92%). Mp. = 248-256 °C (melt/decomp.) (lit. mp. > 230 °C). NMR (CDCl<sub>3</sub>):  $\delta$ (<sup>1</sup>H) = 1.36 (d, 15H, *J* = 3.7Hz); 7.35 (br s, 9H); 7.82 (t, 6H, *J* = 8.6 Hz).  $\delta$ (<sup>31</sup>P) = 30.28 (d, *J* = 143.5 Hz). The NMR results are in agreement with the literature values.

#### *Reaction in dichloromethane*<sup>5</sup>

[Cp\*RhCl<sub>2</sub>]<sub>2</sub> (294mg, 0.476 mmol) and PPh<sub>3</sub> (256 mg, 0.977 mmol) were placed in a flask charged with 12 cm<sup>3</sup> dry DCM. The red solution was stirred at room temperature for 45 min. The solvent was removed *in vacuo*. The resultant sticky orange residue

was recrystallized from dichloromethane-hexane, eventually yielding 531 mg (98%) orange crystals. Mp. = 248-257 °C (melt/decomp.). NMR data are similar to those obtained for the product of the reaction in ethanol.

#### 4.4.3 $\text{Cp}^*\text{RhCl}_2(\text{PMePh}_2)$ (**23**)<sup>5</sup>

450 mg (0.73 mmol)  $[\text{Cp}^*\text{RhCl}_2]_2$  was placed in a Schlenk tube with 15 cm<sup>3</sup> dry dichloromethane. 291 mg (1.46 mmol)  $\text{PMePh}_2$  was transferred, under nitrogen, from a sealed ampoule to the reaction vessel. The mixture was stirred for 40 minutes at room temperature. The solvent was removed *in vacuo*, and the residue recrystallized from DCM/hexane. Reddish brown crystals were obtained in 663 mg (89 %) yield. Mp. = 257 - 260 °C. NMR ( $\text{CDCl}_3$ )  $\delta(^1\text{H}) = 1.41$  (d, 15H,  $J = 3.4$  Hz), 2.14 (d, 3H,  $J = 12.2$  Hz), 7.44 (m, 6H), 7.82 (m, 4H);  $\delta(^{31}\text{P}) = 24.31$  (d,  $J = 142$  Hz). The NMR results are in agreement with the literature values.<sup>5,6</sup>

#### 4.4.4 $\text{Cp}^*\text{RhCl}_2(\text{PMe}_2\text{Ph})$ (**24**)<sup>5</sup>

388 mg (0.63 mmol)  $[\text{Cp}^*\text{RhCl}_2]_2$  was placed in a Schlenk tube with 15cm<sup>3</sup> dry dichloromethane. 171 mg (1.24 mmol)  $\text{PMe}_2\text{Ph}$  was transferred, under nitrogen, from a sealed ampoule to the reaction vessel. The mixture was stirred for 40 minutes at room temperature, and the solvent removed *in vacuo*. The residue was recrystallized from DCM/hexane, furnishing red crystals (507 mg, 90 %). Mp. = 229-231°C.

NMR ( $\text{CDCl}_3$ )  $\delta(^1\text{H}) = 1.44$  (d, 15H,  $J = 3.4$  Hz), 1.87 (d, 6H,  $J = 11.7$  Hz), 7.45 (m, 3H), 7.87 (m, 2H);  $\delta(^{31}\text{P}) = 13.26$  (d,  $J = 139\text{Hz}$ ). The NMR results are in agreement with the literature values.<sup>5,6</sup>

#### 4.4.5 $[\text{Cp}^*\text{RhI}_2]_2$ (**25**)<sup>3</sup>

$[\text{Cp}^*\text{RhCl}_2]_2$  (400 mg, 0.65 mmol) and NaI (1.0 g, 6.7 mmol) were refluxed in 30 cm<sup>3</sup> reagent-grade acetone for 3 hours. The reaction mixture was cooled and the purple-brown crystals removed under suction filtration and washed with small quantities (*ca* 5 – 10 cm<sup>3</sup>) of water, acetone and ether. The yield was 555 mg (87 %).

The complex was pure enough to be used unrecrystallized in further reactions.

Mp = 295°C (decomp) (lit. mp. > 230 °C). NMR (CDCl<sub>3</sub>): δ(<sup>1</sup>H) = 1.99 (s, 15H). The NMR results are in agreement with the literature values.

#### 4.4.6 Cp\*RhI<sub>2</sub>(PPh<sub>3</sub>) (**26**)<sup>3</sup>

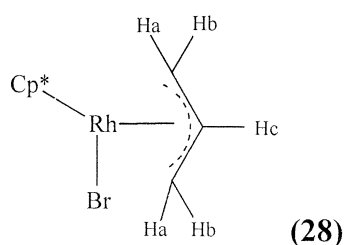
[Cp\*RhI<sub>2</sub>]<sub>2</sub> (500 mg, 0.51 mmol) and triphenylphosphine (1.0 g, 3.82 mmol) were refluxed in 25cm<sup>3</sup> reagent-grade acetone for 5 hours. After the reaction mixture had cooled, the purple crystals were filtered, washed with acetone and dried in air to yield 706mg (92%) of the complex. Mp = 255 -257 °C (lit. mp. > 230 °C). NMR (CDCl<sub>3</sub>): δ(<sup>1</sup>H) = 1.76 (d, 15H, *J* = 4.4 Hz), 7.45 (m, 9H), 7.67 (m, 6H). δ(<sup>31</sup>P) = 27.62 (d, *J* = 148 Hz). The NMR results are in agreement with the literature values.

#### 4.4.7 [Cp\*RhBr<sub>2</sub>]<sub>2</sub> (**27**)<sup>7</sup>

[Cp\*RhCl<sub>2</sub>]<sub>2</sub> (330 mg, 0.53 mmol) and NaBr (1 g, 9.7 mmol) were refluxed in 10cm<sup>3</sup> acetone for 2.5 hrs. The solution was cooled and the solvent removed *in vacuo*. The orange residue was recrystallized from dichloromethane/hexane to yield orange crystals (392 mg, 92 %). Mp. = 285 °C (slow decomp) (literature mp. > 260 °C).<sup>8</sup> NMR (CDCl<sub>3</sub>): δ(<sup>1</sup>H) = 1.73 (s, 15H). The NMR results are in agreement with the literature values.

### 4.5 Rhodium alkenyl complexes

#### 4.5.1 Reaction of [Cp\*RhBr<sub>2</sub>]<sub>2</sub> with MgBr-CH<sub>2</sub>CH=CH<sub>2</sub>



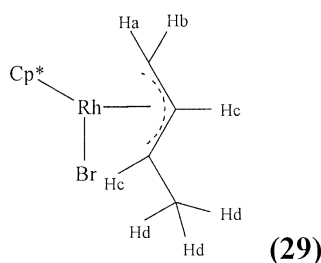
Allylmagnesium bromide (1 mmol) was added to a suspension of [Cp\*RhBr<sub>2</sub>]<sub>2</sub> (160 mg, 0.2mmol) in 10 cm<sup>3</sup> diethyl ether at -78 °C. The reaction mixture was allowed to

warm to room temperature and was stirred for 3 hours. Saturated  $\text{NH}_4\text{Cl}$  solution (*ca*  $3 \text{ cm}^3$ ) was added and the organic layer extracted with benzene (*ca*  $10 \text{ cm}^3$ ) and dried over anhydrous  $\text{MgSO}_4$ . Removal of solvent *in vacuo* furnished a solid red-brown product (110 mg, 76 %). Mp. = 120-122 °C (decomp). NMR ( $\text{CDCl}_3$ ):  $\delta(^1\text{H}) = 1.78$  (s, 15H), 3.14 (d, 2H<sub>a</sub>,  $J = 11.7\text{Hz}$ ), 3.33 (d, 2H<sub>b</sub>,  $J = 6.8\text{Hz}$ ), 3.95 (m, 1H<sub>c</sub>).  $\delta(^{13}\text{C}) = 9.53$  (Cp\* Me), 60.15 (d,  $J = 9.9 \text{ Hz}$ , 2 $\underline{\text{C}}\text{H}_a\text{H}_b$ ), 94.57 (d,  $J = 6.8 \text{ Hz}$ , -C- $\underline{\text{C}}\text{H}_c$ -C-), 98.04 (d,  $J = 6.9 \text{ Hz}$ , Cp\* ring).

Anal. calc. for  $\text{C}_{13}\text{H}_{20}\text{RhBr}$ : C, 43.5; H, 5.6. Found: C, 43.8; H, 5.5%.

Mass spec. FAB: 358/360  $[\text{M}]^+$ , 279  $[\text{M} - \text{Br}]^+$ , 237  $[\text{M} - \text{Br} - \eta^3\text{-C}_3\text{H}_5]^+$ .

#### 4.5.2 Reaction of $[\text{Cp}^*\text{RhBr}_2]_2$ with $\text{MgBr}-(\text{CH}_2)_2\text{CH}=\text{CH}_2$



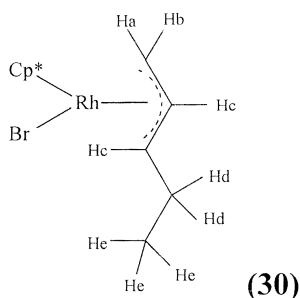
Butenylmagnesium bromide (2.5 mmol) added to a suspension of  $[\text{Cp}^*\text{RhBr}_2]_2$  (400 mg, 0.503 mmol) in  $10 \text{ cm}^3$  diethyl ether at  $-78^\circ\text{C}$ . After stirring for 1 day the reaction was hydrolyzed with saturated  $\text{NH}_4\text{Cl}$  (*ca*  $3 \text{ cm}^3$ ) solution and the organic layer extracted with benzene (*ca*  $10\text{cm}^3$ ). The solvent was removed *in vacuo* and the oily red residue recrystallized from ether/hexane. The product was isolated as orange crystals (270 mg, 72 %). Mp. = 120 - 122°C (melt/decomp).

NMR ( $\text{CDCl}_3$ ):  $\delta(^1\text{H}) = 1.56$  (d, 3H<sub>d</sub>,  $J = 5.4\text{Hz}$ ), 1.76 (s, 15H), 3.11 (d, 1H<sub>a</sub>,  $J = 11.2\text{Hz}$ ), 3.14 (d, 1H<sub>b</sub>,  $J = 6.3\text{Hz}$ ), 3.76 (m, 2H<sub>c</sub>).  $\delta(^{13}\text{C}) = 9.67$  (Cp\* Me), 17.90 ( $\text{CH}_2\text{-}\underline{\text{C}}\text{H}_3$ ), 56.15 (d,  $J = 10.4 \text{ Hz}$ ,  $\underline{\text{C}}\text{H}_a\text{H}_b$ ), 70.20 (d,  $J = 7.6 \text{ Hz}$ ,  $\underline{\text{C}}\text{H}_c\text{-CH}_3$ ), 95.38 (d,  $J = 6.1 \text{ Hz}$ ,  $\text{CH}_a\text{H}_b\text{-}\underline{\text{C}}\text{H}_c$ ), 97.70 (d,  $J = 6.1 \text{ Hz}$ , Cp\* ring).

Anal. calc. for  $\text{C}_{14}\text{H}_{22}\text{RhBr}$ : C, 45.1; H, 5.9. Found: C, 45.4; H 5.8%.

Mass spec. FAB:  $m/e$  372/374  $[\text{M}]^+$ , 293  $[\text{M} - \text{Br}]^+$ , 237  $[\text{M}^+ - \text{Br} - \eta^3\text{-C}_4\text{H}_7\text{-H}]^+$ .

#### 4.5.3 Reaction of $[\text{Cp}^*\text{RhBr}_2]_2$ with $\text{MgBr}-(\text{CH}_2)_3\text{CH}=\text{CH}_2$



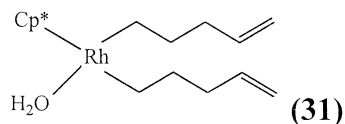
Pentenylmagnesium bromide (1 mmol) was added to a suspension of  $[\text{Cp}^*\text{RhBr}_2]_2$  (160 mg, 0.2 mmol) in 10 cm<sup>3</sup> diethyl ether at -78°C. After stirring for 1 day the reaction was hydrolyzed with saturated  $\text{NH}_4\text{Cl}$  (ca 3 cm<sup>3</sup>) solution and the organic layer extracted with benzene (ca 5 cm<sup>3</sup>). Solvent was removed *in vacuo* and the oily red product was recrystallized from ether/hexane. Mp. = 118-120 °C.

NMR ( $\text{CDCl}_3$ ):  $\delta(^1\text{H}) = 1.16$  (t, 3H<sub>e</sub>, 7.3Hz), 1.77 (s, 15H), 1.93 (m, 2H<sub>d</sub>), 3.11 (d, 1H<sub>a</sub>, 10.1Hz), 3.14 (d, 1H<sub>b</sub>, 6.4Hz), 3.74 (m, 2H<sub>c</sub>).  $\delta(^{13}\text{C}) = 9.72$  (s, Cp\* Me), 15.92 (s, H<sub>3</sub>C-CH<sub>2</sub>-), 26.12 (s, -CH<sub>2</sub>-), 56.22 (d,  $J = 11.5$  Hz, C-H<sub>a</sub>H<sub>b</sub>), 78.21 (d,  $J = 7.6$  Hz, (H<sub>d</sub>)<sub>2</sub>C-CH<sub>c</sub>-), 93.47 (d,  $J = 6.1$  Hz, H<sub>c</sub>C-CH<sub>a</sub>H<sub>b</sub>), 97.76 (d,  $J = 6.1$  Hz, Cp\* ring).

Anal. calc. for C<sub>15</sub>H<sub>24</sub>RhBr: C, 46.6; H, 6.2. Found: C, 46.9; H, 6.0%.

Mass spec. FAB:  $m/e$  385/387  $[\text{M}-\text{H}]^+$ , 307  $[\text{M}-\text{Br}]^+$ , 237  $[\text{M}-\text{Br}-\eta^3\text{-C}_5\text{H}_9-\text{H}]^+$ .

#### 4.5.4 Reaction of $[\text{Cp}^*\text{RhCl}_2]_2$ with $\text{MgBr}-(\text{CH}_2)_3\text{CH}=\text{CH}_2$



A suspension of 130 mg (0.21 mmol)  $[\text{Cp}^*\text{RhCl}_2]_2$  in 10 cm<sup>3</sup> diethyl ether was cooled to -78°C. 2 cm<sup>3</sup> of a 0.5 M solution of pentenylmagnesium bromide was added. The reaction was allowed to attain room temperature and was stirred for 3 hours. The excess Grignard reagent was hydrolyzed with aqueous  $\text{NH}_4\text{Cl}$ . The organic layer was extracted and dried over anhydrous  $\text{MgSO}_4$ . The solvent was removed to yield an orange oil that was dissolved in a small quantity of benzene. The solution was passed

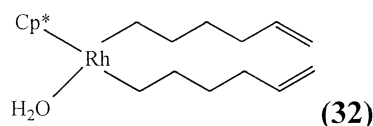
through a short column (5 cm) of deactivated alumina using a benzene eluent. A yellow band was the first and only band to elute and was collected. Other bands, dark red and orange, remained at the surface of the column. The final product was obtained as a yellow oil (48 mg, 29 %).

NMR (CDCl<sub>3</sub>):  $\delta$ (<sup>1</sup>H) = 0.91 (t, 4H, *J* = 7.4Hz), 0.99 (q, 4H, 7.2Hz), 1.26 (s, 15H), 2.05 (q, 4H, *J* = 7.3Hz), 5.0 (m, 4H), 5.8 (m, 2H).

Anal. calc. for C<sub>20</sub>H<sub>26</sub>RhO: C, 60.9; H, 8.9. Found: C, 60.9; H, 8.1 %.

Mass spec. FAB: *m/e* 391 [M - H]<sup>+</sup>, 376 [M - H<sub>2</sub>O]<sup>+</sup>, 307 [M - H<sub>2</sub>O - C<sub>5</sub>H<sub>9</sub>]<sup>+</sup>, 237 (M - H<sub>2</sub>O - 2C<sub>5</sub>H<sub>9</sub> - H)<sup>+</sup>.

#### 4.5.5 Reaction of [Cp\*RhCl<sub>2</sub>]<sub>2</sub> with MgBr-(CH<sub>2</sub>)<sub>4</sub>CH=CH<sub>2</sub>

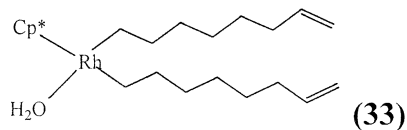


A suspension of 200 mg (0.32 mmol) [Cp\*RhCl<sub>2</sub>]<sub>2</sub> in 10 cm<sup>3</sup> diethyl ether was cooled to -78 °C and 5 equivalents of hexenylmagnesium bromide was added. The reaction was brought to room temperature and allowed to stir for 3 hours. The work-up was identical to that of **31**. The final yield was 97 mg (36 %).

NMR (CDCl<sub>3</sub>):  $\delta$ (<sup>1</sup>H) = 0.90 (t, 4H, *J* = 6.9Hz), 1.29 (s, 15H), 2.04 (q, 4H, *J* = 7.1Hz), 5.0 (m, 4H), 5.8 (m, 2H), 0.98 – 1.72 (br m, 8H).

Anal. calc. for C<sub>22</sub>H<sub>30</sub>RhO: C, 62.6; H, 9.2. Found: C, 63.0; H, 9.4 %.

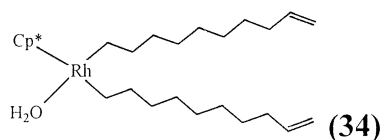
#### 4.5.6 Reaction of [Cp\*RhCl<sub>2</sub>]<sub>2</sub> with MgBr-(CH<sub>2</sub>)<sub>6</sub>CH=CH<sub>2</sub>



4.3 cm<sup>3</sup> of a 0.55 M solution of octenylmagnesium bromide (2.37 mmol) was added to a suspension of [Cp\*RhCl<sub>2</sub>]<sub>2</sub> (290 mg, 0.47 mmol) in 10 cm<sup>3</sup> ether held at -78 °C. The reaction mixture was left stirring at ambient temperature for 3 hours. The reaction work-up was identical to that for complex **31**. The final yield was 162mg (36 %).

NMR (CDCl<sub>3</sub>):  $\delta(^1\text{H}) = 0.89$  (t, 4H,  $J = 7.8\text{Hz}$ ), 1.28 (s, 15H), 2.05 (q, 4H, 7.1Hz), 5.0 (m, 4H), 5.8 (m, 2H), 0.98 – 1.72 (br m, 16H). IR (NaCl disc) = 3420 cm<sup>-1</sup> (O-H stretch). Anal. calc. for C<sub>26</sub>H<sub>38</sub>RhO: C, 65.3; H, 9.8. Found: C, 65.4; H, 9.9 %.

#### 4.5.7 Reaction of [Cp\*RhCl<sub>2</sub>]<sub>2</sub> with MgBr-(CH<sub>2</sub>)<sub>8</sub>CH=CH<sub>2</sub>



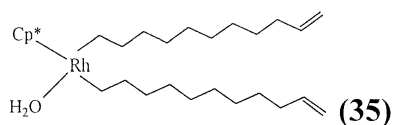
A suspension of [Cp\*RhCl<sub>2</sub>]<sub>2</sub> (135 mg, 0.22 mmol) in 10 cm<sup>3</sup> diethyl ether was held at -78 °C and 1.3 cm<sup>3</sup> of a 0.84 M solution of decenylmagnesium bromide was added. The reaction was stirred at room temperature for 4 hours. The reaction work-up was as described for complex **31**. The yield of the yellow oil was 100 mg (43 %).

NMR (CDCl<sub>3</sub>):  $\delta(^1\text{H}) = 0.89$  (t, 4H,  $J = 7.3\text{Hz}$ ), 1.26 (s, 15H), 2.04 (q, 4H,  $J = 7.1\text{Hz}$ ), 5.0 (m, 4H), 5.8 (m, 2H), 0.99 – 1.71 (br m, 24H).

Anal. calc. for C<sub>30</sub>H<sub>46</sub>RhO: C, 67.4; H, 10.3. Found: C, 67.8; H, 10.4 %.

Mass spec. FAB:  $m/e$  516 [M - H<sub>2</sub>O]<sup>+</sup>, 237 [M - H<sub>2</sub>O - 2C<sub>10</sub>H<sub>19</sub>]<sup>+</sup>.

#### 4.5.8 Reaction of [Cp\*RhCl<sub>2</sub>]<sub>2</sub> with MgBr-(CH<sub>2</sub>)<sub>9</sub>CH=CH<sub>2</sub>



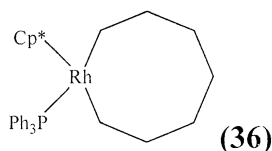
10 cm<sup>3</sup> of a 0.10 M solution of undecenylmagnesium bromide (1 mmol) was added to a suspension of [Cp\*RhCl<sub>2</sub>]<sub>2</sub> (120 mg, 0.19 mmol) in 10 cm<sup>3</sup> ether held at -78 °C. The reaction was stirred at room temperature for 3.5 hours. The reaction work-up was as is described for complex **31**. The final yield of yellow oil was 78 mg (37 %).

NMR (CDCl<sub>3</sub>):  $\delta(^1\text{H}) = 0.91$  (t, 4H,  $J = 7.0\text{Hz}$ ), 1.29 (s, 15H), 2.07 (q, 4H,  $J = 7.1\text{Hz}$ ), 5.0 (m, 4H), 5.8 (m, 4H), 0.99 – 1.71 (br m, 28H). IR (NaCl disc) = 3420 cm<sup>-1</sup> (O-H stretch).

Mass spec. FAB:  $m/e$  544 [M - H<sub>2</sub>O]<sup>+</sup>, 391 [M - H<sub>2</sub>O - C<sub>11</sub>H<sub>21</sub>]<sup>+</sup>, 237 [M - H<sub>2</sub>O - 2C<sub>11</sub>H<sub>21</sub> - H]<sup>+</sup>.

## 4.6 Reactions of rhodium precursors with di-Grignard reagents

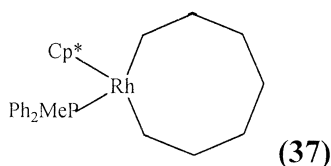
### 4.6.1 Reaction of Cp\*RhCl<sub>2</sub>(PPh<sub>3</sub>) with MgBr-(CH<sub>2</sub>)<sub>7</sub>-MgBr



Cp\*RhCl<sub>2</sub>(PPh<sub>3</sub>) (200 mg, 0.35 mmol) was dried in a Schlenk tube prior to addition of 30 cm<sup>3</sup> dry diethyl ether to the vessel. The tube was cooled to 0 °C and MgBr-(CH<sub>2</sub>)<sub>7</sub>-MgBr (1 mmol) was added. The reaction was stirred at room temperature for 36 hours. The reaction was observed to be changing gradually from a suspension of insoluble Cp\*RhCl<sub>2</sub>(PPh<sub>3</sub>) to an orange solution. The solvent was removed and the product extracted with benzene. It was passed through a 3 cm column of deactivated silica. The yellow band was collected and the solvent was removed to reveal a yellow oil (63 mg, 30%). NMR (C<sub>6</sub>D<sub>6</sub>): δ(<sup>1</sup>H) = 1.53 (d, 15H, *J* = 2.0 Hz), 0.83 – 1.38 (br m, 14H), 7.22 – 7.37 (m, 15H). δ(<sup>31</sup>P) = 56.15 (d, *J* = 186.4 Hz).

Mass spec. FAB: *m/e* 597 [M – H]<sup>+</sup>, 499 [M – 7CH<sub>2</sub> – H]<sup>+</sup>, 424 [M – 7CH<sub>2</sub> – 5CH<sub>3</sub> – H]<sup>+</sup>

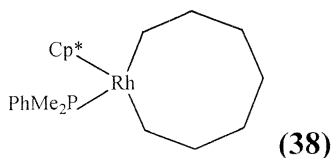
### 4.6.2 Reaction of Cp\*RhCl<sub>2</sub>(PMePh<sub>2</sub>) with MgBr-(CH<sub>2</sub>)<sub>7</sub>-MgBr



A Schlenk tube containing a suspension of dried Cp\*RhCl<sub>2</sub>(PMePh<sub>2</sub>) (330 mg, 0.65 mmol) in 35 cm<sup>3</sup> diethyl ether was cooled in an ice-bath. 2.43 cm<sup>3</sup> of a 0.4 M solution of MgBr-(CH<sub>2</sub>)<sub>7</sub>-MgBr (0.97 mmol) was added, and the reaction stirred at room temperature for 3.5 hrs. The reaction work-up was similar to that of **16**. The yellow oil was isolated in 117 mg (34 %).

NMR (C<sub>6</sub>D<sub>6</sub>): δ(<sup>1</sup>H) = 1.57 (d, 15H, = 2.4 Hz), 0.85 - 1.34 (br m, 17H), 6.99 – 7.36 (m, 10H). δ(<sup>31</sup>P) = 38.77 (d, *J* = 185.4 Hz).

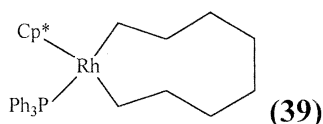
#### 4.6.3 Reaction of Cp\*RhCl<sub>2</sub>(PMe<sub>2</sub>Ph) with MgBr-(CH<sub>2</sub>)<sub>7</sub>-MgBr



A Schlenk tube containing a suspension of dried Cp\*RhCl<sub>2</sub>(PMePh<sub>2</sub>) (160 mg, 0.31 mmol) in 35 cm<sup>3</sup> diethyl ether was cooled in an ice-bath. 1.2 cm<sup>3</sup> of a 0.8 M solution of MgBr-(CH<sub>2</sub>)<sub>7</sub>-MgBr (0.97 mmol) was added, and the reaction stirred at room temperature for 3 hrs. The work-up procedure was similar to that described for complex **16**. The yield of the yellow oil was 49 mg (33%).

NMR (C<sub>6</sub>D<sub>6</sub>): δ(<sup>1</sup>H) = 1.55 (d, 15H, *J* = 2.4 Hz), 0.85 – 1.34 (br m, 20H), 6.89 – 7.38 (m, 5H). δ(<sup>31</sup>P) = 20.96 (d, *J* = 183.1 Hz).

#### 4.6.4 Reaction of Cp\*RhCl<sub>2</sub>(PPh<sub>3</sub>) with MgBr-(CH<sub>2</sub>)<sub>8</sub>-MgBr

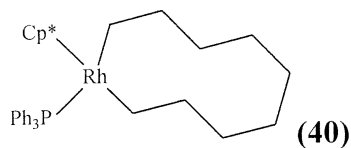


300 mg (0.53 mmol) Cp\*RhCl<sub>2</sub>(PPh<sub>3</sub>) was added to 35 cm<sup>3</sup> diethyl ether in a Schlenk tube. The suspension was cooled to 0 °C, and MgBr-(CH<sub>2</sub>)<sub>8</sub>-MgBr (1.1 mmol) was added. After stirring for 2 hours at room temperature, the reaction mixture was filtered and the product extracted with pentane. The residue, a yellow-brown oil, was dissolved in a little benzene and passed through a 4 cm column of deactivated alumina with benzene as eluent. The yellow band was collected and yielded a yellow oil (123 mg, 38 %).

NMR (C<sub>6</sub>D<sub>6</sub>): δ(<sup>1</sup>H) = 1.59 (d, 15H, *J* = 2.0Hz), 0.88 – 1.37 (m, 16H), 7.10 – 7.45 (m, 15H). δ(<sup>31</sup>P) = 56.33 (d, *J* = 185.4 Hz).

Mass spec. FAB: *m/e* 499 [M – 8CH<sub>2</sub>]<sup>+</sup>, 424 [M – 8CH<sub>2</sub> – 5CH<sub>3</sub> – H]<sup>+</sup>.

#### 4.6.5 Reaction of Cp\*RhCl<sub>2</sub>(PPh<sub>3</sub>) with MgBr-(CH<sub>2</sub>)<sub>9</sub>-MgBr



320mg (0.56mmol) Cp\*RhCl<sub>2</sub>(PPh<sub>3</sub>) was added to 40cm<sup>3</sup> diethyl ether in a Schlenk tube. The suspension was cooled to 0 °C, and 0.85mmol (1.5 molar eq.) MgBr(CH<sub>2</sub>)<sub>9</sub>MgBr was added. The reaction mixture was allowed to stir at room temperature for 1.5 hours, and was seen to turn an orange-yellow as time progressed. Solvent was removed *in vacuo* and the product extracted with benzene. The solvent was removed again, and the residue dissolved in a little benzene and passed through a short column of deactivated alumina (benzene eluent). The yellow band collected furnished a yellow-orange oil of yield 101mg (29 %).

NMR (C<sub>6</sub>D<sub>6</sub>): δ(<sup>1</sup>H) = 1.59 (d, 15H, *J* = 2.0Hz), 0.87 – 1.35 (m, 18H), 7.07 – 7.45 (m, 15H). δ(<sup>31</sup>P) = 56.34 (d, *J* = 185.4).

Mass spec. FAB: *m/e* 499 [M – 9CH<sub>2</sub>]<sup>+</sup>, 424 [M – 9CH<sub>2</sub> – 5CH<sub>3</sub> – H]<sup>+</sup>, 363 [M – PPh<sub>3</sub> – H]<sup>+</sup>.

#### 4.7 Determination of X-ray Crystal Structure of 30

The X-ray crystal structure analysis was carried out at the University of Cape Town. X-ray single crystal intensity data were collected on a Nonius Kappa-CCD diffractometer using graphite monochromated MoK $\alpha$  radiation. Temperature was controlled by an Oxford Cryostream cooling system (Oxford Cryostat). The strategy for the data collections was evaluated using the Bruker Nonius "Collect" program. Data were scaled and reduced using DENZO-SMN software (Otwinowski & Minor, 1997). The structure was solved by direct methods using SHELXS-97 (Sheldrick, 1997) and refined employing full-matrix least-squares with the program SHELXL-97 refining on F<sup>2</sup> (Sheldrick, 1997). Packing diagrams were produced using the program PovRay and graphic interface X-seed (Barbour, 2001).

#### **4.8 Thermal decomposition studies**

All thermal decompositions were carried out under anhydrous, oxygen-free conditions. Approximately 10 mg of a sample was placed in a thoroughly cleaned and dried tube. The tube was degassed and sealed under vacuum. The sample was submerged in a heated oil bath held constant at 170°C. After 2 hours the reaction was quenched by immersion in liquid nitrogen. The sample was extracted with 0.5ml cyclohexane containing the internal standard, chlorobenzene. Decomposition products were analyzed by GC-FID and GC-MS. Products were identified by comparison of their retention times to those of known samples. The product yields were determined by the response relative to the chlorobenzene standard, and the response factors were obtained from standard samples in the following manner: a solution containing a known quantity of the standard and a known quantity of the internal standard chlorobenzene was analyzed by GC-FID. The response factor was calculated by the equation  $f_i = A_i C_s / A_s C_i$ , where  $A$  is the peak area and  $C$  is the concentration of the standard ( $s$ ) or internal standard ( $i$ ).

## **4.9 References**

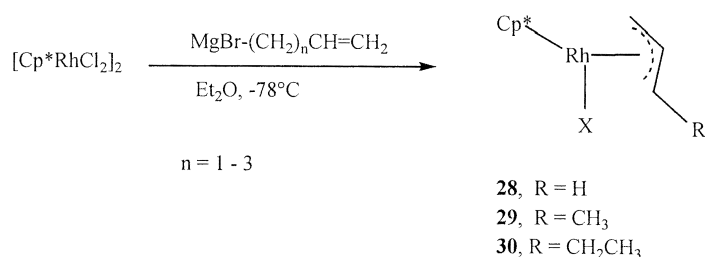
1. G. S. Silverman, in *Handbook of Grignard reagents*, G. S. Silverman and P. E. Rakita (eds.), Marcel Dekker, Inc., 1996.
2. J. X. McDermott, J. F. White and G. M. Whitesides, *J. Am. Chem. Soc.*, 1976, **98**, 6521.
3. J. W. Kang, K. Moseley and P. M. Maitlis, *J. Am. Chem. Soc.*, 1969, **91**, 5970.
4. C. White, A. Yates and P. M. Maitlis, *Inorg. Synth.*, 1992, **29**, 229.
5. W. D. Jones and V. L. Kuykendall, *Inorg. Chem.*, 1991, **30**, 2615.
6. V. Tedesco and W. von Philipsborn, *Magn. Res. Chem.*, 1996, **34**, 373.
7. W. D. Jones and F. J. Fehrer, *Inorg. Chem.*, 1984, **23**, 2376.
8. D. S. Gill and P. M. Maitlis, *J. Organomet. Chem.*, 1975, **87**, 359.

## Chapter 5

### Conclusions and future work

The aim of this project was to investigate different routes to the synthesis of rhodium-containing metallacycloalkanes. A recently-developed route, that had proved to work very well in the preparation of large-ring platinacycloalkanes, involves the synthesis of metal bis-alkenyl complexes. The bis-alkenyl complexes were subjected to Grubbs' ring-closing metathesis, resulting in the formation of platinacycloalkenes which were subsequently hydrogenated to form the corresponding platinacycloalkane.

This method was one of those applied for the preparation of rhodacycloalkanes. Therefore, a series of alkenyl Grignard reagents of the type  $\text{MgBr}-(\text{CH}_2)_n\text{CH}=\text{CH}_2$  ( $n = 1 - 4, 6, 8, 9$ ) were reacted with the rhodium precursors  $[\text{Cp}^*\text{RhX}_2]_2$  ( $\text{X} = \text{Cl}$  or  $\text{Br}$ ). The reactions of propenyl-, butenyl- and pentenylmagnesium bromide with  $[\text{Cp}^*\text{RhBr}_2]_2$  afforded, unexpectedly, a series of allylic complexes of composition  $\text{Cp}^*\text{RhBr}(\text{allyl-R})$  (**28** – **30**) (Scheme 5.1). These were found to be stable, crystalline solids and were isolated in high yields. Two of the three allylic complexes, **28** and **30**, are novel complexes. We were able to grow good crystals of **30**, and an X-ray structure was determined. This confirmed the  $\eta^3$ -allylic structure. Complex **29** is a known compound; however, we have prepared it in high yield by a new route.

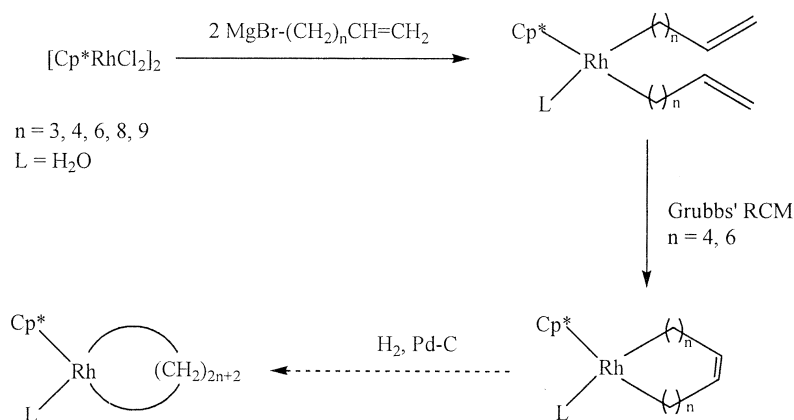


Scheme 5.1

<sup>1</sup>H NMR evidence suggests that the chemical nature of the allylic complex in solution can change according to the polarity of the solvent. The most likely explanation is that in non-polar solvents such as benzene the allylic complex exists in its neutral form, and that when placed in a polar solvent, chloroform, the complex is converted to its

ionic form,  $[\text{Cp}^*\text{Rh}(\text{allyl-R})]^+ \text{Br}^-$ . Further studies, including conductivity measurements, should be carried out in order to prove this claim.

The preparation of a series of new bis-alkenyl rhodium complexes, which had been our initial aim, was achieved by the reaction of intermediate to long-chain alkenyl-Grignard reagents with  $[\text{Cp}^*\text{RhCl}_2]_2$  (Scheme 5.2). The complexes were found to be of composition  $\text{Cp}^*\text{Rh}(\{\text{CH}_2\}_n\text{CH}=\text{CH}_2)_2\text{L}$ . It was determined that  $\text{L} = \text{H}_2\text{O}$ ; the water molecule is believed to arise during the aqueous work-up. Surprisingly, reaction of the bis-alkenyl complexes with  $\text{PPh}_3$  did not cause the expected ligand substitution reaction. It is possible that  $\text{PPh}_3$  is too weakly basic and/or too bulky to coordinate to the rhodium centre. This reaction could be carried out using more strongly basic and less sterically hindered phosphines, such as trimethylphosphine ( $\text{PMe}_3$ ).



**Scheme 5.2**

The bis-alkenyl complexes were isolated in medium-low yields of approximately 40%. The synthesis of bis-alkenyl complexes is only the first in a series of reactions that eventually leads to the preparation of metallacycloalkanes. It is therefore necessary to optimize the yields of these precursors, in order for the bis-alkenyl method to provide a viable alternative to the more conventional methods for the preparation of rhodacycloalkanes.

Nevertheless, the method could still be convenient for the synthesis of large metallacycloalkanes (albeit in low yield) that are difficult or impossible to prepare via other routes. We have carried out ring-closing reactions on a select few of the bis-

alkenyl complexes.  $^1\text{H}$  NMR monitoring indicates that ring-closing to form the rhodacycloalkene does occur. So far we have not been able to isolate the rhodacycloalkene. However, further work in this area could lead to isolation of the product and optimization of the reaction conditions. From then on, it is only one step to the preparation of perhaps, very large rhodacycloalkanes, new molecules that would be potential models for metallacyclic catalytic intermediates.

Due to the problems encountered with the bis-alkenyl route, another method was employed as an alternative for the preparation of rhodacycloalkanes. We attempted to synthesize medium-sized rhodacycloalkanes (8 – 10 ring members) by the reaction of rhodium dihalide precursors with di-Grignard alkyl reagents, a method employed by Diversi *et al.* Diversi's rhodacycles, of which the largest was a 7-membered ring complex, were obtained as stable orange crystals. Our products, however, were obtained as yellow oils. The oils had low stability, making characterization difficult. However,  $^1\text{H}$  and  $^{31}\text{P}$  NMR data were obtained, and the fragmentation patterns observed in the mass spectra indicated the presence of the proposed rhodacycloalkanes.

It was expected that the rhodacyclooctane prepared by ourselves and the rhodacycloheptane prepared by Diversi would exhibit similar properties (Figure 5.1), as the complexes differ only by one ring methylene group. It is surprising, then, that the two molecules should differ so greatly in both form and stability.

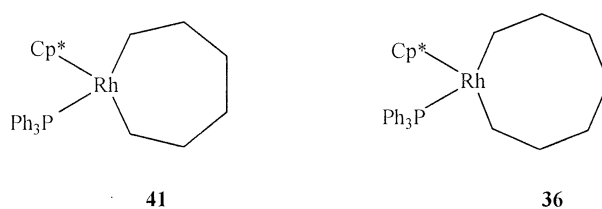


**Figure 5.1 Rhodacycloheptane (41) and rhodacyclooctane (36)**

Decomposition studies were carried out on four of the five rhodacycloalkanes synthesized. A range of different organic decomposition products were detected. Most of these could be explained by the common decomposition pathways of  $\beta$ -H elimination and reductive elimination, and other processes such as alkene

isomerization and hydrogenation. For  $\text{Cp}^*\text{Rh}(\text{CH}_2)_7(\text{PMePh}_2)$  and  $\text{Cp}^*\text{Rh}(\text{CH}_2)_7(\text{PMe}_2\text{Ph})$  the major products were n-heptane and 1- and 2-heptene. For  $\text{Cp}^*\text{Rh}(\text{CH}_2)_9(\text{PPh}_3)$  two of the three major products were 1-nonene and n-nonane. More interestingly, some of the organic products appeared to be formed as a result of carbon-carbon fission reactions, a less common process, but a known one. Thus  $\text{Cp}^*\text{Rh}(\text{CH}_2)_7(\text{PPh}_3)$  underwent thermal decomposition to give 60 % cyclohexane. This result indicates that there is a loss of one carbon from the ring prior to decomposition. This can arise as a result of an  $\alpha$ -carbon abstraction reaction, in which there is migration of a methylene group from the metallacycle ring onto the metal centre.

Future work on rhodacycloalkanes should include reactivity studies of the complexes with reagents such as CO or ethylene. The synthesis of larger-ring complexes, as well as different phosphine derivatives, could be carried out. Full characterization and (assuming that crystals could be grown) X-ray crystal structures could be obtained. Decomposition studies also would be carried out and the results compared with those of the known rhodacycloalkanes and the ones reported in this thesis.

Overall, we have contributed to the development of a new route to the preparation of novel metallacycloalkanes, and in the process have synthesized some novel complexes. Some, like the bis-alkenyl complexes, are unique examples of a rare class of complexes. All have proven to exhibit some interesting properties and behaviour, and this warrants further studies on these fascinating groups of complexes.